

4. SITE 872¹

Shipboard Scientific Party²

HOLE 872A

Date occupied: 2 June 1992
Date departed: 3 June 1992
Time on hole: 1 day
Position: 10°05.850'N, 162°51.960'E
Bottom felt (rig floor, m; drill-pipe measurement): 1094.5
Distance between rig floor and sea level (m): 10.9
Water depth (drill-pipe measurement from sea level, m): 1083.6
Total depth (rig floor, m): 1238.5
Penetration (m): 144.0
Number of cores (including cores with no recovery): 18
Total length of cored section (m): 144.00
Total core recovered (m): 123.63
Core recovery (%): 86
Oldest sediment cored:
Depth (mbsf): 143.7
Nature: phosphatized chalk
Age: middle Eocene
Hard rock:
Depth (mbsf): 144.0
Nature: basalt

HOLE 872B

Date occupied: 3 June 1992
Date departed: 4 June 1992
Time on hole: 1 day, 20 hr, 30 min
Position: 10°05.808'N, 162°51.996'E
Bottom felt (rig floor, m; drill-pipe measurement): 1094.5
Distance between rig floor and sea level (m): 10.9
Water depth (drill-pipe measurement from sea level, m): 1083.6
Total depth (rig floor, m): 1287.0
Penetration (m): 192.5
Number of cores (including cores with no recovery): 3
Total length of cored section (m): 86.30
Total core recovered (m): 25.96
Core recovery (%): 30
Oldest sediment cored:
Depth (mbsf): 136.0
Nature: pelagic sediment infilling fractures in basalt
Age: early Santonian

Hard rock:

Depth (mbsf): 136.0
Nature: basalt

HOLE 872C

Date occupied: 5 June 1992
Date departed: 5 June 1992
Time on hole: 23 hr, 45 min
Position: 10°05.62'N, 162°52.002'E
Bottom felt (rig floor, m; drill-pipe measurement): 1093.0
Distance between rig floor and sea level (m): 10.9
Water depth (drill-pipe measurement from sea level, m): 1082.1
Total depth (rig floor, m): 1242.5
Penetration (m): 148.0
Number of cores (including cores with no recovery): 18
Total length of cored section (m): 148.00
Total core recovered (m): 145.72
Core recovery (%): 98.5
Oldest sediment cored:
Depth (mbsf): 141.7
Nature: foraminifer ooze
Age: late Oligocene
Hard rock:
Depth (mbsf): 141.7
Nature: basalt

Principal results: Site 872 is located at 10°05.85'N, 162°51.96'E at 1084 m water depth, on the central portion of Lo-En Guyot, approximately 148.2 km from Anewetak Atoll in the northern Marshall Islands. Lo-En Guyot and the living atoll Anewetak, located to the northwest, are bathymetric features that share the same volcanic pedestal. In the Marshall Islands area, the association of atolls with adjacent guyots is prevalent (Fig. 1).

The guyots in the Marshall Islands region have pelagic caps that range in thickness from virtually 0 to 150 m. The thickness of an individual pelagic cap appears to be strongly correlated with both the depth of the guyot (related to the length of the depositional history) and the size of the guyot (less erosion near the perimeter of the summit). Of the guyots surveyed on the 1988 cruise of the *Moana Wave* (MW8805), the pelagic cap atop Lo-En Guyot appears to be the most complete in the region. Recovering the pelagic cap sediments was a key objective of drilling on this guyot; therefore, on the basis of the 3.5-kHz echo-sounder records, the position of Site 872 was selected in the thickest portion of the pelagic cap on Lo-En Guyot.

The objectives at this location were (1) to recover pelagic sediments for high-resolution stratigraphy and for reconstructing the paleoceanography in this sector of the Pacific; (2) to relate the acoustic stratigraphy of the pelagic cap to its depositional and diagenetic history and correlate seismic reflectors with those seen in other settings; (3) to date the interface between the pelagic cap and the underlying platform, and to infer the age and cause of platform drowning; (4) to establish the characteristics of platform carbonate facies and facies changes with time; (5) to compare the stratigraphy and facies of Lo-En Guyot with Anewetak; and (6) to establish the age of the basement.

Three holes were drilled at Site 872. Hole 872A is located 150 m northwest of Hole 872B, and Hole 872C is located 106 m north of

¹ Premoli Silva, I., Haggerty, J., Rack, F., et al., 1993. *Proc. ODP, Init. Repts.*, 144; College Station, TX (Ocean Drilling Program).

² Shipboard Scientific Party is as given in the list of participants preceding the contents.

Hole 872B; all three holes were offset 75 m from the acoustic beacon deployed at this site. The unusual distance between the three holes was chosen to prevent or diminish the chance that drilling disturbance in the vicinity of one drill hole would disrupt the physical properties of the ooze within another drill hole in the pelagic cap. Experience with the exceptionally soupy, winnowed foraminifer ooze from Site 871 on Limalok Guyot guided this decision.

Holes 872A and 872C were cored with the advanced hydraulic piston cores (APC) to 143.7 and 139.5 mbsf, respectively, where refusal occurred at the boundary between late Oligocene and middle Eocene sediments. These holes were continued by extended core barrel (XCB) coring to 144 mbsf with a total recovery of 85.9% (Hole 872A) and 148 mbsf with a total recovery of 98.5% (Hole 872C), respectively. Hole 872B was spudded using the rotary core barrel (RCB) system. After spot coring the pelagic cap, cores were recovered from 135.2 to 192.5 mbsf total depth (TD), for a total recovery of 30.1% in Hole 872B.

The APC cores recovered from Hole 872A were winnowed and very soupy, similar to the material recovered from the pelagic cap at Limalok Guyot (Site 871). The lack of cohesion in these sediments when they are drilled, and the subsequent handling of these water-laden cores on deck, result in cores that are poor candidates for high-resolution stratigraphy. To salvage Site 872 for the high-resolution stratigraphy objective, we implemented a different method of handling cores upon arrival on the rig floor when drilling Hole 872C. Excess water at the top of a core was removed with a device, named a piglet, that was inserted into the core liner while the core was upright within the core barrel on the rig floor. Additional excess water was removed after the core was cut into sections. Each section was turned upright to permit water to rise to the top for removal and the core liner was then trimmed at the top of the ooze. In this manner, we were able to recover cores in which the details of mottling, sharp changes in color and lithology, and sedimentary structures could be observed.

Four lithologic units were recognized at Site 872 using a combination of visual core descriptions, augmented with smear slide and thin-section data. Age identification of these units is based on calcareous nannofossils and planktonic foraminifers studied in smear slides, washed residues, and thin-section samples. The units identified are, from top to bottom, as follows:

Unit I (Hole 872A, 0–143.6 mbsf; Hole 872C, 0–141.7 mbsf) consists of white to pale brown nannofossil foraminifer ooze intercalated with foraminifer ooze of Pleistocene to late Oligocene age. Sediment composition allowed the division of Unit I in two subunits. The calcium carbonate content of Unit I is almost 100%, and interstitial water analysis indicates minimal diagenesis. Subunit IA (Hole 872A, 0–30.2 mbsf; Hole 872C, 0–32.9 mbsf) is comprised of white to very pale brown nannofossil foraminifer ooze and intercalated foraminifer ooze of Pleistocene to late Miocene age. Subunit IB (Hole 872A, 30.2–143.6 mbsf; Hole 872C, 32.9–141.7 mbsf) is comprised of very pale brown homogeneous foraminifer ooze with a medium sand texture that is well sorted, winnowed, and of late Miocene to late Oligocene age. The transition between the two subunits is marked by an interval of sediment characterized by a mixture of nannofloras and faunas of different zones followed by a disconformity. This mixed and incomplete interval spans the late middle to early late Miocene. Within the lower Miocene, another disconformity, representing a hiatus of approximately 5 m.y., was observed in Subunit IB at about 100 mbsf in both holes. The sedimentary succession across the Oligocene/Miocene boundary appears to be complete.

Unit II (Hole 872A, 143.6–143.7 mbsf; Hole 872B, 135.2–135.36 mbsf) includes three subunits. Subunit IIA is composed of phosphatized middle Eocene chalk containing pebbles of basalt, conglomerates, and volcanics (Hole 872A, 143.6–143.7 mbsf). Subunit IIB consists of phosphatized volcanoclastic sandstone of indeterminate age (Hole 872B, 135.2–135.3 mbsf). Subunit IIC is comprised of a conglomerate, coated by a shiny dark brown to black veneer that encloses phosphatized lithoclasts, <1 to 3 cm in diameter (Hole 872B, 135.3–135.36 mbsf). The phosphatized lithoclasts contain volcanoclastic debris set in a pelagic limestone matrix of latest Santonian to early Campanian age. The lithoclasts are redeposited in pelagic sediment of late Paleocene age.

Unit III (Hole 872B, 135.36–135.41 mbsf) consists of subangular basalt clasts, 0.5 to 4 cm in size, in a pelagic limestone matrix of late early Santonian age in contact with slightly altered basalt.

Unit IV (Hole 872A, 143.7–144.0 mbsf; Hole 872B, 135.41–192.5 mbsf; Hole 872C, 141.7–148.0 mbsf, 872C) is composed of differentiated alkali olivine basalt as massive flows and flow-top breccias. The uppermost 71 cm of Unit IV in Hole 872B has a few fractures infilled with pelagic sediments of early Santonian age. These pelagic sediments are increasingly phosphatized with depth and contain some reworked planktonic foraminifers of late Turonian age. A sparsely olivine-phyric basalt identifies the uppermost flow in Holes 872A and 872B; in Hole 872C, the upper volcanic flow is a highly altered olivine basalt (142.75–143.10 mbsf) that belongs to a different flow.³ The brecciated flow tops in several flow units in Hole 872B suggest that these flows were erupted subaerially in a short time, which precluded soil development on top of the flows. In Hole 872C, the basalt unit is overlain by a 10-cm-thick dark gray clay that appears to be an alteration product of the basalt. Basalt samples display natural remanent magnetization (NRM) intensities of <10 A/m and usually have a nearly univectorial magnetization. Inclinations of the characteristic remanent magnetization are negative and range from -41° to -61° .

Logging in Hole 872B was initially planned (1) to gain definitive information about the presence or absence of additional sediment intervals in the basalt, and (2) to obtain a clearer understanding of the unconformity between the upper Oligocene foraminifer ooze and the underlying hardground. The condition of the hole was less than favorable; however, with difficulty, it was cleaned to total depth in preparation for logging. However, logging proved to be unsuccessful, as both of the geochemical tools onboard the ship would not properly calibrate during in-pipe checks, and a tool run encountered a bridge only 4 m beneath the pipe. The prospects of obtaining any logging results did not justify additional logging time.

BACKGROUND AND OBJECTIVES

Site 872 (proposed Site Pel-3) is located at $10^{\circ}05.85'N$, $162^{\circ}51.96'E$, in a water depth of 1084 m, on the central summit region of Lo-En Guyot in the northern Marshall Islands. Lo-En Guyot is the sibling edifice of the living atoll Annewetak, located to the northwest; both bathymetric features share the same volcanic pedestal. In the Marshall Islands area, the association of atolls with adjacent guyots is prevalent (Fig. 1).

The guyots in the Marshall Islands region have pelagic caps that range in thickness from virtually 0 to 150 m. The thickness of an individual pelagic cap appears to be strongly correlated with both the depth of the guyot (related to the length of the depositional history) and the size of the guyot (less erosion near the perimeter of the summit). Of the guyots surveyed on the 1988 cruise of the *Moana Wave* (MW8805), the pelagic cap atop Lo-En Guyot appears to be the most complete in the region and was a key objective, therefore, of drilling on this guyot.

Rock dredges, obtained during Cruise MW8805 from the southern side of Lo-En Guyot, contain breccia composed of angular fragments of vesicular basalt floating in a calcareous matrix of shallow-water debris and planktonic foraminifers (Lincoln et al., in press). The most abundant planktonic foraminifers are specimens belonging to *Favusella washitensis* and possibly other species of favusellids. Associated in these rocks are also common specimens of the calpionellid species *Colomiella recta*. The stratigraphic distribution of *Favusella* is from early Albian to Cenomanian; the distribution of *Colomiella* is from late Aptian to early Albian. Both of these species, although planktonic, generally occur in a near-shore environment and are missing in the

³ In Hole 872C, the basement contact at the top of Lithologic Unit IV is placed at 141.7 mbsf within Section 144-872C-17X-CC. The actual depth of this contact is thought to be at 142.5 to 142.75 mbsf based on a change in drilling parameters.

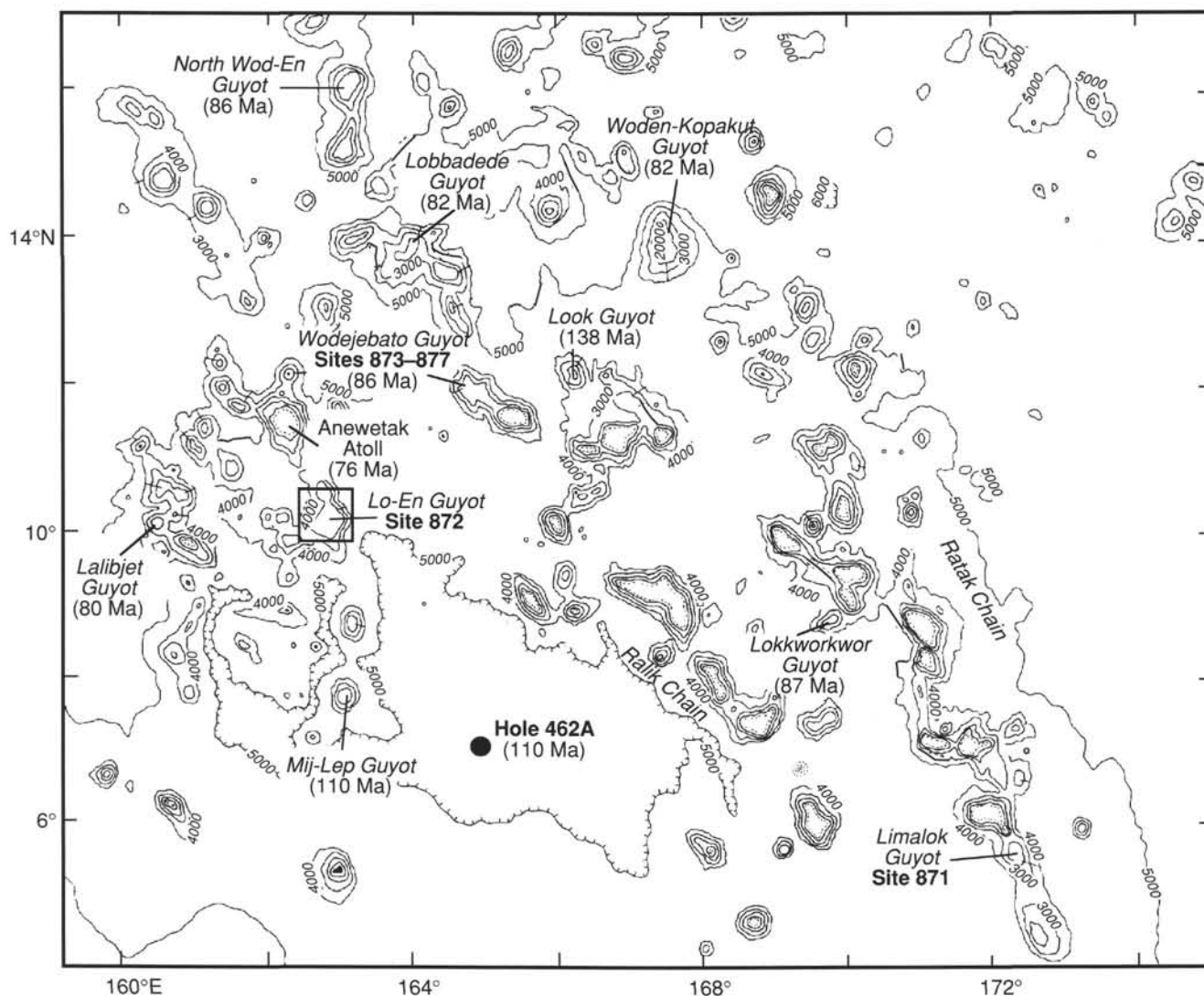


Figure 1. Bathymetry around the Marshall Islands. Contour interval is 1000 m, and the ages shown in parentheses are radiometric dates of basalts collected over a number of different surveys. Radiometric ages from Davis et al. (1989) and Pringle (1992). Figure revised from Hein et al. (1990). The locations of Lo-En Guyot and Site 872 are indicated.

open-ocean, deep-water deposits. Their occurrence indicates that a shallow-marine environment existed at least in the early to middle Albian on Lo-En Guyot. This interpretation of age and environment is supported by the presence of poorly preserved specimens of the planktonic foraminifer *Praeglobotruncana stephani*, which demonstrates that Lo-En Guyot was already in a pelagic regime by latest Albian time.

The shallow-water debris contained within the matrix of this breccia are abundant bryozoan fragments, echinoid debris, sponge spicules, and possibly rudist fragments. Numerous agglutinated foraminifer specimens related to *Vercorsella* and/or *Sabaudia* also occur; their presence suggests that a carbonate platform was alive on Lo-En Guyot by Aptian-Albian time. The dredged rocks were probably deposited in an outer slope environment, as indicated by the mixture of basalt fragments, shallow-water debris, and open-marine planktonic foraminifers (Lincoln et al., in press).

The same dredge haul on Lo-En Guyot includes a manganese-encrusted foraminifer limestone that is conceivably Coniacian in age. The planktonic foraminifer assemblage contains whiteinellids and marginotruncanids, as well as one specimen of *Dicarinella*

concovata; this may identify the assemblage, therefore, as belonging to the *Dicarinella concovata* Zone. Another breccia from this dredge haul is composed of angular basalt pebbles floating in a planktonic foraminifer-rich matrix attributable to the *Globotruncanella elevata* Zone of early Campanian age (Lincoln et al., in press).

All the dredge haul data demonstrate that Lo-En Guyot (1) erupted before early Albian time, (2) supported a shallow-water carbonate environment during most of the Albian, and (3) subsided into the pelagic realm by latest Albian time. No evidence exists that this guyot returned to sea level during the Late Cretaceous, although the Campanian age of volcanic breccias recovered from the flanks of this guyot could indicate an erosional event potentially caused by uplift that coincides with the eruption of adjacent Anewetak Atoll. The radiometric age of 75.9 ± 0.6 Ma for Anewetak basalt indicates that Lo-En's sibling erupted during passage over either the Rurutu or Rarotonga hotspots in the Late Cretaceous (Lincoln et al., in press); this coincides with the Late Cretaceous uplift events at nearby Wodejebato and Ruwituntun. The SeaMARC II side-scan imagery of Lo-En Guyot shows two

volcanic cones that breach the surface of the pelagic cap along the central, southwestern region of the summit of the guyot (see "Underway and Site Geophysics" section, this chapter). These volcanic cones have not been radiometrically dated and may be related to Late Cretaceous or younger volcanism.

The primary objectives planned for Site 872 (Pel-3) were (1) to recover pelagic sediments for high-resolution stratigraphy and for reconstruction of the paleoceanography of this sector of the Pacific; (2) to relate the acoustic stratigraphy of the pelagic cap to its depositional and diagenetic history and correlate reflectors with those seen in other settings; (3) to date the interface between the pelagic cap and the underlying platform, and to infer the age and cause of platform drowning; (4) to establish the characteristics of the shallow-water facies and changes with time; (5) to compare the stratigraphy and facies of Lo-En Guyot with its living sibling Anewetak; and (6) to establish the age of the basement.

Drilling at Site 872, in the central portion of Lo-En Guyot, did not recover a carbonate platform; therefore, the carbonate platform objectives cannot be addressed directly. Cores from the pelagic cap, as well as the igneous edifice, were recovered, but the anticipated carbonate platform was absent. The remainder of the primary objectives can be addressed with the preliminary shipboard studies and additional shore-based studies.

OPERATIONS

Site 871 to Site 872

The ship track to the second drill site led to the northwest between Jaluit and Ailinglapalap atolls, then passed south of Ujae Atoll, in the Republic of the Marshall Islands. An average transit speed of 11.8 kt was maintained. A 200-in.³ water gun was streamed, and the approach survey began about 10 nmi southeast of proposed Site Pel-3. The seismic line was shot along a south-east-northwest transect over only the southern portion of Lo-En Guyot; a sonobuoy experiment was simultaneously conducted during the seismic profiling. When proposed Site Pel-3 was crossed, the profile continued about 6 nmi before the ship reversed course and recrossed the site. A positioning beacon was dropped at 1352L (L = local time) on 2 June 1992 to begin operations at Site 872. The total distance traveled, including surveys, was 644 nmi.

Site 872 (Pel-3)—Lo-En Guyot

Site 872 (proposed Site Pel-3) is centrally located on Lo-En Guyot, a sibling guyot adjacent to Anewetak Atoll and on the same volcanic pedestal. The setting, geology, and operational plan were virtually identical to those of Site 871, except that the limestone section was expected to be older and better indurated. The site location was chosen to obtain the maximum thickness of the pelagic cap on top of the guyot.

Hole 872A

The seismic gear was recovered following the beacon launch; the vessel took station on the beacon and the pipe trip began. The trip was faster than at Hole 871A because of the shallower water depth and because it was not necessary to drift and measure the drill string. A "geoset" drag-type outer bit was used with the APC/XCB bottom-hole assembly (BHA), primarily to provide smoother drilling and greater compatibility with the XCB shoe in the limestone section. Special subs were added to the BHA to provide the option of using the motor-driven core barrel (MDCB) to core limestone at the bottom of the planned APC/XCB holes. Again, a "pig" was pumped through the drill string to dislodge any loose rust before APC operations began.

The initial spud attempt was at 1730L on 2 June 1992, but the APC assembly apparently did not seat at the landing sub because pressure did not build up with pump circulation. The APC was recovered, inspected, and found to be still pinned together. It was run back to the BHA and landed about 15 m too high. The pig had only traveled down the drill string to the MDCB latch sub, where it became lodged when circulation could bypass it through the slots in the inner wall of the sub. The pig eventually was dislodged through vigorous "spudding" with the APC and using high pump circulation rates with the wireline blowout preventer (BOP) closed. A successful spud was accomplished at 1800L. The recovery of a mud-line core indicated a seafloor depth of 1094.5 m below the dual-elevator stool (DES) or 1083.6 m below sea level.

Further delays were experienced as coring continued. A shear-pin stub jammed the APC after Core 144-872A-2H; it was disassembled and rescoped. Core 144-872A-3H had no recovery because the core-catcher flapper had stuck open. After Core 144-872A-8H, a fuse blew on the coring winch control and an additional half hour of downtime ensued. As soon as mechanical problems abated, hole trouble began. Below about 70 mbsf, soupy foraminifer ooze flowed into the hole and accumulated around and above the BHA. The drill string became stuck while Core 144-872A-11H was being retrieved from 100 mbsf and an over-pull of 130,000 lb was required to free it.

Cores 144-872A-5H to -12H were magnetically oriented; heat-flow data were collected during recovery of Cores 144-872A-4H, -7H, and -10H using the Adara shoe. The orientation and heat-flow programs had to be discontinued because of adverse hole conditions. Coring continued with the liberal use of mud flushes, and the hole seemed to stabilize below 120 mbsf. Incomplete strokes of the core barrel on Cores 144-872A-11H and -12H appear to coincide with a reflector on the 3.5-kHz echo sounder record, but no hard strata were noted in the cores or by drilling parameters. Full stroke then was regained until Core 144-872A-17H (to 143.7 mbsf), when the core barrel struck middle Eocene phosphatized foraminifer limestone that contained fragments of basalt and a reworked, phosphatized Santonian pebbly conglomerate.

Coring then switched to the XCB mode. Core 144-872A-18X encountered hard drilling with an extremely low rate of penetration (ROP). The core barrel was pulled after only 30 cm of penetration; it contained 24 cm of basalt core.

Plans to attempt MDCB cores of limestone were abandoned because of the unexpected occurrence of basalt. A second APC hole was postponed until another method of handling the highly fluid sediment cores could be initiated. Operational plans were confused further because we had intended to protect a deep RCB penetration against the unstable pelagic section by emplacing a drill-in casing (DIC) string through the soft upper sediments. Not knowing whether more sediments existed below the basalt unit, we decided to take a maximum positioning offset from Hole 872A and drill at least 50 m into hard rock. If only basalt was encountered, the site would be abandoned. If more sediments were found, the hole would continue toward the original objectives and hole conditions would be dealt with as conditions dictated.

Hole 872B

During the round trip of the drill string, the vessel was offset to a point 75 m southeast of the beacon (and 150 m southeast of Hole 872A). A backup beacon was launched at the new location while the pipe trip was in progress. Hole 872B was spudded at 1900L on 3 June 1992 and washed to 77 mbsf. Coring with the RCB began at 77 mbsf in an attempt to recover ooze associated with the approximate sub-bottom depth of the seismic reflector

and also the interval not recovered by the APC in Hole 872A. After three successive cores, to 106 mbsf, only a few lumps of firm foraminifer ooze were recovered and hole problems returned. The hole was drilled ahead from 106 to 135 mbsf, the "wash barrel" was recovered, and continuous coring began.

Fragments of a hardground, as well as a phosphatized limestone conglomerate in contact with the underlying basalt, were recovered from Hole 872B at 135.4 mbsf. The basalt was quite hard and dense; coring ROP averaged only about 3 m/hr. Hole conditions stabilized by the time hard-rock coring began, and operations proceeded smoothly with an average ROP of about 2.8 m/hr and a core recovery rate of over 50% (Table 1).

The drill string unexpectedly became stuck just after the core barrel for Core 144-872B-9R was dropped, apparently the result of loose rocks in the hole beside the BHA. The bit was about 13 m above total depth, so circulation continued at a slightly elevated pressure; however, the pipe could not be rotated or moved vertically. After several minutes of "working" the pipe to free it (as much as 150,000 lb up and 60,000 lb down), multiple attempts were made to jar the BHA loose with the drilling jars. Unfortu-

nately, the jars could not be cocked for either up or down blows by introducing left-hand torque. After left-hand torque had been put into the string several times, about 14,000 ft-lb was applied and the pipe suddenly spun to the left and came free in the hole. The weight indicator showed a loss of about 34,000 lb, indicating that a BHA connection had backed off! The free upper portion of the drill string was kept just above the backed-off connection while the motion compensator was activated; the string was lowered carefully with slow rotation and moderate circulation. An abrupt rise in circulating pressure, followed by weight and torque indications, showed that the connection reengaged successfully. When only moderate right-hand torque was applied, the stuck BHA suddenly broke free and normal parameters were regained.

Only one core remained to fulfill the drilling objectives of the hole; the operation was completed with the undertorqued connection. A mud flush was circulated and the final core was cut and recovered without incident.

The contact of the pelagic cap with the hardground, the contact of the conglomerate with the basalt, and the presence or absence of sediments in the basalt, were of particular scientific interest so preparations were made to log the hole. A wiper trip was made to prepare the hole for logging. The condition of the hole was found to be less favorable than anticipated; the string encountered about 30,000 lb drag as it was lowered from 90 mbsf to the basalt contact at 145 mbsf. Considerable difficulty was experienced in working the bit past a ledge at the contact, but the hole eventually was cleaned out to total depth. Another viscous mud flush then was circulated and the bit was released with the rotary shifting tool (RST). The end of the drill string was pulled to just below the basalt contact for logging, with the intention of raising the string past the contact as the logging tool approached from below.

Logging proved to be unsuccessful because both geochemical tools on board the ship would not calibrate properly during in-pipe checks. When the second backup tool also failed to calibrate in the pipe, an attempt was made to record a log anyway. Only 4 m beneath the pipe, the tool encountered a bridge that had formed during the elapsed 4 hr from the wiper trip. The prospects of obtaining any logging results did not justify additional logging time. The logging tools were recovered and rigged down.

The drill string was recovered; the BHA was changed to the APC/XCB configuration. All BHA connections were checked for torque, and the connection between the body and the lower sub of the drilling jar was identified as the back-off culprit.

Hole 872C

On 5 June 1992, the first APC core found the seafloor at 1093 m from driller's datum. The soft pelagic section was cored in an effort to duplicate Hole 872A and fill in unrecovered gaps in the section. To salvage Site 872 for the high-resolution stratigraphy objective, we implemented a different method of handling cores upon arrival on the rig floor.

Excess water at the top of a core was removed with a device (named a "piglet") that was inserted into the core liner while the core was upright within the core barrel on the rig floor. The surficial water flowed through the central portion of the piglet until the piglet contacted the upper surface of the sediment. The core barrel was then placed horizontally for removal of the core liner and draining of excess water. The piglet inside the core liner prevented the sediment from sloshing during the removal of the liner from the horizontally placed core barrel and during the transport of the core to the catwalk for subsequent labeling and cutting into sections. After the core was cut into sections, each section was turned upright to permit additional excess water to rise to the top for removal, and the resulting void was removed by trimming the core liner to prevent the resuspension and disturbance of the sediment. In this manner, we were able to achieve

Table 1. Coring summary, Site 872.

| Core no. | Date (June 1992) | Time (Z) | Depth (mbsf) | Cored (m) | Recovered (m) | Recovery (%) |
|------------------|------------------------|-------------|-----------------|--------------|------------------|-----------------|
| 144-872A- | | | | | | |
| 1H | 2 | 0715 | 0-7.5 | 7.5 | 7.69 | 102.0 |
| 2H | 2 | 0750 | 7.5-17.0 | 9.5 | 8.57 | 90.2 |
| 3H | 2 | 0845 | 17.0-26.5 | 9.5 | 0.00 | 0.0 |
| 4H | 2 | 0940 | 26.5-36.0 | 9.5 | 7.68 | 80.8 |
| 5H | 2 | 1005 | 36.0-45.5 | 9.5 | 8.16 | 85.9 |
| 6H | 2 | 1035 | 45.5-55.0 | 9.5 | 8.76 | 92.2 |
| 7H | 2 | 1135 | 55.0-64.5 | 9.5 | 8.72 | 91.8 |
| 8H | 2 | 1210 | 64.5-74.0 | 9.5 | 9.41 | 99.0 |
| 9H | 2 | 1340 | 74.0-83.5 | 9.5 | 9.21 | 96.9 |
| 10H | 2 | 1435 | 83.5-93.0 | 9.5 | 9.05 | 95.2 |
| 11H | 2 | 1510 | 93.0-100.0 | 7.0 | 7.24 | 103.0 |
| 12H | 2 | 1650 | 100.0-102.0 | 2.0 | 0.00 | 0.0 |
| 13H | 2 | 1745 | 102.0-111.5 | 9.5 | 8.51 | 89.6 |
| 14H | 2 | 1810 | 111.5-121.0 | 9.5 | 8.21 | 86.4 |
| 15H | 2 | 1845 | 121.0-130.5 | 9.5 | 8.79 | 92.5 |
| 16H | 2 | 1920 | 130.5-140.0 | 9.5 | 9.00 | 94.7 |
| 17H | 2 | 2010 | 140.0-143.7 | 3.7 | 4.39 | 118.0 |
| 18X | 2 | 2305 | 143.7-144.0 | 0.3 | 0.24 | 80.0 |
| Coring totals | | | | 144.0 | 123.63 | 85.9 |
| 144-872B- | | | | | | |
| 1R | 3 | 0800 | 77.3-87.0 | 9.7 | 0.08 | 0.8 |
| 2R | 3 | 0845 | 87.0-96.6 | 9.6 | 0.05 | 0.5 |
| 3R | 3 | 0930 | 96.6-106.3 | 9.7 | 0.05 | 0.5 |
| 4R | 3 | 1225 | 135.2-144.8 | 9.6 | 0.74 | 7.7 |
| 5R | 3 | 1635 | 144.8-154.5 | 9.7 | 4.37 | 45.0 |
| 6R | 3 | 2020 | 154.5-164.0 | 9.5 | 0.87 | 9.2 |
| 7R | 3 | 2315 | 164.0-173.1 | 9.1 | 8.07 | 88.7 |
| 8R | 4 | 0455 | 173.1-182.6 | 9.5 | 4.50 | 47.3 |
| 9R | 4 | 0945 | 182.6-192.5 | 9.9 | 7.23 | 73.0 |
| Coring totals | | | | 86.3 | 25.96 | 30.1 |
| 144-872C- | | | | | | |
| 1H | 5 | 0355 | 0.0-9.0 | 9.0 | 8.84 | 98.2 |
| 2H | 5 | 0415 | 9.0-18.5 | 9.5 | 9.29 | 97.8 |
| 3H | 5 | 0445 | 18.5-28.0 | 9.5 | 9.81 | 103.0 |
| 4H | 5 | 0505 | 28.0-37.5 | 9.5 | 9.14 | 96.2 |
| 5H | 5 | 0530 | 37.5-47.0 | 9.5 | 8.73 | 91.9 |
| 6H | 5 | 0600 | 47.0-56.5 | 9.5 | 8.99 | 94.6 |
| 7H | 5 | 0630 | 56.5-66.0 | 9.5 | 9.07 | 95.5 |
| 8H | 5 | 0705 | 66.0-75.5 | 9.5 | 9.42 | 99.1 |
| 9H | 5 | 0755 | 75.5-85.0 | 9.5 | 9.44 | 99.3 |
| 10H | 5 | 0830 | 85.0-94.5 | 9.5 | 9.76 | 103.0 |
| 11H | 5 | 0905 | 94.5-104.0 | 9.5 | 8.75 | 92.1 |
| 12H | 5 | 0940 | 104.0-106.0 | 2.0 | 3.08 | 154.0 |
| 13H | 5 | 1020 | 106.0-115.5 | 9.5 | 9.49 | 99.9 |
| 14H | 5 | 1105 | 115.5-125.0 | 9.5 | 9.50 | 100.0 |
| 15H | 5 | 1135 | 125.0-130.0 | 5.0 | 7.82 | 156.0 |
| 16H | 5 | 1210 | 130.0-139.5 | 9.5 | 9.15 | 96.3 |
| 17X | 5 | 1450 | 139.5-146.0 | 6.5 | 3.73 | 57.4 |
| 18X | 5 | 1700 | 146.0-148.0 | 2.0 | 1.71 | 85.5 |
| Coring totals | | | | 148.0 | 145.72 | 98.5 |

recovery of cores in which details of mottling, sharp changes in color and lithology, and sedimentary structures could be observed.

Magnetic orientation was attempted for all APC cores starting with Core 144-872C-4H. An incomplete stroke was indicated on Core 144-872C-12H from 104 mbsf, but full stroke was regained on Cores 144-872C-13H and -14H. Cores 144-872C-15H and -16H had incomplete stroke in upper Oligocene foraminifer ooze.

The XCB system was used to core from 139.5 mbsf. A hard contact was encountered in Core 144-872C-17X, where upper Oligocene foraminifer ooze was found to overlie clay and basalt; the contact was noted by changes in the drilling parameters at 142.5 mbsf.⁴ Core 144-872C-17X became jammed immediately upon encountering the harder material. The ROP through the unrecovered 4.5 m seemed high for the XCB in basalt; an additional core was attempted in an effort to recover more transitional material from the contact zone. A higher circulation rate was used for Core 144-872C-18X, which penetrated 2 m in 1 hr. The core barrel recovered 1.71 m of nicely trimmed core of altered basalt.

As sedimentary strata were not located within the 50 m drilled beneath the basalt contact, the achievable objectives of the site were considered fulfilled and the drill string and beacons were recovered. *JOIDES Resolution* departed the site at 0800L on 6 June 1992.

UNDERWAY AND SITE GEOPHYSICS

Introduction

West of the Ralik Chain, over a 1000 km northwest of Limalok Guyot, a cluster of volcanoes marks the westernmost extent of the southern Marshall Islands (Fig. 1). This volcanic cluster consists of two atolls flanked by a number of guyots. Ujlan Atoll lies on the western edge of the cluster, Anewetak Atoll (formerly Eniwetok Atoll) marks the northern perimeter, and Lo-En Guyot forms the eastern edge.

Information on the reefs and volcanoes within this cluster comes primarily from drilling on Anewetak Atoll during Operation Crossroads in the late 1940s. Two holes drilled on Anewetak during Operation Crossroads reached volcanic basement. Hole F-1, located on Elugelab Island in the northwest, struck volcanic basement at 1405 m; Hole E-1, located on Parry Island in the southeast, encountered basalt cuttings at 1267 m and solid basalt at 1282 m (Schlanger, 1963). Shallow-water carbonate sediments of Eocene age lie directly over the basalt. Seismic refraction studies at Anewetak (Raitt, 1957) showed that the upper surface of the atoll's volcanic foundation slopes gently to the northwest, and that basement was shallower beneath Anewetak Atoll and Parry Island than beneath Elugelab Island. The basalt, originally dated by K/Ar methods as being in the range of 51.4 to 61.4 Ma, has subsequently been dated by ⁴⁰Ar/³⁹Ar methods to obtain a total fusion age of ~77 Ma (M.S. Pringle, unpubl. data).

Lo-En Guyot, centered about 10°10'N and 163°52'E, lies ~150 km south-southeast of Anewetak Atoll. Before the site survey work conducted in 1988, little was known about the detailed morphology of Lo-En Guyot. A ridge extending from the south flank of Anewetak Atoll connects the edifice with that of Lo-En Guyot. In plan-view, Lo-En's edifice resembles a square with a maximum width slightly >50 km. A small seamount lies north of this edifice, straddling the ridge between Lo-En Guyot and Anewetak Atoll. Two more small seamounts with diameters <14 km lie west-southwest of Lo-En Guyot.

Site Survey—*Moana Wave* Cruises MW8805 and MW9009

As mentioned above, little was known about Lo-En Guyot before the site survey work of *Moana Wave* Cruises MW8805 and MW9009. Cruise MW8805 conducted the original site survey of this guyot, collecting a suite of geophysical data that included SeaMARC II side-scan sonar images and swath-map bathymetry, digital single-channel seismic data, 3.5-kHz echo-sounder bathymetry, and gravity and magnetics measurements. In addition to the geophysical data, basalt and limestone were recovered in three dredges from various depths along the flanks of Lo-En Guyot. Cruise MW9009 returned to Lo-En Guyot to collect six-channel seismic data over the summit and to dredge a cone-shaped feature identified in the Cruise MW8805 data.

Lincoln et al. (in press), as part of a regional overview on the mid-Cretaceous and Late Cretaceous volcanic and tectonic history of the Marshall Islands, cite the contents of Cruise MW8805 rock dredge (RD) 33 as evidence for the existence of a shallow-water carbonate bank on top of Lo-En Guyot during the mid-Cretaceous. Sample RD33, taken from the southwest flank of Lo-En at ~2400 m depth, contained breccia consisting of angular fragments of vesicular basalt floating in a calcareous matrix of shallow-water debris and planktonic foraminifers. The planktonic foraminifers suggest a middle to late Albian age for these rocks. Two other dredges across this guyot (RD34 and RD35) sampled shallower portions of the slope. Samples RD34 and RD35 recovered rocks of similar lithology from depths of ~1900 and ~1775 m, respectively. These rocks consisted of rounded basalt cobbles and basalt pebbles in a matrix containing planktonic foraminifers of Paleogene age. Although no direct evidence existed in the Cruise MW8805 data for Late Cretaceous volcanism or reef growth on Lo-En Guyot, Lincoln et al. (in press) postulated that uplift and subaerial exposure of this edifice was likely around the time of volcanic activity on Anewetak Atoll (~77 Ma).

SeaMARC II bathymetry over Lo-En shows the gross morphology of the edifice (Fig. 2). The summit approaches a maximum diameter of ~40 km in a north-south direction. In general, the 1400-m contour marks the first break in slope down from the summit. In the side-scan images, a high-backscatter band marks the edge of the summit (Fig. 3). The flanks of the guyot maintain a fairly uniform gradient of 15°, except in areas where shelves extend away from the summit. These shelves are most prominent along the north and south flanks of the guyot, and they commonly have slopes of <6° across their tops (Fig. 2). The southern shelf is ~6 km wide, whereas the northern shelf merges with the ridge connecting Lo-En Guyot and Anewetak Atoll. Along the west flank of Lo-En Guyot, low-backscatter terraces ~0.5 km wide lie downslope from the summit edge (Fig. 3).

A thick layer of pelagic sediments covers the central portion of Lo-En's summit (Fig. 4). Cropping out from these pelagic sediments are a number of high-backscatter cones and lobes (Fig. 3). These features are especially prominent across the southern shelf. It is impossible to determine the origin of the cones (either igneous or sedimentary) from the side-scan and bathymetric data alone. During Cruise MW8805, the ship fortuitously crossed one of the summit cones (Figs. 3–4). This particular cone exhibited a high magnetic signature, which suggests a volcanic origin. Attempts to sample this feature during Cruise MW9009 were unsuccessful.

Two profiles representative of the single-channel seismic data collected during Cruise MW8805 are shown in Figure 4. Profile A–A' crosses the summit in a north-south direction. Along this profile the presumed volcanic cone crops out from the pelagic sediments. Profile B–B' is an east-west crossing of the summit that was used to pick the location of proposed Site Pel-3. The

⁴ See Footnote 3.

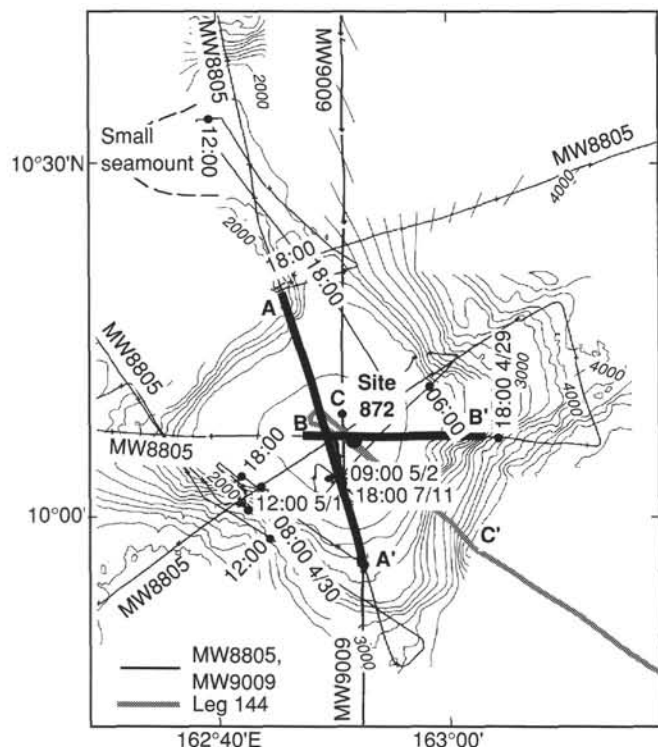


Figure 2. Contoured SeaMARC II bathymetry of Lo-En Guyot. Contour interval is 200 m. The ship tracks shown in this figure represent the seismic coverage across this guyot. Profiles A-A' and B-B' were collected during a 1988 *Moana Wave* cruise (MW8805), and Profile C-C' was collected during Leg 144.

reflectors annotated in this profile mark the boundaries of the presumed sedimentary units overlying the volcanic basement. The interpretation of this profile (at Pel-3) placed a sequence of pelagic sediments 0.18 s two-way traveltime (TWT) over a relatively thin (<0.2 s) carbonate platform. The primary focus of drilling on Lo-En Guyot was the sampling of this thick sequence of pelagic sediments and the associated internal reflectors. Unfortunately, Figure 4 does not clearly show the individual reflector packets within the pelagic sequence. Beneath the pelagic sequence, a carbonate platform 0.14 s TWT thick presumably overlies volcanic basement, and the "deep reflector" annotated in Figure 4 represents some sort of structure within the volcanic complex.

Site Survey—Leg 144

Magnetics data in addition to 3.5- and 12-kHz echo-sounder bathymetric data were collected during the transit from Site 871 to Lo-En Guyot. The site survey over Lo-En Guyot consisted of a northwest-oriented line intersecting the Cruise MW8805 single-channel line at the location of Site Pel-3 (Fig. 2). We deployed the seismic gear at 2230Z on Julian Day (JD) 153, with a ship's heading of 305° and a ship speed of ~6 kt. We initially used a 200-in.³ water gun as a source, but the gun began to malfunction around 2245Z and was recovered shortly thereafter. An 80-in.³ water gun was deployed in its place. A quick repair of the 200-in.³ gun allowed us to deploy it again near the edge of the summit, at 2340Z. Upon cresting the summit edge, we launched a sonobuoy at 2357Z and received a strong signal and some possible refractions for ~1 hr. Site Pel-3 was crossed on JD 154 at 0059Z, and we turned shortly after to a heading of ~115°. The beacon marking

Site 872 was dropped on the return line at 0252Z. By 0300Z the seismic gear was recovered, and by 0315Z the ship was on station.

The purpose of running the survey line across the southeast slope of Lo-En Guyot was to collect data along its flank over which no previous coverage existed. Both echo-sounder and seismic profiles show a topographic high along the perimeter of the summit (Figs. 5–6). The height of this feature above the first slope break is 98 m. Behind this perimeter high, and beneath the accumulated pelagic sediments, the topography remains hummocky for ~1.5 km. The pelagic sediments thicken toward the center of the summit, reaching a maximum thickness of 0.18 s TWT at the location of Site 872. A packet of strong reflectors 0.04 s TWT thick forms the uppermost sequence of these pelagic sediments. Deeper within the section, two reflectors spaced ~0.02 s TWT apart appear to shallow toward the margin of the summit in relation to the relatively flat platform reflector. The platform reflector itself exhibits relief of <0.01 s TWT, except directly behind the perimeter high. The seismic data collected during Leg 144 does not show much structure beneath the pelagic-platform interface (Fig. 6).

LITHOSTRATIGRAPHY

Drilling results from the three holes on Lo-En Guyot are summarized in a single lithostratigraphic framework (Fig. 7 and Table 2). Lithologic units are identified by color, carbonate and clay content, fossil and particle constituents, lithification, and sedimentary structures. Four major units were recognized (Fig. 7): Unit I, nannofossil and foraminifer oozes; Unit II, fragments of an iron manganese crust, phosphatized chalk that contains pebbles of the underlying unit, phosphatized volcanoclastic sandstone, and pieces of phosphatized conglomerate consisting of volcanoclastic pebbles in planktonic foraminifer limestone matrix; Unit III, subangular basalt clasts within a planktonic foraminifer limestone; and Unit IV, basalt. In Hole 872B, crevasses and fractures in the upper flows of the basalt are infiltrated by planktonic foraminifer limestone from the overlying unit; in Hole 872C, a thin clay layer encloses a few basalt clasts (Interval 144-872C-17X-CC, 28–38 cm).

Unit I

Intervals: Hole 872A, Core 144-872A-1H through Section 144-872A-17H-3; Hole 872B, Core 144-872B-1R through to -3R; Hole 872C, Core 144-872C-1H through Section 144-872C-17X-CC, 20 cm
 Depth: Hole 872A, 0–143.6 mbsf; Hole 872B, 77.3–106.3 mbsf; Hole 872C, 0–141.7 mbsf
 Age: Hole 872A, Pleistocene to late Oligocene; Hole 872B, middle to early Miocene; and Hole 872C, Pleistocene to late Oligocene

Unit I consists of white (10YR 8/2) to pale brown (10YR 7/3) nannofossil foraminifer ooze intercalated with foraminifer ooze, which grades downhole into foraminifer ooze. A small amount of terrigenous clay is dispersed within the ooze. The calcium carbonate content averages 96.9% (see "Organic Geochemistry" section, this chapter). Unit I is divided into two subunits based on a downhole decrease in nannofossil abundance, a corresponding coarsening of the sediment texture, and a minor change in color.

Subunit IA

Intervals: Hole 872A, Core 144-872A-1H to Section 144-872A-4H-3, 72 cm; Hole 872C, Core 144-872C-1H to Section 144-872C-4H-3
 Depth: Hole 872A, 0–30.2 mbsf; Hole 872C, 0–32.9 mbsf
 Age: Holes 872A and 872C, Pleistocene to late Miocene

Subunit IA consists mainly of white (10YR 8/2) foraminifer ooze, which is interbedded with subordinate, very pale brown (10YR 8/3) nannofossil foraminifer ooze in vague layers and bands several centimeters to tens of centimeters thick. In Hole 872C, several beds of foraminifer ooze 5 to 22 cm thick are

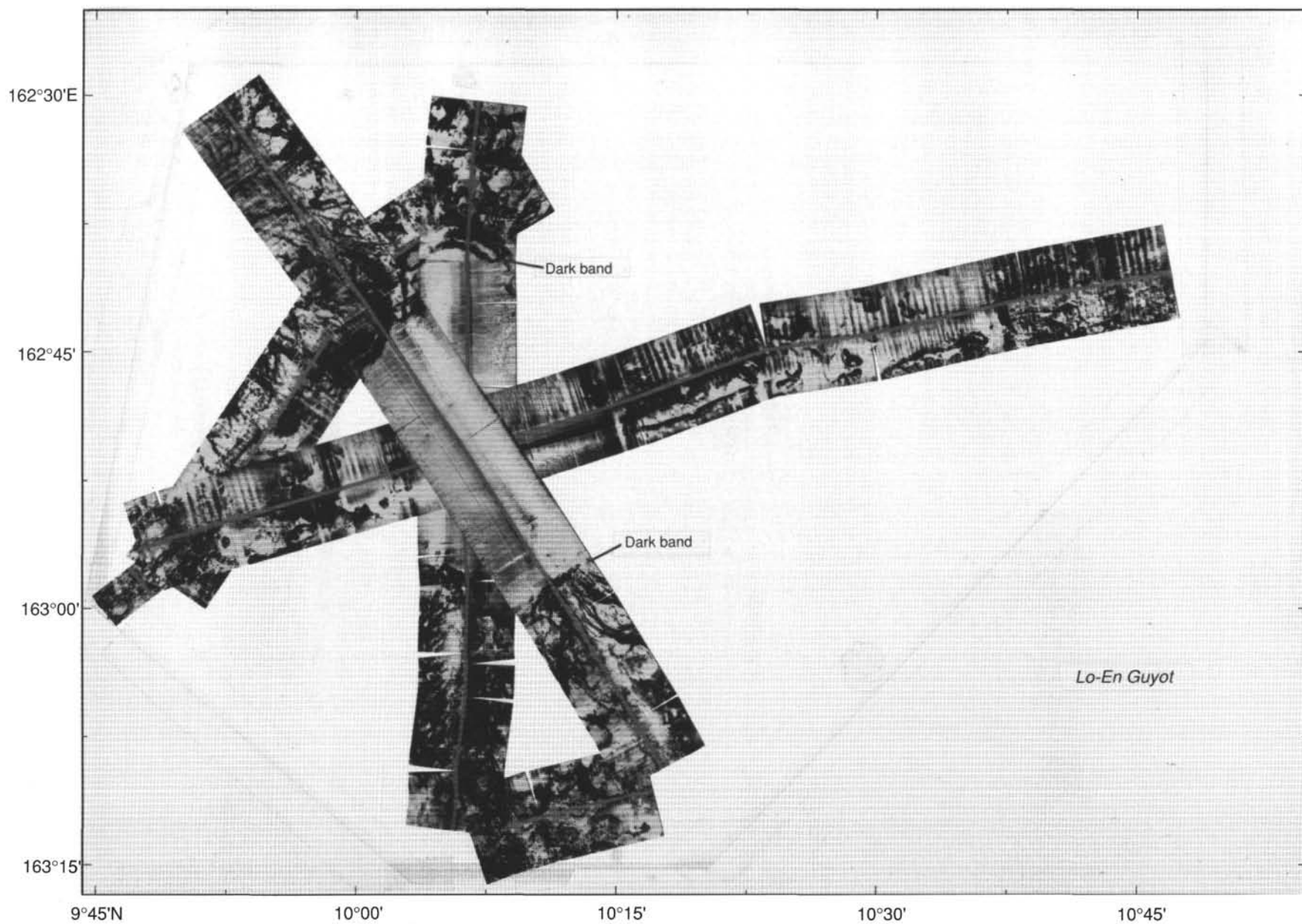


Figure 3. Side-scan images over Lo-En Guyot. In this image, dark tones represent high backscatter features, and light-gray to white tones represent low backscatter features. The dark band represents the edge of the summit.

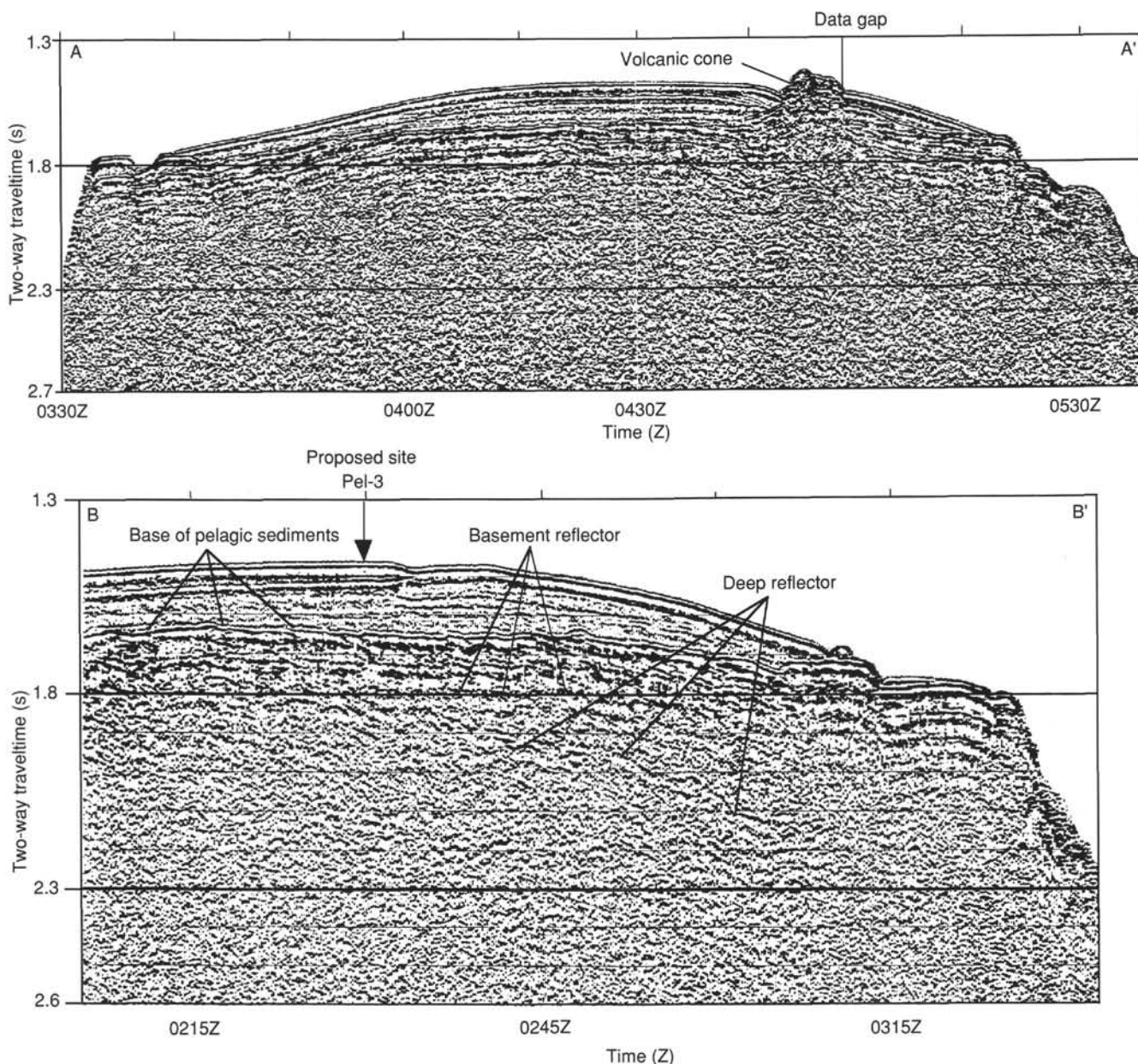


Figure 4. Single-channel seismic Profiles A-A' and B-B' collected during Cruise MW8805 across Lo-En Guyot. Profile A-A' shows the presumed volcanic cone that crops out from the pelagic sediments, whereas Profile B-B' is the seismic line from which Site 872 was selected. An arrow marks the location of the site directly above the thickest sequence of the pelagic sediments. The basement reflector marked on this profile represents the bottom of the presumed carbonate complex. The deep reflector suggests a change in the character of the basement.

intercalated within the nannofossil foraminifer ooze. The boundaries between beds are sharp. Locally, gray, circular spots, about 1 cm in diameter, are found in the ooze; they are probably burrows.

The ooze in Hole 872A is strongly disturbed by drilling and is soupy, which precludes recognition of any sedimentary structures. This problem was addressed by changes in core handling for Hole 872C; cores were stored vertically, then water was drained from the top of the core and from each core section and the resulting void was removed by trimming the core liner before the cores were split. This resulted in somewhat improved preservation of sedimentary structures in the upper cores; toward the lower part of the unit, however, no significant difference in

drilling disturbance was detected between the different core handling techniques.

At the top of Subunit IA (Cores 144-872A-1H and -2H and Cores 144-872C-1H and -2H), the ooze contains light yellowish brown (10YR 6/4) specks. The specks are either limonite or phosphatic stains on the tests of planktonic foraminifers. Pinkish gray (5YR 6/2) laminae that are 1 cm thick are present in Core 144-872A-2H-6.

Subunit IB

Intervals: Hole 872A, Sections 144-872A-4H-3, 72 cm, through -17H-3; Hole 872B, Cores 144-872B-1R to -3R; Hole 872C, Sections 144-872C-4H-4 to -17X-CC, 20 cm

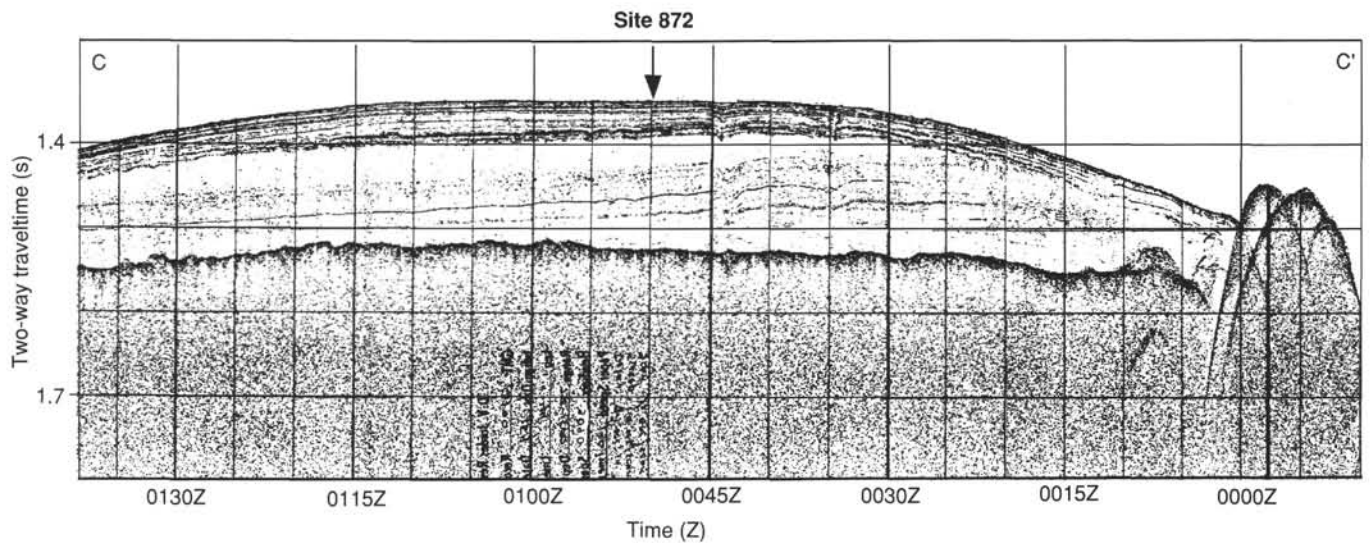


Figure 5. Profile C-C' of 3.5-kHz echo sounder collected during Leg 144 over Lo-En Guyot.

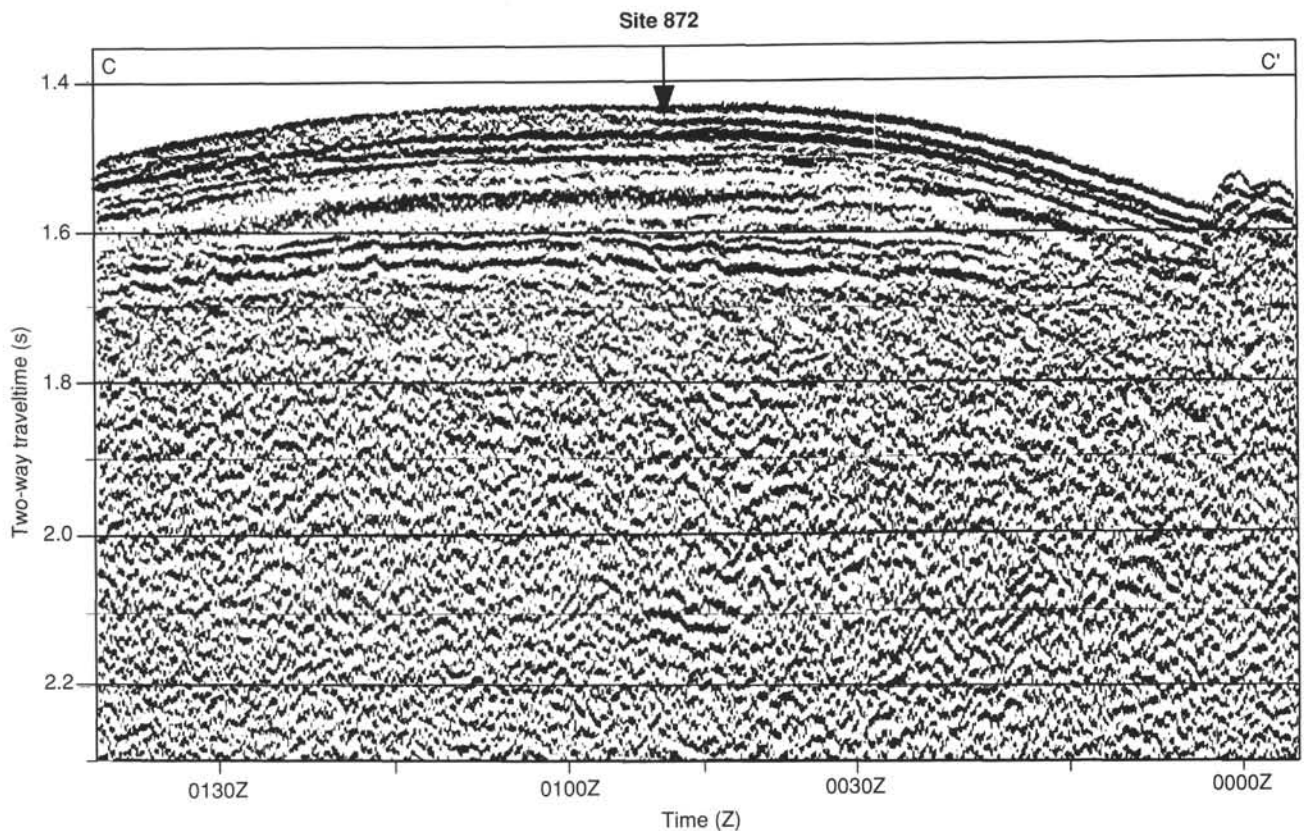


Figure 6. Single-channel seismic Profile C-C' collected during Leg 144 over Lo-En Guyot with the location of Site 872.

Depth: Hole 872A, 30.2–143.6 mbsf; Hole 872B, 77.3–106.3 mbsf;
 Hole 872C, 32.9–141.7 mbsf;
 Age: Hole 872A, late Miocene to late Oligocene; Hole 872B, middle
 to early Miocene; Hole 872C, late Miocene to late Oligocene

The boundary between Subunits IA and IB is placed at the disappearance downhole of color banding. Subunit IB consists of very pale brown (10YR 7/3), homogenous foraminifer ooze. The

ooze is soupy and is comprised of fine to medium sand-sized foraminifer tests. Nannofossils are a minor component in these sediments (<5%); clay minerals, zeolites, sponge spicules, and radiolarians occur as traces. Lumps of slightly consolidated ooze, up to 1 cm in diameter, were recovered from Core 144-872A-7H-6 to the base of Core 144-872A-11H, and in Cores 144-872C-8H to -11H. These lumps are friable and crumble easily. The occurrence of these lumps may indicate the initial stages of sediment consoli-

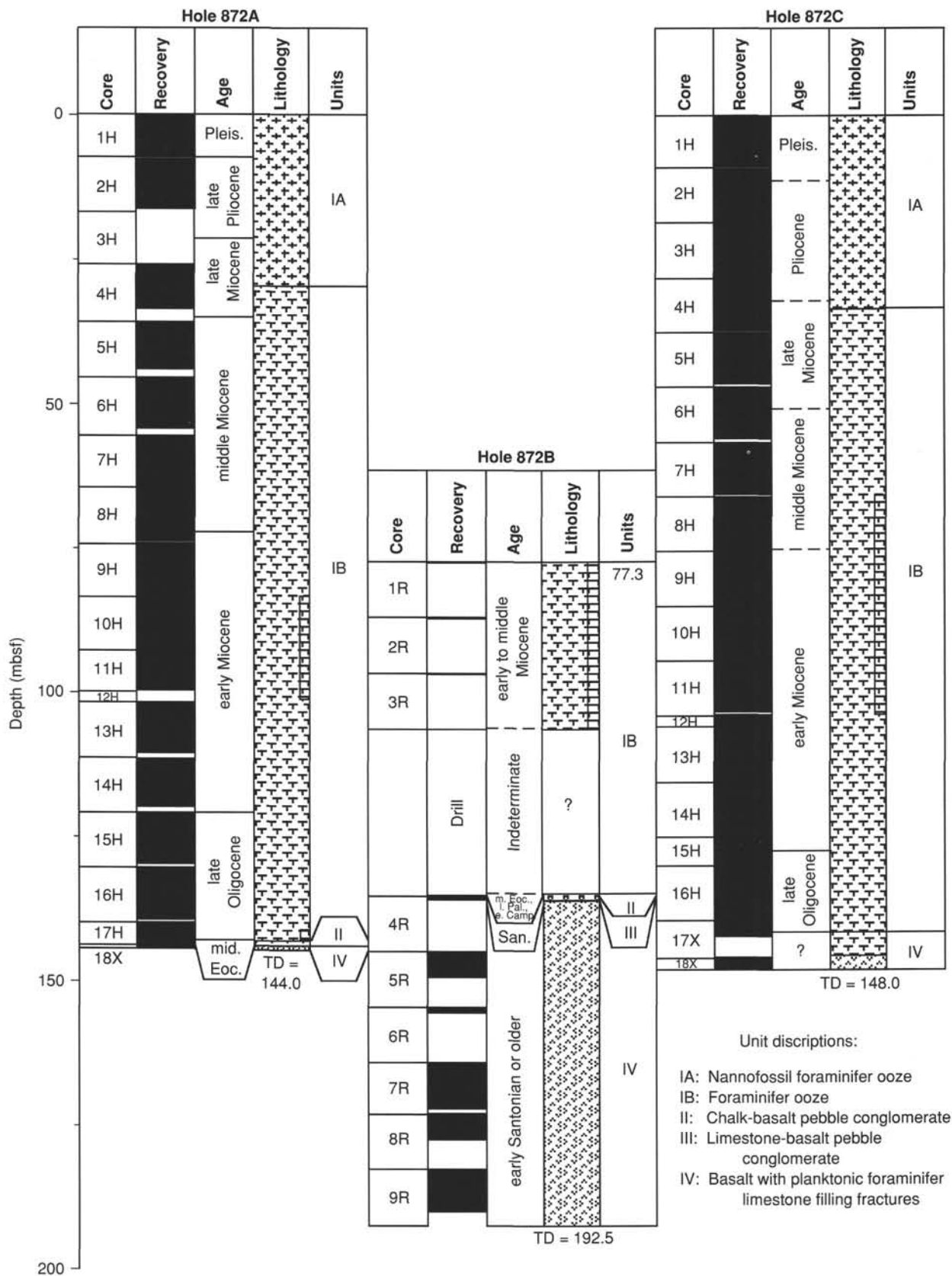


Figure 7. Lithostratigraphic summary of Site 872. TD = total depth.

Table 2. Summary of lithostratigraphic units, Site 872.

| Unit/ subunit | Core, section, interval (cm) | Depth (mbsf) | Age | Description |
|------------------|---------------------------------|-----------------|--------------------------------|--|
| IA | 144-872A-1H to -4H-3, 72 cm | 0.0–30.2 | Pleistocene to late Miocene | Intercalated nannofossil foraminifer and foraminifer ooze. |
| | 144-872C-1H to -4H-3 | 0.0–32.9 | | |
| IB | 144-872A-4H-3, 72 cm, to -17H | 30.2–143.6 | late Miocene to late Oligocene | Foraminifer ooze. |
| | 144-872B-1R to -3R | 77.3–106.3 | | |
| | 144-872C-4H-4 to -17X | 32.9–141.7 | | |
| IIA | 144-872A-17H-CC, 0–10 cm | 143.6–143.7 | middle Eocene | Phosphatized chalk that contains pebbles of the underlying unit. |
| IIB | 144-872B-4R-1, 0–10 cm | 135.2–135.30 | ? | Phosphatized volcaniclastic sandstone; age relationship with adjacent subunits uncertain. |
| IIC | 144-872B-4R-1, 10–16 cm | 135.30–135.36 | late Paleocene | Pieces of phosphatized conglomerate consisting of volcaniclastic pebbles in pelagic limestone of latest Santonian to early Campanian age. These conglomerate pieces are redeposited in pelagic sediment of late Paleocene age. |
| III | 144-872B-4R-1, 16–21 cm | 135.36–135.40 | late early Santonian | Subangular basalt clasts in a pelagic limestone matrix. |
| IV | 144-872A-18X | 143.7–144.0 | | |
| | 144-872B-4R-1, 21 cm, to -9R | 135.41–192.5 | early Santonian or older | Basalt with fractures filled by planktonic foraminifer limestone in upper 71 cm. |
| | 144-872C-17X-CC, 20 cm, to -18X | 141.7–148.0 | ? | Basalt. |

ation occurring from about 66 to 100 mbsf. The pelagic ooze found below Cores 144-872A-8H and 144-872C-8H is white (10YR 8/2). In Core 144-872A-12R, the ooze contains yellowish brown foraminifer tests possibly stained by iron (Fe) or manganese (Mn). Specks of very pale brown color (10YR 8/3) are abundant in Cores 144-872A-15H to -17H. They are most common in Section 144-872A-17H-3, which gives a “salt and pepper” appearance to the sediment. In Core 144-872A-17H, at the base of Subunit IB, the nannofossil content increases to 20%–65%. Minor phosphate impregnation within a thin bed of foraminifer ooze was noted in Interval 144-872C-17X-CC, 20–28 cm; it may delineate a brief period of slow deposition.

Unit II

Intervals: Hole 872A, Interval 144-872A-17H-CC; 0–10 cm; Hole 872B, Interval 144-872B-4R-1, 0–16 cm;
Depth: Hole 872A, 143.6–143.7 mbsf; Hole 872B, 135.2–135.4 mbsf
Age: Hole 872A, middle Eocene; Hole 872B, indeterminate

Unit II consists of numerous fragments of several different lithologies: phosphatized chalk and limestone, manganese crusts, volcaniclastic sandstones, and reworked pieces of Unit III. Unit II is divided into three subunits based on variations in lithology and its position in the recovered core. However, all pieces within Unit II are small enough (the largest is 4 cm) to have caved from the walls of the above hole or to have been displaced inside the core during drilling and recovery.

Subunit IIA

Intervals: Interval 144-872A-17H-CC, 0–10 cm
Depth: 143.6–143.7
Age: middle Eocene

Subunit IIA consists of chalk fragments, a fragment of phosphatic and manganiferous crust; loose basalt and volcaniclastic pebbles with shiny, polished surfaces; and fragments of basalt-pebble conglomerate with pelagic limestone matrix (late Santonian in age) that have been reworked from the underlying unit. Some of the smaller pebbles are cemented within the chalk, but most are loose. Some of the larger pebbles have chalk cemented to surfaces. We assume that the larger pebbles broke loose from the chalk as it disintegrated during drilling. The uppermost several millimeters of a 1-cm-thick fragment of phosphatic crust is laminated with Fe/Mn dendrites at the top. Below the phosphate laminae, the crust is a lithified, yellow foraminifer chalk with several small pebbles intercalated within the chalk. Near the surface of the crust are several cemented pebbles, a few millimeters in size, with soft foraminifer ooze trapped around them.

Another fragment of a yellowish chalk has a burrow infilled with soft foraminifer ooze and several pebbles up to 5 mm in size, including a fragment of volcanic glass (Fig. 8). The sediment in the burrow fill has been assigned an Oligocene age based on the identification of foraminifers, but the chalk has been assigned a middle Eocene age (see “Biostratigraphy” section, this chapter).

The loose pebbles that co-occur with chalk fragments in Section 144-872A-17H-CC are polished, somewhat rounded or flattened in shape, and dark brown to blackish in color. One of the pebbles is a fragment of a conglomerate that is about 2 cm across; it is rounded and coated by phosphate. This lithoclast is composed of two rounded pebbles of highly altered volcaniclastic sandstone and one pebble of vesicular basalt, all of which are cemented by phosphatized foraminifer limestone matrix (Fig. 9). Poorly pre-

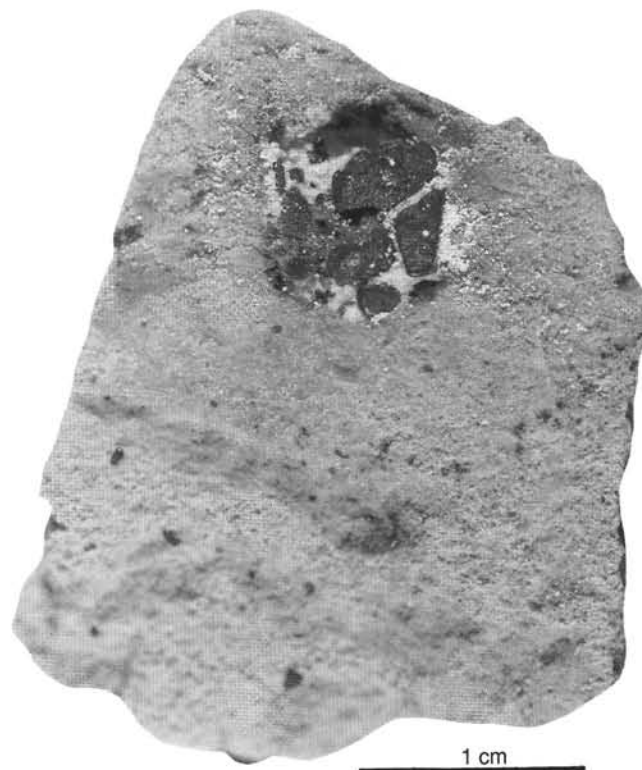


Figure 8. Close-up core photograph of a fragment of chalk from Subunit IIA, with a filled boring (Interval 144-872A-17H-CC, 0–5 cm).

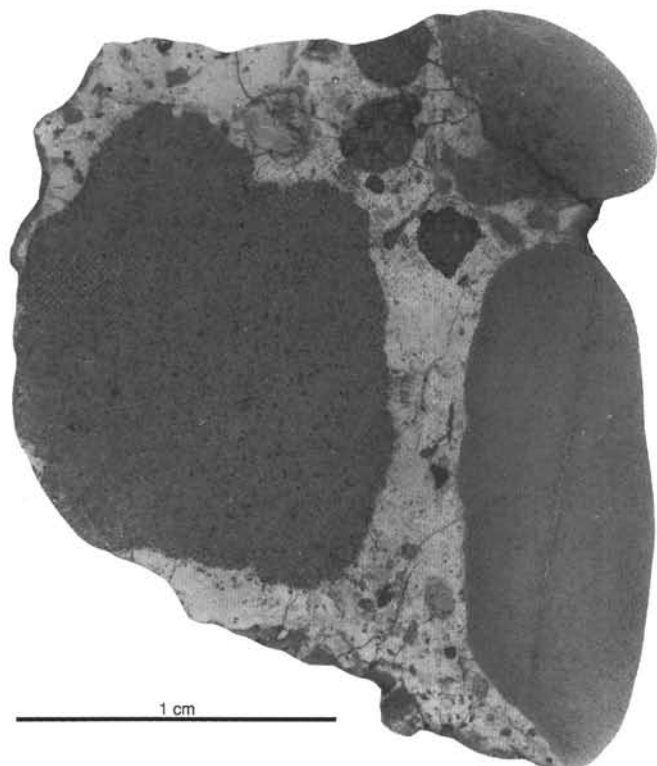


Figure 9. Close-up photograph of a thin section made from pebble conglomerate reworked from Unit III into Subunit IIA (from Interval 144-872A-17H-CC, 0–10 cm).

served tests of planktonic foraminifers occur in the matrix; they have been assigned a late Santonian age (see “Biostratigraphy” section, this chapter). This pebble is a reworked fragment of Unit III (see description below). These larger pebbles have middle Eocene foraminifer chalk cemented to some surfaces; we assume they were originally incorporated within the chalk and were later freed during the drilling process.

Subunit IIB

Interval: Interval 144-872B-4R-1, 0–10 cm
Depth: 135.2–135.3 mbsf
Age: indeterminate

Subunit IIB consists of several pieces of highly altered volcanoclastic sandstones that have oxidized, dark brown upper surfaces. The sandstone is composed of fine-grained, highly altered volcanic grains; one piece has trace amounts of very fine micritic carbonate grains. One clast in this unit has traces of carbonate cement on its surface. It is uncertain whether these volcanoclastic cobbles are part of a distinct volcanoclastic bed or are clasts broken from a friable chalky matrix. The position of this subunit relative to adjacent subunits is uncertain; the largest piece of Subunit IIB is only 4 cm long, and all pieces of adjacent subunits are smaller still. Any or all of these fragments could have caved from previously drilled intervals or could have been displaced in the core during drilling or recovery. The age of Subunit IIB is indeterminate.

Subunit IIC

Interval: Interval 144-872B-4R-1, 10–16 cm
Depth: 135.3–135.36 mbsf
Age: late Paleocene

Several pebbles of conglomerate and altered basalt, up to 2 cm in diameter and coated by a thin, phosphate film, comprise Subunit IIC. Several pebbles are brown in color, have a shiny surface, and are partially covered by a sandy carbonate cement, indicating that they were broken from their matrix during drilling (Fig. 10). At least one of these pebbles is a two-generation conglomerate (Fig. 10). Thin-section examination showed that small pebbles of basalt and highly altered carbonate rock were cemented by a foraminifer-rich packstone during early Campanian time. This matrix contains some volcanic glass shards. After lithification the rock was phosphatized and partly coated by iron manganese crust. The conglomerate was then fractured and the pieces reworked and cemented by a planktonic foraminifer limestone matrix of late Paleocene age. The late Paleocene matrix contains small volcanoclastic pebbles.

Unit III

Interval: Interval 144-872B-4R-1, 16–21 cm
Depth: 135.36–135.41 mbsf
Age: late Santonian

The phosphatic pebbles in Interval 144-872B-4R-1, 0–16 cm, are underlain by a limestone with basalt clasts (Fig. 11). The lower contact between the limestone and the basalt is irregular but sharp and welded. Clasts within the limestone are subangular and 0.5–5 cm in diameter; they have a basaltic composition. The basalt is finely crystalline, with trachytic texture and dark-rimmed feldspar laths. The clasts are probably derived from a basalt flow. One of the clasts is triangular in shape and oriented with the sharp edge downward, which may indicate that the clasts fell into the carbonate mud or were carried downslope in a gravity flow. It could also be interpreted that the carbonate layer is the fill of a wider fracture and not a continuous planktonic limestone conglomerate bed. The pelagic foraminifer limestone contains about 40% planktonic foraminifers, 1%–2% ostracodes, and traces of volcanic grains; these are surrounded by a clotted, micritic matrix. Noticeably absent are any benthic or shallow-water fossils in the limestone. The phosphatized pebble conglomerates with limestone matrix

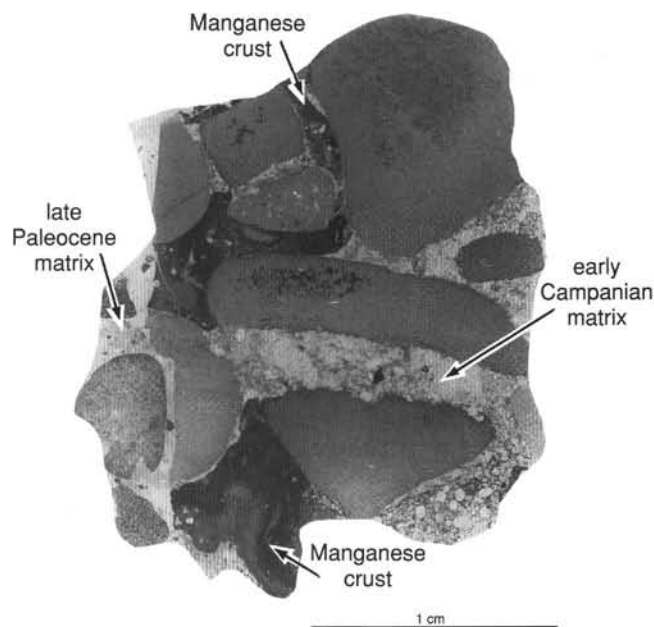


Figure 10. Close-up photograph of a thin section made from pebble conglomerate reworked from Unit III into Subunit IIC (from Interval 144-872B-4R-1, 13–16 cm).

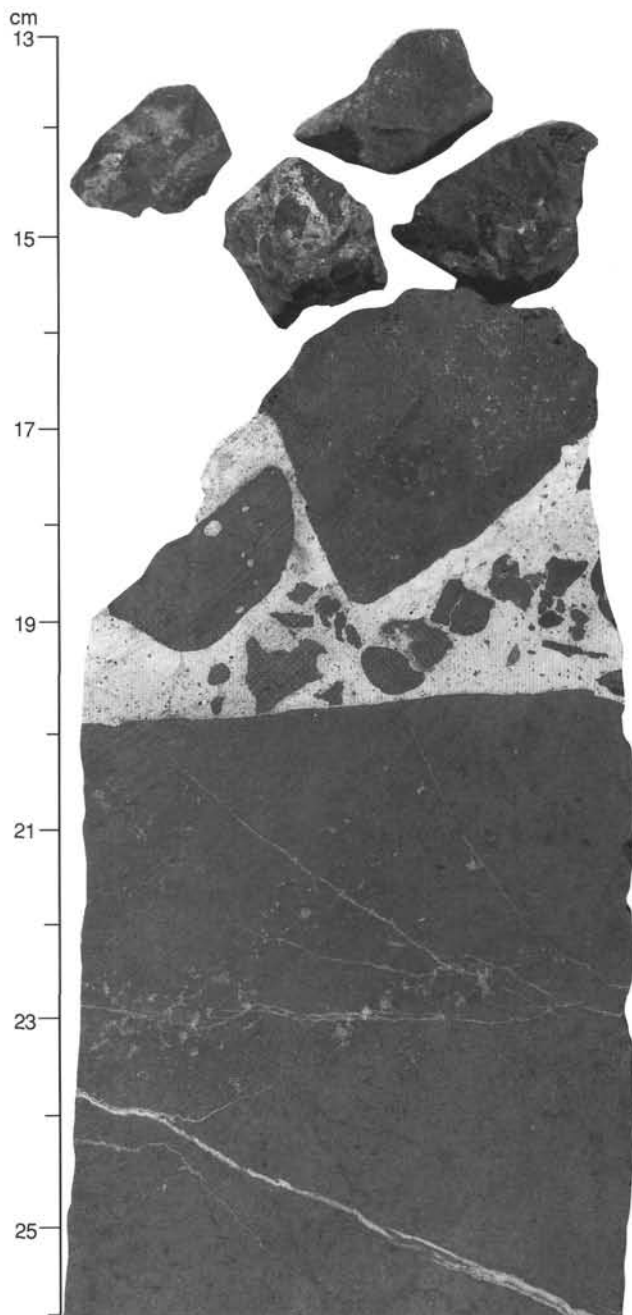


Figure 11. Close-up core photograph of pebbles in Subunit IIC and of the underlying pebbly limestone of Unit III (Interval 144-872B-4R-1, 13–26 cm). Note the sharp, welded boundary between the basalt and Unit III, and the angular shape of basalt clasts incorporated into it.

described from Subunits IIA and IIC are thought to be reworked from Unit III.

Unit IV

Interval: Hole 872A, Core 144-872A-18X; Hole 872B, Section 144-872B-4R-1, 21 cm, to Core 144-872B-9R; Hole 872C, Section 144-872C-17X-CC, 20 cm, through Core 144-872C-18X
 Depth: Hole 872A, 143.7–144.0 mbsf; Hole 872B, 135.4–192.5 mbsf; Hole 872C 141.7–148.0 mbsf
 Age: Hole 872A, indeterminate; Hole 872B, early Santonian or older; Hole 872C, indeterminate

Unit IV is composed of basalt. Detailed descriptions of these rocks are given in the “Igneous Petrography” section (this chapter). However, two aspects of the volcanic basement are sedimentologically significant and need to be mentioned here. Five crevasses or fractures within the upper 71 cm of the basalt are filled by foraminifer limestone (Core 144-872B-4R; Fig. 12). The infillings of these fractures are 1 mm to >1 cm thick, white to pale red (10R 6/3), phosphatized, foraminifer limestone. Foraminifers are mostly planktonic and poorly preserved; few benthic foraminifers are present. Additional components of the limestone are ostracodes, pellets, probably crustacean fecal pellets (*Favreina*), a fish tooth, a fragment of a sponge or a coral, and sand-sized debris of weathered basalt. The matrix is clotted and pelleted lime mud, which is locally bioturbated. The fracture fill is early Santonian (see “Biostratigraphy” section, this chapter).

A very different lithologic development was found in Core 144-872C-17X, where the top of a highly altered, greenish, microcrystalline, vesicular basalt is overlain by 10 cm of a dark-gray clay with several basalt fragments. The clay is overlain by a foraminifer ooze of Oligocene age (see “Biostratigraphy” section, this chapter). The contact between the clay and overlying ooze was not recovered.

Preliminary Interpretation of Depositional History

An important lesson to be learned from the drilling at Lo-En Guyot is that, even in holes drilled 75 m apart, stratigraphic sequences may differ significantly. In Hole 872C, altered basaltic basement is overlain by a veneer of unfossiliferous dark clay, which in turn is overlain by upper Oligocene foraminifer ooze (for all stratigraphic age data, see “Biostratigraphy” section, this chapter). However, in Hole 872B, cracks in the basalt are filled by lower Santonian limestone. The microfossil assemblage in the limestone suggests that the basalt surface was submerged in inner to middle neritic depths at the time of deposition. Why no indica-



Figure 12. Close-up photograph of a fracture within the basalt infilled by pelagic carbonate (Interval 144-872B-4R-1, 60–67 cm).

tion of this submergence is recorded in Hole 872C, located 75 m distant from Hole 872B, remains unexplained.

The presence of a foraminifer packstone within fractures at the top of the subaerially(?) formed basalt (see "Igneous Petrology" section, this chapter) in Core 144-872B-4R indicates possible flooding of the basaltic basement during early Santonian time. Pelagic sediments rained down into basalt fractures and filled intergranular space between volcanic pebbles on the surface of the guyot. Based on ages of the pebble conglomerate matrixes, this pelagic sedimentation lasted at least through early Campanian. Volcanic glass shards in the matrix of one conglomerate with a Campanian matrix may suggest nearby volcanic activity. It is uncertain whether the volcanoclastic sands of Subunit IIB may be related to the volcanic fragments in the pelagic limestone of Late Cretaceous age.

Apparently, a period of nondeposition occurred between the early Campanian and the late Paleocene; many of the pebbles within chinks of late Paleocene and middle Eocene age were coated with phosphatic deposits and thin manganese crusts before redeposition. Evidence also exists that the conglomerate of Unit III was eroded following lithification; at least one conglomerate pebble (Interval 144-872B-4R-1, 13–16 cm; Fig. 11) was fractured across both clasts and matrix before redeposition into a younger pelagic matrix during late Paleocene time.

The phosphatized crust fragments within the Subunit IIA chalk suggest a period of post-middle Eocene nondeposition that lasted until the late Oligocene, when deposition of the foraminifer ooze of Subunit IB began. Deposition of the ooze continued with several short breaks into the Pleistocene. Manganese, or iron-stained foraminifer tests, which give a speckled appearance to the ooze in Holes 872A and 872C (Cores 144-872A-1H and -2H, and Cores 144-872C-1H and -2H), may indicate slowed or interrupted deposition at these levels. However, no paleontologic hiatus was noted in either Core 144-872A-2H or Core 144-872C-2H. This may indicate that the observed stained tests are caused by contamination from the surface. The Oligocene to Miocene foraminifer ooze was winnowed by bottom currents. The depositional conditions changed slightly during the Pliocene to Pleistocene, when increases in the nannofossil content within the ooze point to a decreased intensity of the current activity.

Lo-En Guyot is morphologically a classic guyot with a flat upper surface. Drilling on the guyot did not recover any platform limestone, or any indication of a carbonate platform near the site. All the drilling evidence points to persistent pelagic deposition over the center of the guyot. However, as Site 872 was located near the center of the guyot where the pelagic cap is thickest, this result does not exclude the possibility of a fringing carbonate platform closer to the seaward edge of the guyot.

The flat upper surface of Lo-En Guyot cannot be explained by a continuous carbonate platform cap. However, based on the drilling results, we cannot say whether the flat surface of the guyot was produced by erosion of the entire volcano to a peneplain or by a fringing reef buildup combined with erosion of the central cone. The erosional setting could have been subaerial or submarine, by wave planation. The time of earliest erosion is less speculative than the mechanism. It must have been before the early Santonian, the age of pelagic sediments overlying and filling the cracks of the eroded basalt surface. Evidence is also present for later periods of erosion before or during the late Paleocene and perhaps in the middle Eocene.

Lo-En Guyot thus stands in sharp contrast to other guyots (e.g., Limalok Guyot; see "Site 871" chapter, this volume) in that it lacks a continuous cover of platform carbonate over its top. Such a finding documents significant differences in the geologic histories of individual guyots in this region.

BIOSTRATIGRAPHY

Introduction

Three holes were drilled at Site 872. Holes 872A and 872C were drilled with the APC and APC/XCB, respectively, for the purpose of coring the pelagic cap of Lo-En Guyot; Hole 872B was rotary drilled to penetrate and core horizons below the pelagic cap. Sediments spanning the Santonian through the Pleistocene were recovered. Age dating and paleoenvironmental interpretations were based on calcareous microplankton fossils, with additional paleoecologic information provided by benthic foraminifers, palynomorphs, and diatoms.

Calcareous Nannofossils

Holes 872A and 872C

Time constraints limited nannofossil analysis largely to core-catcher samples, although some detailed work was done on selected cores from Hole 872A. The following discussion is restricted to the record in Hole 872A except in the few cases where results from Hole 872C differ significantly from those of Hole 872A.

The interval from Samples 144-872A-1H-1, 25–26 cm, through -1H-1, 85–86 cm, contains *Emiliania huxleyi* and *Pontosphaera indoceanica*, indicating the *Emiliania huxleyi* Zone of late Pleistocene age. The assemblages are dominated by *Gephyrocapsa* spp. This dominance, as well as the presence of *P. indoceanica*, indicate that the uppermost Pleistocene zone (*Emiliania huxleyi* Acme Zone) is either contained in the upper 24 cm of the hole or is absent. The underlying *Gephyrocapsa oceanica* Zone occurs in Samples 144-872A-1H-1, 135–136 cm, and -1H-2, 25–26 cm (1.35–1.75 mbsf), based on the absence of both *E. huxleyi* and *Pseudoemiliania lacunosa*. The interval from Samples 144-872A-1H-2, 85–86 cm, through -1H-4, 25–26 cm (2.35–4.75 mbsf) contains *P. lacunosa* but lacks *Helicosphaera sellii*. Samples in this interval are dominated by the larger *Gephyrocapsa* spp. such as *G. oceanica*. The association of these species, in combination with the dominance of the *G. oceanica* group, indicates the *P. lacunosa* Zone of middle to early Pleistocene age. Samples 144-872A-1H-5, 85–86 cm, through -1H-5, 25–26 cm, also contain *P. lacunosa* and lack *H. sellii*, but they are dominated by the small *Gephyrocapsa* spp. This association indicates the small *Gephyrocapsa* Zone of early Pleistocene age. Samples 144-872A-1H-4, 5, 85–86 cm, and -1H-CC have been assigned to the *Helicosphaera sellii* Zone of early Pleistocene age. Sample 144-872A-2H-1, 0–1 cm, is assigned to the *Calcidiscus macintyre* Zone based on the occurrence of *C. macintyre* and the absence of discoasters. The presence of rare *Gephyrocapsa oceanica* indicates an early Pleistocene age, although planktonic foraminifers suggest that this sample is late Pliocene in age (Zone N21, see below).

Core 144-872A-2H contains upper Pliocene nannofossil foraminifer ooze in which at least two subzones are represented. Sample 144-872A-2H-2, 25–26 cm (9.25 mbsf), contains *Discoaster brouweri* and *Discoaster triradiatus* without *Discoaster pentaradiatus* or *Discoaster surculus*, indicating Subzone CN12d of late Pliocene age. Sample 144-872A-2H-CC (17.0 mbsf) contains a more abundant discoaster assemblage, including *D. brouweri*, *D. pentaradiatus*, *D. asymmetricus*, *D. blackstockae*, and *D. trstellifer* but lacking *Discoaster tamalis*. This association indicates Subzone CN12b of late Pliocene age.

Sediment was not recovered in Core 144-872A-3H. Sample 144-872C-3H-CC (28.0 mbsf) contains a lower Pliocene assemblage that includes *Reticulofenestra pseudumbilica*, *Sphenolithus abies*, *Amaurolithus delicatus*, and *Ceratolithus rugosus* but lacks *Pseudoemiliania lacunosa* and *Discoaster asymmet-*

ricus. This assemblage indicates Subzone CN10c of early Pliocene age.

The interval from Samples 144-872A-4H-1, 50–51 cm, through -4H-3, 50–51 cm (27.0–30.5 mbsf), contains well-preserved nanofossils, including *Discoaster quinqueramus*, *Discoaster berggrenii*, and *Amaurolithus primus*, which indicates Subzone CN9b of late Miocene age. Sample 144-872A-4H-5, 50–51 cm (33.0 mbsf), is assigned to Zone CN8 of late Miocene age based on the presence of *Discoaster neohamatus* and the absence of *D. quinqueramus*, *D. berggrenii*, *Discoaster hamatus*, and *Catinaster* spp.

Age determinations in the interval from Sections 144-872A-4H-CC through -5H-2 (36.0–39.0 mbsf) are difficult because of pervasive assemblage mixing. Samples within this interval contain *Discoaster hamatus*, *Discoaster quinqueramus*, *Discoaster berggrenii*, *Catinaster coalitus*, and *Catinaster calyculus*. The association of these species is most easily explained by the mixing of taxa from Subzones CN7b and CN9b (both of late Miocene age). In addition, rare *Discoaster tamalis*, representative of late Pliocene Subzone CN12a, occur in some samples within this interval. Although it is impossible to determine whether this mixing is the result of reworking or downhole contamination, the presence of the upper Pliocene *D. tamalis* suggests the latter interpretation. Planktonic foraminifer data also indicate significant downhole contamination within this interval (see below). If the interpretation of downhole contamination is accepted, then this interval may be assigned to Subzone CN7b of early late Miocene age. This is in concert with the unmixed Subzone CN7b assemblages that immediately underlie the mixed interval.

The interval from Samples 144-872A-5H-3, 50–51 cm, through -5H-CC (39.5–44.16 mbsf) contains *Discoaster hamatus*, *Catinaster coalitus*, and *Catinaster calyculus*, indicating Subzone CN7b of early late Miocene age. Sample 144-872A-6H-1, 50–51 cm (50.0 mbsf), contains a slightly older assemblage (Zone CN6) that includes *Catinaster coalitus* but lacks *Discoaster hamatus* and *Catinaster calyculus*. The apparent absence of Subzone CN7a suggests a small disconformity at the core break between Cores 144-872A-5H and -6H.

Samples 144-872A-6H-CC through -8H-3, 50–51 cm (54.26–68 mbsf), contain *Discoaster exilis* but lack *Catinaster coalitus* and *Sphenolithus heteromorphus*, indicating Zone CN5 of middle Miocene age. The presence of *Discoaster kugleri* in samples from Sample 144-872A-6H-CC through Core 144-872A-7H indicates Subzone CN5b. This species is apparently absent in Samples 144-872A-8H-1, 50–51 cm, through -8H-3, 50–51 cm (66.50–68.0 mbsf), suggesting Subzone CN5a, although this may be an artifact of relatively poorer preservation and insufficient observation.

The interval from Sample 144-872A-8H-4, 50–51 cm, through Core 144-872A-11H (66.5–100 mbsf) is assigned to the combined Zone CN3/4 based on the occurrence of *Sphenolithus heteromorphus*. Separation of these zones is normally based on the presence or absence of *Helicosphaera ampliapertura*. This species, however, is known to favor areas near continental margins and is notoriously rare or absent in remote oceanic locations. Thus, it is not useful for zonal division at the Lo-En Guyot site.

Lower Miocene Zone CN2, identified by the presence of *Sphenolithus belemnus*, occurs within Core 144-872A-12H (100–102 mbsf). The thinness of this zone (2 m) is probably caused by the existence of a hiatus, as suggested by the planktonic foraminifers (see below). However, it might be attributable, at least in part, to the short APC stroke of this core. An incomplete stroke of 2 m occurred at a similar stratigraphic level in Hole 872C. Cores 144-872A-13H and -14H (102.0–121.0 mbsf) contain *Cyclicargolithus abisectus*, *Cyclicargolithus floridanus*, and *Sphenolithus*

delphix but lack *Sphenolithus belemnus*, *Dictyococcites bisectus*, *Zygrhablithus bijugatus*, and *Sphenolithus ciperoensis*, indicating Zone CN1 of early Miocene age. The abundance of *Triquetrorhabdulus carinatus* in Sample 144-872A-14H-CC indicates Subzones CN1a and CN1b of earliest Miocene age.

Core 144-872A-15H (121.0–130.5 mbsf) contains assemblages of Subzone CP19b of latest Oligocene age. Species present include *Sphenolithus ciperoensis*, *Dictyococcites bisectus*, *Zygrhablithus bijugatus*, *Cyclicargolithus abisectus*, and *Triquetrorhabdulus carinatus*. Samples 144-872A-17H-3, 50–51 cm, through -17H-CC (143.5–143.7 mbsf) contain *Sphenolithus distentus* and *S. ciperoensis*, indicating Subzone CP19a of late Oligocene age.

Section 144-872A-17H-CC contains material of three distinct ages. The soft, white foraminifer ooze of Subzone CP19a (late Oligocene age) is intermixed with tan, pebble-bearing foraminifer chalk. This tan chalk contains *Dictyococcites bisectus*, *Toweius magnicrassus*, and *Chiasmolithus gigas*, indicating Subzone CP13b of middle Eocene age. The white Oligocene ooze fills burrows within some pieces of the middle Eocene chalk.

In addition to the Paleogene material, nanofossils occur in the pelagic limestone matrix of a conglomeratic clast. Nanofossils from this matrix were identified in thin section. Small patches (burrows?) within the matrix contain well-preserved nanofossils indicative of the *Fasciculithus tympaniformis* Zone (CP4) of early late Paleocene age. The bulk of the matrix contains several biostratigraphically restricted forms that suggest a Santonian age. The presence of *Micula concava* and *Reinhardtites anthophorus* indicate a maximum age of late early Santonian (CC15). The presence of *Stoverius coronatus*, *Stoverius biarcus*, *Gephyrorhabdus coronadventis*, and common *Aspidolithus parvus expansus* and *Arkhangelskiella specillata* without *Aspidolithus parvus parvus* or *Aspidolithus parvus constrictus* restricts the minimum age of this assemblage to the latest Santonian (CC17). This age assignment corroborates the late Santonian age provided from planktonic foraminifer evidence (Fig. 13).

Hole 872B

Hole 872B was washed down to a depth of 77.3 mbsf. Cores 144-872B-1R through -3R recovered part of the Neogene pelagic cap from 77.3 to 106.3 mbsf. Samples 144-872B-1R-CC and -2R-CC (77.38 and 87.05 mbsf, respectively) contain nanofossil assemblages with *Sphenolithus heteromorphus*, *Reticulofenestra pseudoumbilica*, and rare *Calcidiscus macintyreii*, indicating the *Sphenolithus heteromorphus* Zone (CN4) of middle Miocene age. Sample 144-872B-3R-CC (96.65 mbsf) contains *Sphenolithus belemnus*, *Sphenolithus conicus*, *Cyclicargolithus abisectus*, and *Cyclicargolithus floridanus*, indicating the *Sphenolithus belemnus* Zone (CN2) of early Miocene age (Fig. 14).

The underlying 28.9 m were washed and coring resumed at a depth of 135.2 mbsf. Core 144-872B-4R recovered basalts with thin sediment layers (Fig. 15). The nanofossil content was investigated both in smear slides and thin sections prepared from all the sediment layers. Sample 144-872B-4R-1, 20–22 cm, contains common, moderately preserved nanofloras, including *Lithastrinus septenarius*, *Eiffellithus eximius*, *Reinhardtites anthophorus*, and *Micula decussata*, indicating Zone CC15 of early Santonian age. Sample 144-872B-4R-1, 61–62 cm, contains very rare and poorly preserved specimens of *Eiffellithus eximius* and *Marthasterites furcatus*, indicating an age no older than the late Turonian. Only a few specimens of *Eiffellithus eximius* were observed in Sample 144-872B-4R-1, 68–70 cm, which cannot be older than early Turonian. Planktonic foraminifer assemblages from this interval are more diagnostic (see below) and indicate a Santonian age.

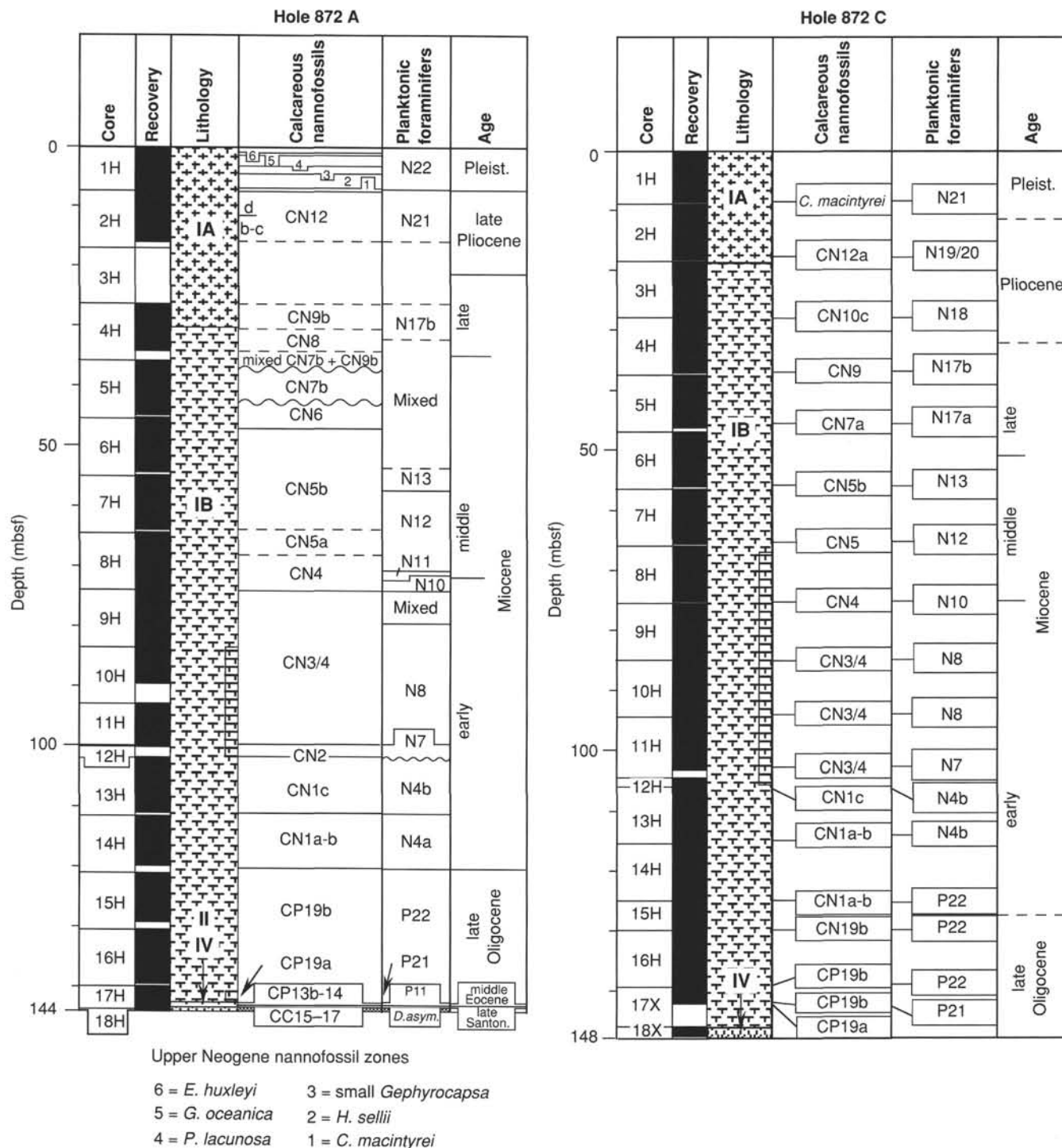


Figure 13. Biostratigraphy of Holes 872A and 872C, Lo-En Guyot.

Planktonic Foraminifers

Holes 872A and 872C

Planktonic foraminifers are very abundant throughout the pelagic sequence at Site 872 (Lo-En Guyot). Core-catcher samples from Holes 872A and 872C were examined. Further sampling was conducted on cores from Hole 872A to constrain the zonal boundaries more tightly. Figure 13 shows the planktonic foraminifer biostratigraphy obtained from these holes.

Processes such as dissolution, current winnowing, erosion, and redeposition of sediment on the guyot have contributed to the variable preservation observed at this site. For much of the sequence, relatively well-preserved individuals are accompanied by broken, peeled, or dissolved specimens. The fine fraction (45–150 μm) is often dominated by broken and etched fragments. Reworking of older material is encountered at various levels in the sequence. Downhole contamination causes additional problems and is in some cases severe, particularly in the top one or two sections of cores. Downhole contaminants are usually Pleistocene

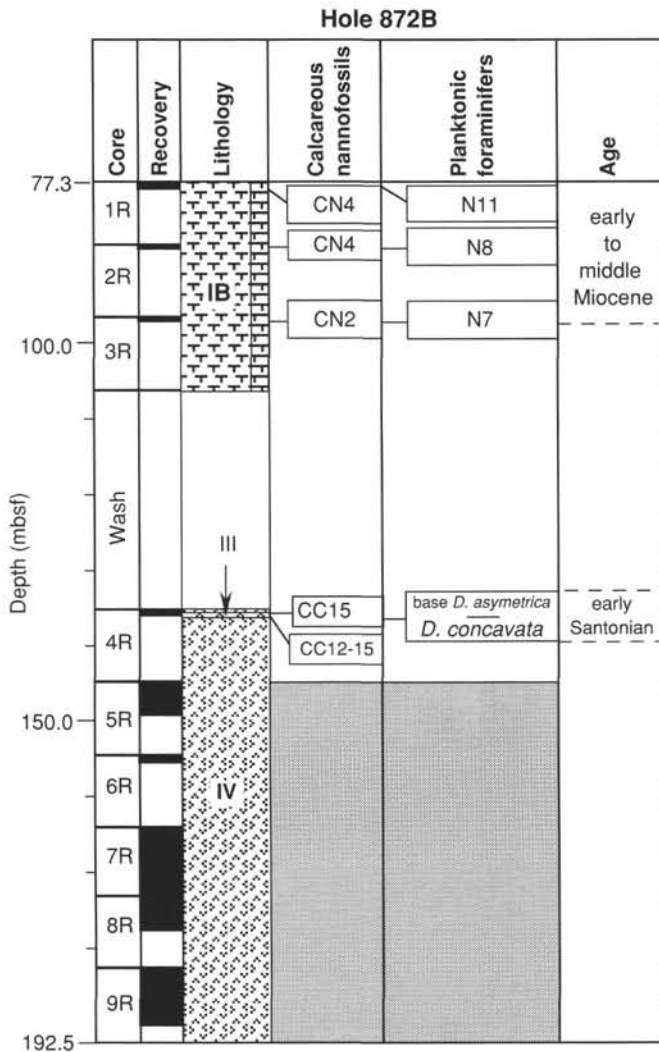


Figure 14. Biostratigraphy of Hole 872B, Lo-En Guyot.

in age, often being discolored by iron staining. These occur through much of the sequence to the level of Core 144-872A-9H.

The following discussion is centered on the faunal sequence observed in Hole 872A. The record from Hole 872C was found to be comparable. Reference is made to Hole 872C only at those levels where additional information is available from that hole.

Sample 144-872A-1H-3, 59–61 cm (3.59 mbsf), contains *Truncorotalia truncatulinoides*, *Globorotalia tumida*, and *Pulleniatina obliquiloculata* and is Pleistocene in age (Zone N22). Samples 144-872A-1H-CC, -2H-3, 59–61 cm, and 144-872A-2H-CC yield an upper Pliocene (Zone N21) assemblage containing *Truncorotalia tosaensis*, *Globigerinoides fistulosus*, *Globorotalia tumida*, and *G. tumida flexuosa*. Material from Core 144-872A-3H was not recovered, but an upper Miocene (Zone N18) assemblage was found at a comparable depth in Hole 872C (Sample 144-872C-3H-CC), which includes frequent *Sphaeroidinellopsis* (but no *Sphaeroidinella*) associated with *Globigerina nepenthes* and *Globorotalia tumida*. In Sample 144-872A-4H-CC, a slightly older assemblage of late Miocene age (Subzone N17a) was found, including *Globoquadrina dehiscens*, *Globigerinoides obliquus*, and a few *Sphaeroidinellopsis seminulina*, but no *Pulleniatina* or *Globorotalia tumida*.

One sample was taken from each section of Cores 144-872A-5H and -6H. This interval is problematic for several reasons,

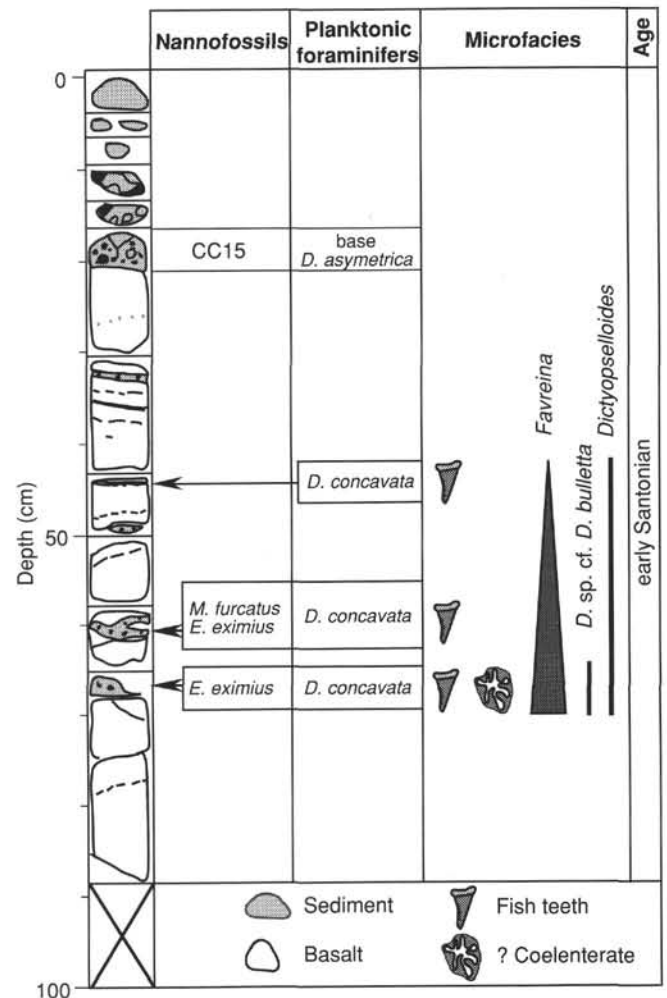


Figure 15. Biostratigraphy and microfacies of sediments recovered in Section 144-872B-4R-1, Lo-En Guyot.

which include variable preservation, severe downhole contamination, extensive reworking, and the scarcity of important marker species of the upper middle and upper Miocene, such as *Neogloboquadrina acostaensis* and *Paragloborotalia siakensis*. This interval has not been zoned by planktonic foraminifers, although a nannofossil zonation is available (Fig. 13). Reworked taxa include Oligocene and lower Miocene species.

A less mixed fauna was found in Sample 144-872A-6H-CC, containing *G. praemenardii* and a few *Paragloborotalia siakensis* but no *Globigerina nepenthes*. This assemblage is representative of Zone N13 of middle Miocene age. The boundary between Zones N13 and N12 is placed between Samples 144-872A-7H-2, 59–61 cm (57.09 mbsf), and -7H-3, 59–61 cm (57.72 mbsf), the latter containing the index species *Globorotalia fohsi robusta* and *G. fohsi lobata*. These advanced members of the *G. fohsi* lineage, which are definitive of Zone N12, occur throughout the lower part of Core 144-872A-7H to Sample 144-872A-7H-CC.

Sample 144-872A-8H-5, 59–61 cm (71.09 mbsf), contains *Globorotalia praefohsi* (sensu Blow, 1969) and *G. peripheroacuta* but lacks fully keeled individuals of *G. fohsi*; this sample belongs to Zone N11 of middle Miocene age. Sample 144-872A-8H-CC contains *Globorotalia peripheroacuta* and *Orbulina universa*, but it lacks the more advanced representatives of the *G. fohsi* group and is consequently assigned to Zone N10. Samples 144-872A-9H-CC, -10H-CC, and -11H-CC contain *Globigerinoides bisphericus*,

Praeorbulina sicana, *P. transitoria*, and *P. glomerosa curva*, but they lack *Orbulina* spp. This assemblage is assigned to Zone N8 of late early Miocene age.

Sample 144-872A-12H-CC lacks *Praeorbulina* spp. but does contain forms transitional from *Globigerinoides trilobus* to *G. bisphericus*; for this reason it is assigned to Zone N7. Samples 144-872A-13H-3, 59–61 cm, and -13H-CC contain *Globigerinoides* spp. and *Globoquadrina dehiscens* in conjunction with members of the “*Globigerina*” *ciperoensis* group and common *Paragloborotalia kugleri*. The occurrence of *P. kugleri* in abundance is taken as good evidence of Subzone N4b (earliest Miocene age), even though the species does occur sporadically through some higher parts of the sequence as a result of reworking. The disconformity separating Zone N7 and Subzone N4b occurs between Cores 144-872A-12H and -13H. This disconformity was also detected at a similar stratigraphic depth in Hole 872C. The short APC stroke of both Cores 144-872A-12H and 144-872C-12H may be related to this disconformity.

Sample 144-872A-14H-CC is also assigned to Subzone N4b. Rare, well-preserved, middle Eocene planktonic foraminifers (*Truncorotaloides topilensis* and *Morozovella crassata*) were found reworked in Samples 144-872A-13H-CC and -14H-CC.

An upper Oligocene (Zone P22) fauna lacking typically Miocene forms such as *Globigerinoides* spp. and *Globoquadrina dehiscens* but containing common “*Globigerina*” *ciperoensis* and “*G.*” *angulisuturalis* was found in Samples 144-872A-15H-3, 58–60 cm, -15H-CC, -16H-3, 58–60 cm, and -16H-CC. The latter two samples, in particular, show a distinctly mixed preservation style. A high proportion (30%–40%) of the fauna in the >150- μ m size fraction is strongly discolored to an orange-brown color from iron staining and/or phosphatization. These specimens are well sorted with respect to their size, occurring only rarely as fragments in the 45–150 μ m fraction. Samples 144-872A-17H-3, 58–60 cm, and 144-872C-17X-CC contain common *Paragloborotalia opima* associated with members of the “*Globigerina*” *ciperoensis* lineage, including the important marker species “*G.*” *angulisuturalis*. This assemblage indicates Zone P21 of late Oligocene age.

Section 144-872A-17H-CC consists of several lithified fragments, in which rounded phosphatic clasts are set in a matrix of indurated foraminifer chalk. In this chalk, planktonic foraminifers are recrystallized, iron stained, and phosphatized. The marker species *Globigerinatheka index*, *Hantkenina mexicana*, *Clavigerinella eocanica*, *Morozovella aragonensis*, and *Truncorotaloides topilensis* were identified. This assemblage is attributed to Zone P11 of middle Eocene age. Burrows, occurring in a few fragments, contain concentrations of small phosphatized clasts and well-preserved, white, Oligocene planktonic foraminifers. A superficial dusting of Oligocene (Zone P21–P22) ooze occurs on several fragments.

The phosphatized pebbles in this section belong to a conglomerate consisting of altered volcanic elements cemented by partially phosphatized chalk that is rich in planktonic foraminifers. Tests of planktonic foraminifers, observed in thin section, are partially or totally phosphatized; this has not modified the characteristic profiles of the various species, however. The assemblage includes *Dicarinella concavata* gr., *Marginotruncana sigali*, *M. pseudolinneiana*, *Contusotruncana fornicata*, *Heterohelix globulosa*, *H. reussi*, *Globigerinelloides prairiehillensis*, *G. bollii*, and *Ventilabrella glabrata* associated with rare *Globo-truncanita elevata* and *G. stuartiformis*. This assemblage is characteristic of the upper part of the *Dicarinella asymetrica* Zone of late Santonian age.

Hole 872B

The first three cores of Hole 872B recovered pelagic ooze containing abundant planktonic foraminifers. Sample 144-872B-1R-CC contains *Globo-rotalia praefohsi* but no advanced representatives of the *G. fohsi* lineage; it is assigned to Zone N11 of middle Miocene age. Sample 144-872B-2R-CC contains *Globigerinoides bisphericus* and *Praeorbulina sicana* but lacks *Orbulina*; it is assigned to Zone N8 of early to middle Miocene age. Sample 144-872B-3R-CC lacks *Praeorbulina sicana* but contains forms transitional from *Globigerinoides trilobus* to *G. bisphericus*, indicating the higher part of Zone N7 of early Miocene age.

Core 144-872B-4R recovered pelagic sediments cementing volcanic rock fragments, infilling cracks in the basalt, or as interbedded layers between lava flows (Figs. 14–15). A pebble, belonging to Subunit IIC (Sample 144-872B-4R-1, 13–16 cm) is a conglomerate with two generations of matrix (Fig. 10). The older matrix contains a rich planktonic fauna attributable to the *Globo-truncanita elevata* Zone of early Campanian age. The younger matrix is barren of planktonic foraminifers. Sample 144-872B-4R-1, 18–22 cm, yields common to abundant, rather well-preserved planktonic foraminifers. The assemblage includes common marginotruncanids (e.g., *M. sigali*, *M. schneegansi*, *M. pseudolinneiana*, *M. coronata*), several *Dicarinella concavata*, *Globigerinelloides bollii*, *Heterohelix reussi*, rare *Contusotruncana fornicata*, *Archaeoglobigerina cretacea*, *Globo-truncana linneiana*, *Ventilabrella eggeri*, and *V. glabrata*. This assemblage is indicative of the *Dicarinella asymetrica* Zone (even in the absence of the nominate species) and is Santonian in age (possibly early Santonian).

In the lower samples (Samples 144-872B-4R-1, 46–48 cm, -4R-1, 60–62 cm, and -4R-1, 68–71 cm; Fig. 15), planktonic foraminifer assemblages are substantially similar to those in the previous sample, although they seem to display a slightly older character. The abundant marginotruncanids and *Heterohelix reussi* and common *Dicarinella concavata* are associated with rare whiteinellids and *Dicarinella primitiva* along with rare, possibly older forms attributable to *Dicarinella hagni* and *Marginotruncana marianosi* in Sample 144-872B-4R-1, 68–71 cm. The bulk of the planktonic faunas in all three layers are indicative of the *Dicarinella concavata* Zone of early Santonian age, but the supposed older forms are known to become extinct in the late Turonian. Poor recovery and the discontinuous record make it difficult to determine whether the older aspect of the assemblage is related to reworking or to preservation. There is evidence in favor of both hypotheses. On the one hand, the occurrence of shallow-water foraminifers and other skeletal organisms within the faunal-rich pelagic sediments would support the possibility of some transport and reworking. On the other hand, the decrease in state of preservation and increase of degree of phosphatization downhole may account for the apparent older aspect of the fauna. Other notable features of this sequence are the occurrence of several medium-sized, perfectly preserved fish teeth, the sharp downhole increase in the abundance of fecal pellets (*Favreina* sp.), and the occurrence of a few benthic foraminifers indicative of shallow-water environment (see below; Fig. 15).

Benthic Foraminifers

Two species of benthic foraminifers were found in the sediments infilling the basalt cracks in Core 144-872B-4R (Fig. 15): *Dictyopselloides* sp. (Samples 144-872B-4R-1, 46–48 cm, -4R-1, 60–62 cm, and -4R-1, 68–71 cm) and *Dorothia* sp. cf. *D. bullella* (Sample 144-872B-4R-1, 68–71 cm). The latter species is known

from the Upper Cretaceous; the genus *Dictyopselloides* is known from the Santonian of France and Spain.

These benthic foraminifers are usually reported from the inner to middle neritic deposits ("circalittoral" of French authors) at a paleodepth of 10 to 100 m, with a maximum paleodepth of approximately 200 m. The association of these species in the crack infillings suggests a relatively shallow paleodepth, although the possibility of post-mortem transport or reworking cannot be eliminated.

Palynology

Palynomorphs

Palynologic analyses were performed on 15 core-catcher samples (Samples 144-872A-1H-CC through -11H-CC and Samples 144-872A-13H-CC through -16H-CC) through the entire thickness of the pelagic cap in Hole 872A. Samples vary from nannofossil foraminifer ooze to foraminifer ooze. Treatment with 20% HCl alone was sufficient to concentrate the organic fraction for visual analysis. For each sample two microscope slides were prepared: one containing unsieved residue for total kerogen and palynofacies analysis, the other containing residue sieved at 20 μm for biostratigraphic analysis.

Dinoflagellates occur only in the three uppermost core catchers (Samples 144-872A-1H-CC, -2H-CC, and -4H-CC; Sample 144-872A-3H-CC was not recovered). For each of these samples (ages from calcareous plankton fossils in parenthesis), the following taxa were recognized:

1. Sample 144-872A-1H-CC (early Pleistocene): *Impagidinium aculeatum*, *I. japonicum*, *I. striatum*, *Impagidinium* sp. cf. *I. patulum*, *Operculodinium israelianum*, and *Spiniferites* sp.

2. Sample 144-872A-2H-CC (early late Pliocene): *Impagidinium aculeatum*, *I. japonicum*, *I. patulum*, *I. striatum*, *Operculodinium centrocarpum* (s.l.), *Polysphaeridium* sp., and *Incertae sedis* sp. 1 of Edwards (1985).

3. Sample 144-872A-4H-CC (late Miocene): *Impagidinium aculeatum*, *Impagidinium* sp. cf. *I. paradoxum*?, and *Impagidinium* sp. cf. *I. striatum*.

Of all the taxa found in these core-catcher samples, only one—*Incertae sedis* sp. 1 of Edwards (1985)—has a restricted range within the upper Cenozoic. *Incertae sedis* sp. 1 of Edwards (1985), recorded here for the first time from Pacific Ocean sediments, is confined to the Neogene in the North Atlantic (see Head et al., 1989, p. 441, for a discussion of occurrences) where it occurs as high as the lower upper Pliocene (M.J. Head, unpubl. data).

Neither embryophyte spores nor pollen were found, although spores(?) of probable algal origin were found in Samples 144-872A-3H-CC and -4H-CC, and possible copepod eggs were recovered from Sample 144-872A-2H-CC.

Palynofacies

Several categories of organic remains were recognized at 1000 \times magnification within the >20- μm organic residue fraction. The most commonly represented category consists of rounded and subrounded clasts of granular amorphogen, up to about 150 μm in diameter and enclosing numerous fine, colorless mineral particles. The larger, rounded, and somewhat elongated clasts are interpreted to be fecal pellets, and the smaller clasts to be fragments of them. A second category comprises the organic infilling of foraminifer chambers. As with the fecal pellets, these foraminifer infillings generally appear as rounded clasts of granular amorphogen, but they have a denser, finer texture and sharp, rather than diffuse, margins. Other categories recorded are dinoflag-

ellates, woody tissues (from higher plants), and foraminifer linings that are thick walled and of amber color.

Visual kerogen analysis of the >20- μm fraction permits recognition of three palynofacies units (Fig. 16), as follows:

Palynofacies Unit 1 (Samples 144-872A-1H-CC through -4H-CC) is defined by the presence of dinoflagellates, these occurring in trace amounts. Well-preserved fecal pellets dominate, and rare foraminifer infillings, trace amounts of woody tissues, and occasional trace amounts of foraminifer linings also occur. Organic remains generally have excellent preservation.

Palynofacies Unit 2 is recognized in Samples 144-872A-5H-CC through -13H-CC. Its top is defined by the downhole disappearance of dinoflagellates and its base by the top of Palynofacies Unit 3. It is characterized by dominant to abundant amounts of moderately to well-preserved fecal pellets, rare to common foraminifer infillings, trace amounts of woody tissues, and occasional trace amounts of foraminifer linings. Organic remains are generally moderately to well preserved so that the absence of dinoflagellates—which are much more resistant to degradation than are fecal pellets—cannot be attributed to preservational loss.

Palynofacies Unit 3 is recognized in Samples 144-872A-14H-CC through -16H-CC. Its top is defined by a downhole decrease in both the preservation and relative abundance of fecal pellets, and a relative increase in foraminifer linings. In addition, rare to common foraminifer infillings and occasional trace amounts of woody tissues are present. Organic remains are generally moderately to rather poorly preserved. Commonly present are transparent membranous tissues, with pyrite impregnation implying some degree of anaerobic decomposition within the lower sediments of the pelagic cap at this site.

Differences between Palynofacies Units 2 and 3 are interpreted as being largely taphonomic. The uphole appearance of dinoflagellates, marking the base of Palynofacies Unit 1, seems to be a primary feature and is discussed in detail below.

Paleoenvironmental Interpretation Based on Dinoflagellate Assemblages

The presence of dinoflagellate cysts in the upper 40 m (Palynofacies Unit 1) of the pelagic cap at Site 872 represents the first discovery of dinoflagellates as a result of drilling on western Pacific guyots and atolls. The scarcity of sporopollenin dinoflagellate cysts in the oceanic Pacific region is indicated by their absence in palynologically examined sediments recovered during ODP Leg 129 (Lancelot, Larson, et al., 1990) and ODP Leg 143 (Sager, Winterer, et al., in press) as well as their absence from Site 871 sediments (see "Biostratigraphy" section, "Site 871" chapter, this volume).

The dinoflagellate assemblages at Site 872 are dominated by the genus *Impagidinium* and are thus oceanic in character, although a single specimen of *Operculodinium israelianum* suggests some inner neritic influence. In view of the recorded absence of dinoflagellate cysts elsewhere in this part of the Pacific, their presence at Site 872 is intriguing. Perhaps they flourished around emergent islands to the east and were swept in suspension by surface or subsurface currents to Lo-En Guyot. Their absence from Palynologic Unit 2 (and possibly Unit 3) might be caused by winnowing but it is not a preservational bias: the presence of relatively fragile fecal pellets in these sediments argues against the preservational loss of dinoflagellate cysts by oxidation.

Inspection of unsieved residues of samples from Hole 872A revealed an increase in silt-sized (up to about 10 μm) quartz grains within those samples containing dinoflagellate cysts. The silt grains are angular to subrounded and probably represent eolian deposition. It is hypothesized that the apparent link between

increased silt and dinoflagellate occurrence is related to a sustained shift in atmospheric and oceanic circulation beginning during the late Miocene.

Siliceous Microfossils and Their Diagenetic Products

The acid-insoluble silt and sand fraction of the sediments from the pelagic cap at this site contain authigenic silicates, such as the zeolites: phillipsite and clinoptilolite (Fig. 16). Trace remains of siliceous microfossils, such as the dissolution-resistant sponge spicules and radiolarians, occur sporadically, generally where the abundance of zeolites decreases. This association may indicate the presence of a relict assemblage derived from more abundant siliceous microfossils, the majority of which were dissolved and provided silica for zeolite formation.

A special situation was encountered in a sample from the top of Core 144-872A-13H. Here, the HCl-insoluble residue was dominated by light, slightly vesicular ash and by iron oxides. In addition, isolated diatoms were found. None of the species encountered yields significant stratigraphic information. Most of the valves belong to marine planktonic diatoms. These, and the presence of a resting spore, imply a shelf or slope environment. In addition, one valve of the freshwater diatom *Aulacosira granulata* was found. The unique presence of diatoms in this sample, which is also rich in silicic ash, suggests that the silica dissolved from this ash protected the diatom shells from dissolution.

Summary

The oldest sediment preserved on Lo-En Guyot consists of Santonian pelagic limestone occurring as crack fillings and a volcanic pebble conglomeratic matrix lying atop basaltic basement in Core 144-872B-4R. Planktonic foraminifers and, to a lesser extent, calcareous nannofossils constrain the age of this material as early Santonian, although there are indications that the lowermost pelagic limestone may be slightly older than that at the top of the sequence. The presence of middle neritic benthic foraminifers in the lowest material may indicate either a relatively shallow pelagic paleoenvironment or transport of shallow-water material into a deeper site of deposition. The Santonian fossils are extensively phosphatized, indicating an extended period of exposure at the seafloor. The presence of middle Eocene sediments directly overlying the Santonian limestones indicates a substantial disconformity with a hiatus of approximately 35 m.y.

The Santonian limestones are mantled by a thin conglomeratic chalk with recrystallized, iron-stained, and/or phosphatized middle Eocene (Zone P11) planktonic foraminifers and partially or wholly replaced (phosphatized?) calcareous nannofossils. A pebble from this interval is a conglomerate with a lower Campanian matrix that was subsequently bored and filled with ooze during the early late Paleocene. The middle Eocene mantle of conglomeratic chalk is, in turn, overlain by upper Oligocene and Neogene pelagic carbonates. Prolonged exposure at the seafloor is indicated also for the middle Eocene conglomeratic chalk by the extensive recrystallization and phosphatization of the microfossils. The hiatus of the disconformity overlying the middle Eocene sediment suggests seafloor exposure may have been as long as approximately 15 m.y.

A 140-m-thick sequence of upper Oligocene through Pleistocene foraminifer ooze was deposited atop the middle Eocene exposure surface. Calcareous microplankton stratigraphy indicates that sedimentation was relatively continuous from the late Oligocene (Zone P21/Subzone CP19a) through the Pleistocene, with only minor periods of nondeposition and/or erosion during the early Miocene (Zone N7 overlying Subzone N4b; hiatus = approximately 5 m.y.), middle Miocene (Subzone CN7a missing;

hiatus = <1 m.y.), and late Miocene (Subzone CN9a missing; hiatus = approximately 2 m.y.). An additional break in sediment preservation may occur in the lower Pliocene, although this interval may be represented by a relatively condensed sequence in Cores 144-872C-3H and -4H (which have not been investigated in detail as a result of time constraints). The abnormally high ratio of planktonic foraminifers to nannofossils throughout most of the Oligocene and Miocene sequence indicates significant winnowing of the sediment. This current activity apparently waned during the Pliocene and Pleistocene, as evidenced by the relative increase in the volume of nannofossils in the oozes.

PALEOMAGNETISM

Initial magnetic susceptibility was measured at an interval of 5 cm on most whole-round cores from the pelagic sediment and on the archive half of split cores containing basalt at Site 872 (Fig. 17). The susceptibility in the pelagic sediments is generally low or negative, with larger values (typically at the tops of cores) probably the result of rust contamination. A downcore decrease in susceptibility, similar to the reduction noted at Site 871, occurs at approximately 30 mbsf. Susceptibility values in the basalt are much higher (ca. 10^{-4} to 10^{-3} cgs). Low values of susceptibility from about 186 to 190 mbsf in Hole 872B correspond to an altered vesicular ankaramite flow (Unit 18; see "Igneous Petrology" section, this chapter), which is also characterized by an order of magnitude lower magnetization than the remaining lavas from Site 872.

The pelagic sediment at Hole 872A was too soupy and disturbed to yield reliable magnetic results. At Hole 872C, an attempt was made to improve the quality of the cores containing pelagic sediment. The 1.5-m-long core sections were stored in a vertical position for 2–3 hr, the excess water was drained from each section, and the resulting void was removed to prevent the resuspension and disturbance of the sediment. We measured Cores 144-872C-1H through -4H as a test of whether this procedure might preserve the magnetic signal better. The resulting magnetic data (Fig. 18) have exclusively positive inclinations, presumably related to reorientation during the coring process. Thus, no magnetostratigraphic data were obtained from the pelagic sediment. We will measure discrete samples in detail on land to examine whether the pelagic sediment has any reliable remanent magnetization.

Thirteen discrete samples of basalt were measured with the pass-through cryogenic magnetometer after alternating-field (AF) demagnetization (Table 3). The majority of the basalt samples have nearly univectorial magnetization and a characteristic direction that is well defined by AF demagnetization (Figs. 19–20). The NRM intensity of the basalt is <10 A/m. In addition to a low NRM intensity (0.23 A/m), the ankaramite flow mentioned above (Sample 144-872B-9R-5, 131–133 cm) also exhibits a different demagnetization behavior, with little reduction in intensity after AF demagnetization in a field of 90 mT (Fig. 21).

The inclinations of the characteristic remanent magnetization are negative, except for Sample 144-872B-8R-4, 6–8 cm, which showed a positive inclination. Subsequent measurement of a sample from lower in the same section (Sample 144-872B-8R-4, 43–45 cm) and two samples from higher in the same flow unit (Samples 144-872B-8R-1, 70–72 cm, and -8R-2, 89–91 cm) yielded negative inclinations. Thus, the positive inclination of this single sample seems to be the result of a section of core that has been inverted.

Basement inclinations range from -41° to -61° , which is steeper than that of the basalts at Site 871 ($+2^\circ$ to -32°). The simplest interpretation of the data from Lo-En Guyot is that the direction represents a normal polarity magnetization acquired at

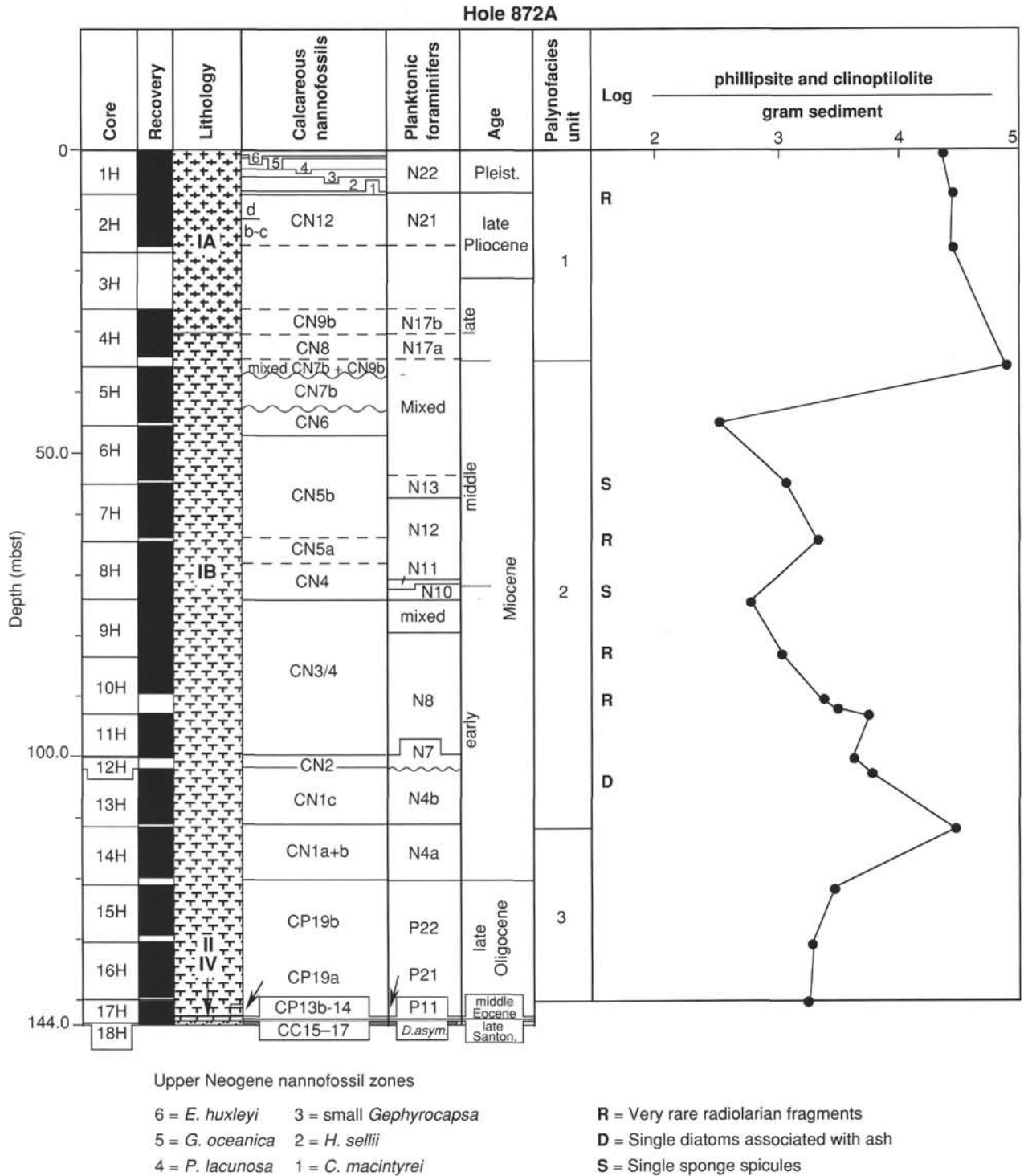


Figure 16. Palynofacies units and siliceous microfossil and zeolite abundances for Hole 872A.

a paleolatitude of approximately 30°S. The present latitude of the Lo-En Guyot is about 10°N, so the guyot may have moved north about 40° in latitude after its formation.

SEDIMENTATION RATES

Pelagic Cap

Pelagic sediment accumulation rates for Site 872 (Lo-En Guyot) are estimated using micropaleontologic data from Hole

872A, the hole in which the greatest biostratigraphic resolution was achieved (see "Biostratigraphy" section, this chapter). Paleomagnetic data are not available because of the disturbed nature of pelagic sediments at this site (see "Paleomagnetism" section, this chapter). Age assignments for calcareous nanofossils and planktonic foraminifers, as shown in Table 4, are taken from Berggren, Kent, and Flynn (1985) and Berggren, Kent, and Van Couvering (1985). Sediment accumulation is plotted graphically in Figure 22.

Table 3. Results of demagnetization of basalts from Cores 144-872B-5R to -9R and Core 144-872C-18X.

| Core, section, interval (cm) | Inclination (degrees) |
|------------------------------|-----------------------|
| 144-872B- | |
| 5R-1, 47-49 | -50.2 |
| 5R-3, 102-104 | -41.6 |
| 6R-1, 40-42 | -48.0 |
| 7R-1, 31-33 | -43.3 |
| 7R-4, 67-69 | -55.8 |
| 7R-7, 74-76 | -48.7 |
| 8R-1, 70-72 | -51.3 |
| 8R-2, 89-91 | -43.9 |
| *8R-4, 6-8 | 54.4 |
| 8R-4, 43-45 | -52.2 |
| 9R-2, 92-94 | -61.0 |
| 9R-5, 131-133 | -42.5 |
| 144-872C- | |
| 18X-2, 26-28 | -47.5 |

*Section apparently inverted.

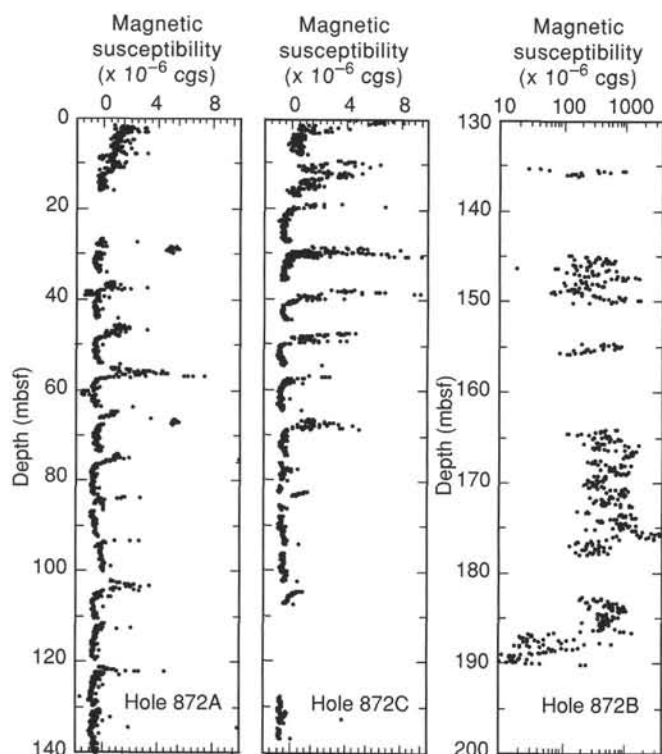


Figure 17. Magnetic susceptibility variations at Site 872. Note change of scale for Hole 872C.

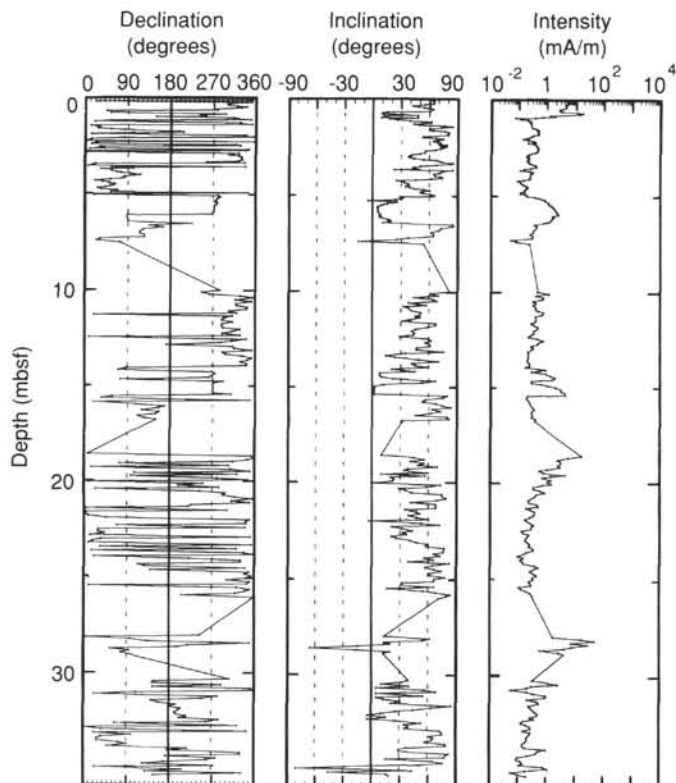


Figure 18. Declination, inclination, and intensity variations for Cores 144-872C-1H to -4H.

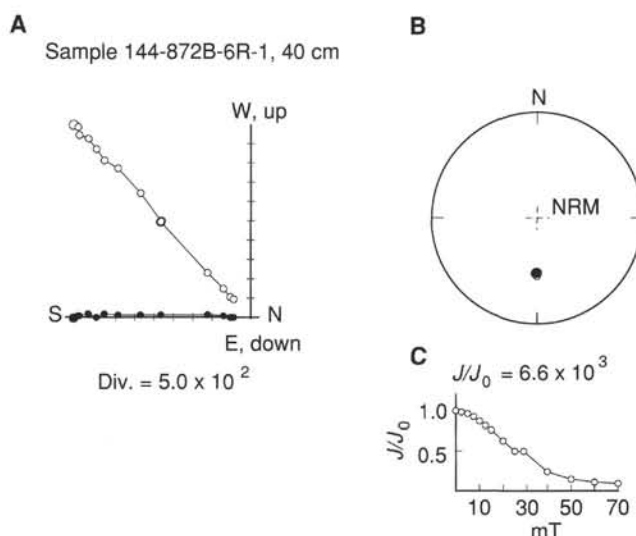


Figure 19. Alternating-field (AF) demagnetization results for basalt Sample 144-872B-6R-1, 40 cm. Demagnetization fields are 0, 2.5, 5, 7.5, 10, 12.5, 15, 20, 29, 40, 50, 60, and 70 mT. **A.** Orthogonal vector plot of progressive AF demagnetization. Closed circles represent horizontal component of the magnetization, and open circles represent vertical component. **B.** Stereonet plot of vector end-points after progressive demagnetization. **C.** Variation of intensity after progressive AF demagnetization.

Following a long hiatus that extended from the middle Eocene (nanfossil Subzone CP13b–Zone CP14, planktonic foraminifer Zone P11) through the late Oligocene (nanfossil Subzone CP19a, planktonic foraminifer Zone P21), foraminifer ooze began to accumulate on the guyot at a rate of approximately 7 m/m.y. Sediment accumulation continued at a similar rate through the Oligocene/Miocene boundary interval to the early Miocene. A significant part of the lower Miocene interval is missing. Thereafter, sediment accumulated at an accelerated rate of 15–16 m/m.y. A condensed interval of middle Miocene age, spanning planktonic foraminifer Zones N10–N12 is present in Core 144-872A-8H. After this, for most of the later part of the middle Miocene, sediment once again accumulated at a relatively rapid rate (10–20 m/m.y.). Sediment accumulation rates for the remaining part of the sequence (i.e., the upper Miocene, Pliocene, and Pleistocene) are difficult to estimate given the existence of several

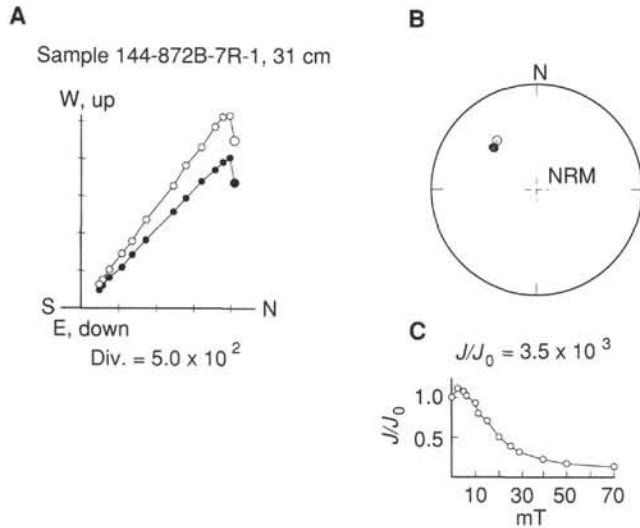


Figure 20. Alternating-field (AF) demagnetization results for basalt Sample 144-872B-7R-1, 31 cm. Demagnetization fields are 0, 2.5, 5, 7.5, 10, 12.5, 15, 20, 25, 30, 40, 50, and 70 mT. Other plot conventions are identical to Figure 19.

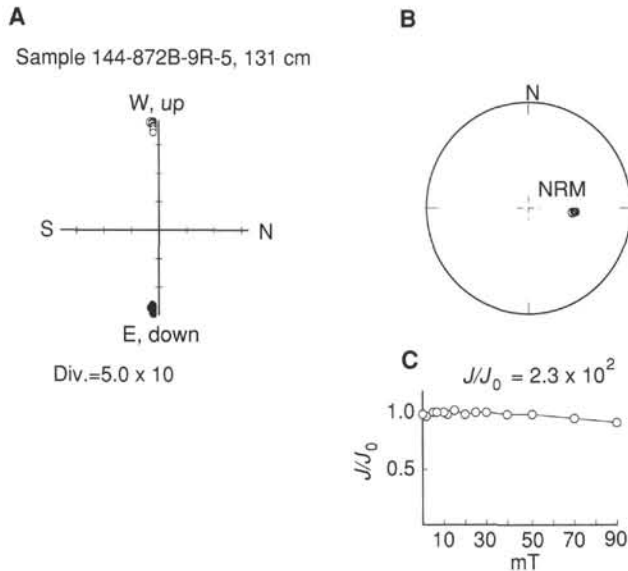


Figure 21. Alternating-field (AF) demagnetization results for basalt Sample 144-872B-9R-5, 131 cm. Demagnetization fields are 0, 2.5, 5, 7.5, 10, 12.5, 15, 20, 29, 40, 50, 70, and 90 mT. Other plot conventions are identical to Figure 19.

short disconformities, but they appear to be on the order of 5 m/m.y.

A hiatus in the lower Miocene, spanning planktonic foraminifer Zones N5 and N6, is inferred between Cores 144-872A-12H and -13H. A similar hiatus is noted at approximately the same sub-bottom depth in Hole 872C. The hiatus represents approximately 5 m.y. of missing time. It should be noted that for the twelfth core of both holes an incomplete stroke of the APC was recorded, which may indicate some physical change at this level. Higher in the sequence, in Cores 144-872A-4H and -5H, reworking of Oligocene and middle Miocene planktonic foraminifers suggests the presence of one or more disconformities, although these approach the limit of biostratigraphic resolu-

Table 4. Biohorizons used to compute sediment accumulation rates for the pelagic cap of Hole 872A.

| Code | Datum | Age (Ma) | Top depth (mbsf) | Base depth (mbsf) |
|--------------------------|---------------------------------|----------|------------------|-------------------|
| Calcareous nannofossils: | | | | |
| C1 | FAD <i>E. huxleyi</i> | 0.28 | 0.85 | 1.35 |
| C2 | LAD <i>P. lacunosa</i> | 0.47 | 1.75 | 2.35 |
| C3 | LAD <i>H. sellii</i> | 1.37 | 5.85 | 6.25 |
| C4 | LAD <i>C. macintyreii</i> | 1.45 | 7.50 | 7.50 |
| C5 | LAD <i>D. brouweri</i> | 1.90 | 7.50 | 7.75 |
| C6 | LAD <i>D. quinqueramus</i> | 5.60 | 17.00 | 26.50 |
| C7 | LAD <i>D. hamatus</i> | 8.85 | 36.00 | 45.50 |
| C8 | LAD <i>C. coalitus</i> | 9.00 | 36.00 | 45.50 |
| C9 | FAD <i>D. hamatus</i> | 10.00 | 45.50 | 46.00 |
| C10 | FAD <i>C. coalitus</i> | 10.80 | 47.00 | 47.50 |
| C11 | LAD <i>S. heteromorphus</i> | 14.40 | 68.00 | 70.00 |
| C12 | FAD <i>S. heteromorphus</i> | 17.10 | 100.00 | 102.00 |
| C13 | LAD <i>S. belemnos</i> | 17.40 | 100.00 | 102.00 |
| C14 | FAD <i>S. belemnos</i> | 21.50 | 102.00 | 111.50 |
| C15 | LAD <i>S. ciproensis</i> | 25.20 | 121.00 | 130.50 |
| C16 | LAD <i>S. distentus</i> | 28.20 | 130.50 | 140.00 |
| Planktonic foraminifers: | | | | |
| F1 | FAD <i>T. truncatulinoides</i> | 1.90 | 3.59 | 7.50 |
| F2 | FAD <i>T. tosaensis</i> | 3.10 | 17.00 | 30.09 |
| F3 | FAD <i>S. dehiscens</i> | 5.10 | 17.00 | 30.09 |
| F4 | FAD <i>G. tumida</i> | 5.20 | 17.00 | 30.09 |
| F5 | FAD <i>P. primalis</i> | 5.80 | 30.09 | 36.00 |
| F6 | LAD <i>G. fohsi robusta</i> | 11.50 | 57.09 | 57.72 |
| F7 | FAD <i>G. fohsi lobata</i> | 13.10 | 69.59 | 71.09 |
| F8 | FAD <i>G. praefohsi</i> | 13.90 | 71.09 | 72.59 |
| F9 | FAD <i>G. peripheroacuta</i> | 14.90 | 74.00 | 83.50 |
| F10 | FAD <i>Orbulina</i> | 15.20 | 74.00 | 83.50 |
| F11 | FAD <i>P. sicana</i> | 16.60 | 100.00 | 102.00 |
| F12 | LAD <i>P. kugleri</i> | 21.80 | 102.50 | 105.59 |
| F13 | FAD <i>G. dehiscens</i> | 23.20 | 111.50 | 115.08 |
| F14 | FAD <i>Globigerinoides</i> spp. | 24.30 | 121.00 | 124.58 |
| F15 | LAD <i>P. opima</i> | 28.20 | 140.00 | 143.58 |

Notes: Ages given are those from Berggren et al. (1985a, 1985b). "Top depth" denotes the lowest sample above a biohorizon; "Base depth" denotes the highest sample below the biohorizon. FAD = first appearance datum, and LAD = last appearance datum.

tion. The absence of nannofossil Subzone CN7a in Core 144-872A-5H is probably because of a short hiatus. Also, nannofossil Zone CN8 (0.65 m.y.) was not found in Core 144-872A-4H, suggesting another minor gap in the record, although the assemblage is very mixed at this level. An additional hiatus is possible in the unrecovered interval represented by Core 144-872A-3H, although if it does occur, it cannot be a major break because an early Pliocene assemblage of planktonic foraminifers and nannofossils was found in the core catcher of Core 144-872C-3H.

Sediment accumulation rates on Lo-En Guyot are generally comparable with those observed on Limalok (see "Sedimentation Rates" section, "Site 871" chapter, this volume). However, accumulation on Lo-En was significantly slower through the middle Miocene and Pleistocene.

INORGANIC GEOCHEMISTRY

Interstitial Waters

Interstitial waters were taken from 12 core samples in Hole 872A and analyzed according to the methods outlined in the "Explanatory Notes" chapter (this volume). All of these samples came from calcareous oozes comprising the pelagic cap in the upper 143 m. No interstitial water samples were taken from the underlying units. Shipboard interstitial water data from Site 872 are presented in Table 5.

Salinity and Chlorinity

Pore-water salinity values of samples from Hole 872A are indicative of normal seawater (consistently 35.5 ppt). Chlorinity

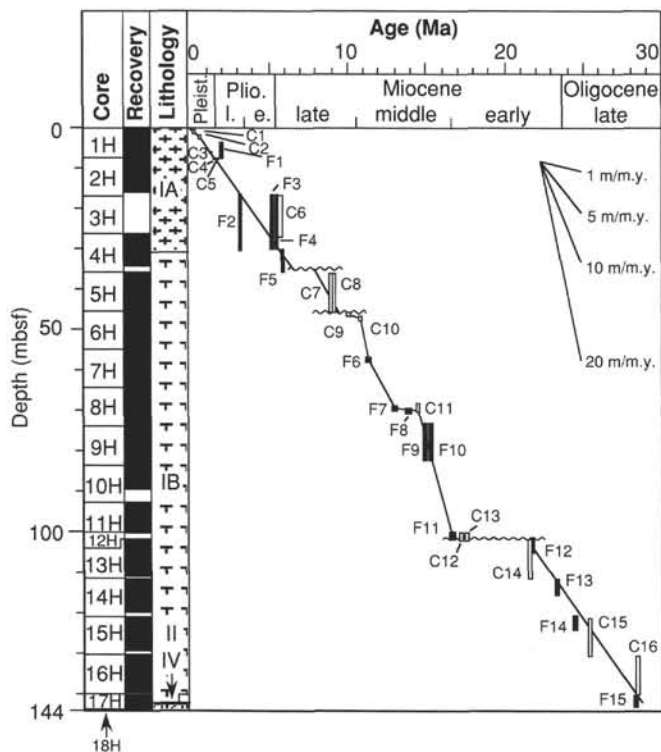


Figure 22. Sediment accumulation rates for the pelagic cap of Hole 872A. Bars represent the upper and lower limits of a biohorizon as constrained by sampling. Foraminifer biohorizons are indicated by filled bars, and calcareous nannofossils by open bars. Codes for biohorizons are keyed to Table 4.

measurements of these samples are also in the range of normal seawater (555–565 mM) and show no significant depth trend (Fig. 23).

Alkalinity, pH, Calcium, Magnesium, Sodium, Potassium, Rubidium, and Lithium

Calcium, magnesium, sodium, potassium, rubidium, and lithium concentrations remain constant with depth and are similar to seawater, with pore waters moderately enriched (~1–1.5 mM) with respect to seawater calcium concentrations (Fig. 23). The pH and alkalinity values that were measured have mean values of 7.63 and 2.42, respectively, and show no depth trend.

Silica

Silica concentrations of the interstitial water samples from Hole 872A range from 116.93 to 132.13 μM , show no depth trend, and reflect deep-sea concentrations.

Sulfate and Ammonium

Ammonium concentrations in the interstitial water samples from Hole 872A vary from 5.43 to 125.76 μM but show no systematic depth trend (Fig. 23). Sulfate pore-water concentrations are generally invariant with depth and indicative of normal seawater. The maximum ammonium pore-water concentration (125.76 μM) coincides with the minimum sulfate pore-water concentration (27.52 mM) in Sample 144-872A-2H-5, 145–150 cm, indicating some localized sulfate reduction and organic-matter decomposition at 6 m (Fig. 23).

Fluoride and Strontium

Fluoride and strontium concentrations in interstitial water samples from Hole 872A vary from 79 to 90 μM and from 104 to 115 μM , respectively, and are consistently enriched with respect to normal seawater (Table 5). Although the depth trends for fluoride and strontium are not simple, some covariation is present between these constituents (Fig. 23).

ORGANIC GEOCHEMISTRY

At Site 872, in addition to safety monitoring for hydrocarbon gases, 23 samples were analyzed to determine the content of inorganic carbon (IC). No determinations were made of total organic carbon, nitrogen, sulfur, and hydrogen because of malfunctioning instruments. The procedures used for the analytical program are described in the "Organic Geochemistry" section, "Explanatory Notes" chapter (this volume).

Volatile Hydrocarbons

The shipboard safety and pollution monitoring program requires regular measurements of light hydrocarbon gases (C_1 to C_3) in cores immediately after retrieval onto the core deck. Fifteen headspace gas samples were obtained from the pelagic carbonate ooze in Hole 872A. The results of the headspace gas analyses are given in Table 6. Very low concentrations of volatile hydrocarbon gases were detected. Methane concentrations varied from 2 to 3 ppm. The concentrations are only slightly higher than the general background of methane in the laboratory and on the core deck, which was found to vary from 1.8 to 2.1 ppm. Traces of ethane and propane were found in two of the samples. The very low

Table 5. Surface seawater and interstitial water geochemical data, Site 872.

| Core, section, interval (cm) | Depth (mbsf) | pH | Alkalinity (mM) | Salinity (g/kg) | Cl^- (mM) | Mg^{2+} (mM) | Ca^{2+} (mM) | SO_4^{2-} (mM) | NH_4^+ (μM) | SiO_2 (μM) | K^+ (mM) | Rb (μM) | Sr^{2+} (μM) | Na^+ (mM) | F (μM) | Li (μM) |
|------------------------------|--------------|------|-----------------|-----------------|--------------------|-----------------------|-----------------------|-------------------------|-----------------------------------|----------------------------------|-------------------|----------------------|------------------------------------|--------------------|---------------------|----------------------|
| Surface seawater | 0 | 8.01 | 2.30 | 35.0 | 555 | 53.34 | 10.65 | 28.9 | 7 | 11 | 10.00 | 1.40 | 91 | 498 | 70 | 26 |
| 144-872A- | | | | | | | | | | | | | | | | |
| 1H-4, 145–150 | 5.95 | 7.86 | 2.62 | 35.5 | 555 | 53.06 | 11.74 | 27.5 | 125 | 117 | 9.47 | 1.63 | 109 | 482 | 87 | 27 |
| 2H-5, 145–150 | 14.95 | 7.61 | 2.31 | 35.5 | 556 | 53.70 | 12.14 | 28.5 | 11 | 126 | 9.86 | 1.55 | 109 | 491 | 90 | 27 |
| 4H-4, 145–150 | 32.45 | 7.32 | 2.25 | 35.5 | 556 | 53.78 | 12.31 | 28.6 | 15 | 132 | 9.52 | 1.56 | 115 | 501 | 84 | 26 |
| 5H-5, 145–150 | 43.45 | 7.60 | 2.27 | 35.5 | 560 | 53.95 | 11.97 | 28.8 | 5 | 115 | 9.18 | 1.58 | 105 | 502 | 86 | 27 |
| 6H-5, 140–150 | 52.90 | 7.66 | 2.33 | 35.5 | 565 | 52.86 | 12.18 | 28.7 | 17 | 117 | 9.33 | 1.53 | 106 | 497 | 88 | 26 |
| 7H-5, 140–150 | 62.40 | 7.63 | 2.31 | 35.5 | 562 | 54.06 | 12.18 | 28.6 | 13 | 128 | 9.23 | 1.57 | 109 | 497 | 88 | 26 |
| 8H-5, 143–150 | 71.93 | 7.54 | 2.40 | 35.5 | 555 | 54.02 | 12.22 | 29.0 | 7 | 136 | 9.47 | 1.58 | 111 | 505 | 79 | 27 |
| 9H-5, 143–150 | 81.43 | 7.63 | 2.38 | 35.5 | 559 | 54.01 | 11.99 | 28.9 | 40 | 132 | 9.52 | 1.53 | 105 | 505 | 85 | 27 |
| 10H-5, 140–150 | 90.90 | 7.56 | 2.35 | 35.5 | 562 | 52.24 | 11.99 | 28.7 | 16 | 126 | 9.38 | 1.53 | 106 | 493 | 81 | 26 |
| 11H-4, 143–150 | 98.93 | 7.67 | 2.46 | 35.5 | 563 | 53.39 | 12.06 | 28.7 | 17 | 126 | 9.47 | 1.57 | 104 | 502 | 85 | 27 |
| 14H-5, 143–150 | 118.93 | 7.72 | 2.74 | 35.5 | 563 | 53.54 | 11.66 | 28.9 | 22 | 123 | 9.52 | 1.59 | 106 | 502 | 79 | 27 |
| 17H-2, 143–150 | 142.93 | 7.76 | 2.63 | 35.5 | 564 | 53.80 | 11.64 | 28.7 | 39 | 128 | 9.57 | 1.61 | 107 | 501 | 82 | 26 |

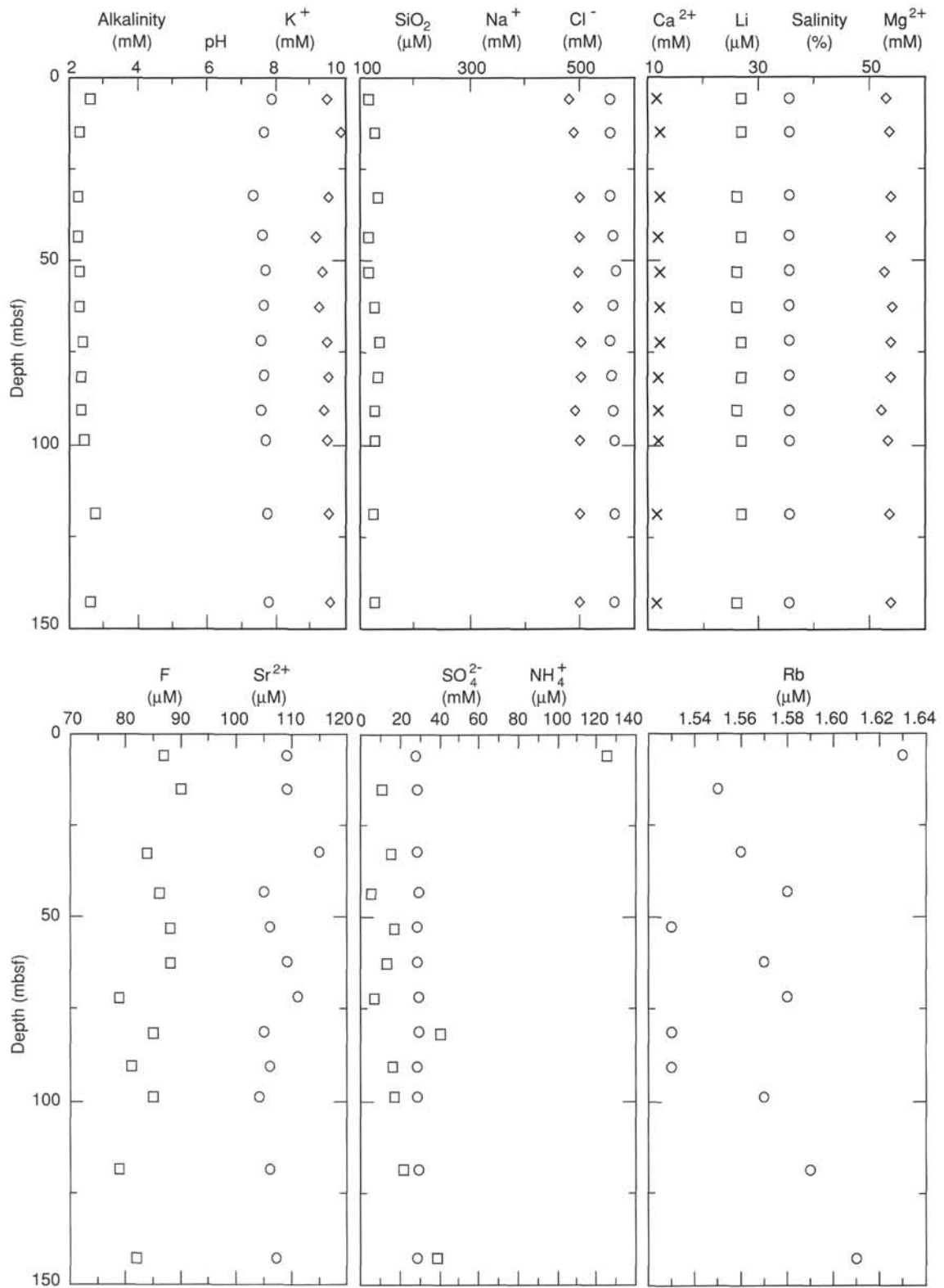


Figure 23. Concentrations of interstitial pore-water parameters vs. depth, Hole 872A. Concentration values remain constant at near seawater values throughout the 143 m of the pelagic cap, with the exception of minor elevations in calcium, fluoride, and strontium and localized sulfate depletion together with ammonium enrichment (see text for details).

Table 6. Results of headspace gas analyses, Hole 872A.

| Core, section, interval (cm) | Methane (ppm) | Ethane (ppm) | Propane (ppm) |
|------------------------------|---------------|--------------|---------------|
| 144-872A- | | | |
| 1H-5, 0-5 | 2.2 | Tr | Tr |
| 2H-6, 0-5 | 2.7 | None | Tr |
| 4H-6, 0-5 | 2.0 | None | None |
| 5H-6, 0-5 | 2.6 | None | None |
| 6H-6, 0-5 | 2.0 | None | None |
| 7H-6, 0-5 | 2.0 | None | None |
| 8H-6, 0-5 | 2.3 | None | None |
| 9H-6, 0-5 | 2.5 | None | None |
| 10H-6, 0-5 | 2.0 | None | None |
| 11H-5, 0-5 | 2.0 | None | None |
| 13H-6, 0-5 | 1.9 | None | None |
| 14H-6, 0-5 | 2.0 | None | None |
| 15H-6, 0-5 | 2.0 | None | None |
| 16H-5, 0-5 | 2.5 | None | None |
| 17H-3, 0-5 | 2.8 | Tr | None |
| Laboratory background | 2.1 | None | None |
| Core deck background | 1.9 | None | None |

Notes: Tr = trace, and None = no gas detected.

volatile gas concentration in the pelagic cap can be ascribed to low concentrations of organic carbon in these sediments (TOC below 0.5%; see paragraph on organic carbon).

Carbonate Carbon

Inorganic carbon content (IC) was measured in 23 samples from Holes 872A and 872B with the Coulometrics carbon dioxide coulometer. No carbonate determinations were performed on samples from Hole 872C. In Hole 872A, one sample from each core of the pelagic cap was analyzed for IC. Most of the samples were obtained from the material squeezed for pore-water analysis, as described in the "Inorganic Geochemistry" section, "Explanatory Notes" chapter (this volume). By using this approach, samples should be virtually free of pore water before drying and no pore-water precipitates are expected. Nevertheless, a few samples desalted before coulometer analysis were found to be significantly higher in IC than the squeeze-cake samples (see Fig. 24), probably reflecting minor amounts of pore-water salts precipitated during sample handling. Thus, the most accurate carbonate determinations are obtained from desalted samples. This procedure should be applied for precise carbonate determinations of pelagic oozes in the future. In Hole 872B, which contained indurated limestones, three microsamples (approximately 100 mg) were collected by hand drilling, using a standard 5-mm drill bit.

The IC and calcium carbonate values for Holes 872A and 872B are given in Table 7. Calcium carbonate content was very high in all samples from the pelagic cap, ranging from 94% to 99% (average = 96.9%, standard deviation = 1.39). The minor fluctuations with depth seen in Hole 872A (Fig. 24) can probably be ascribed to analytical error (see above) and are not considered significant except for the shift toward lower calcium carbonate values in the bottom of the hole (Core 144-872A-17H). The carbonate content of the limestone matrix of the basalt breccias in Core 144-872B-4R-1 was between 91% and 97%.

Organic Carbon and Total Sulfur

Because of malfunctioning analytical instruments, no determinations were made of organic carbon and total sulfur.

Organic Matter Type and Thermal Maturation Level

Shipboard geochemical characterizations of organic matter are normally performed by Rock-Eval (RE) and pyrolysis gas chro-

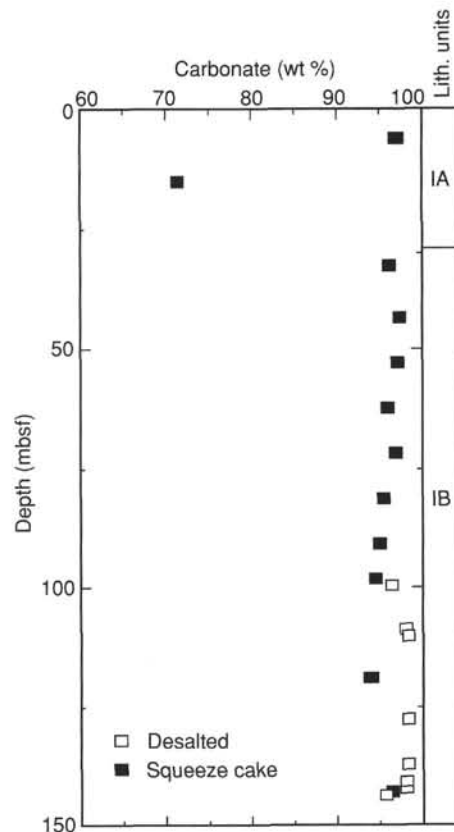


Figure 24. Carbonate content of sediments in Holes 872A and 872B, calculated as calcium carbonate. Also shown are the major lithologic units, as given in the "Lithostratigraphy" section (this chapter).

Table 7. Results of geochemical analyses, Holes 872A and 872B.

| Core, section, interval (cm) | Lithology | Depth (mbsf) | IC (wt%) | CaCO ₃ (wt%) |
|------------------------------|-----------------|--------------|----------|-------------------------|
| 144-872A- | | | | |
| 1H-4, 145-150 | Calcareous ooze | 5.95 | 11.66 | 97.15 |
| 2H-5, 145-150 | Calcareous ooze | 14.95 | 8.59 | 71.57 |
| 4H-4, 145-150 | Calcareous ooze | 32.45 | 11.55 | 96.23 |
| 5H-5, 145-150 | Calcareous ooze | 43.45 | 11.71 | 97.57 |
| 6H-5, 145-150 | Calcareous ooze | 52.90 | 11.68 | 97.32 |
| 7H-5, 145-150 | Calcareous ooze | 62.40 | 11.54 | 96.15 |
| 8H-5, 143-145 | Calcareous ooze | 71.93 | 11.64 | 96.98 |
| 9H-5, 143-145 | Calcareous ooze | 81.43 | 11.47 | 95.57 |
| 10H-5, 140-150 | Calcareous ooze | 90.90 | 11.42 | 95.15 |
| 11H-4, 69-71 | Calcareous ooze | 98.19 | 11.35 | 94.57 |
| 11H-5, 69-71 | Calcareous ooze | 99.69 | 11.59 | 96.57 |
| 13H-5, 69-71 | Calcareous ooze | 108.69 | 11.80 | 98.32 |
| 13H-6, 69-71 | Calcareous ooze | 110.19 | 11.82 | 98.48 |
| 14H-5, 143-150 | Calcareous ooze | 118.93 | 11.29 | 94.07 |
| 15H-5, 69-71 | Calcareous ooze | 127.69 | 11.83 | 98.57 |
| 16H-5, 69-71 | Calcareous ooze | 137.19 | 11.83 | 98.57 |
| 17H-1, 69-71 | Calcareous ooze | 140.69 | 11.80 | 98.32 |
| 17H-2, 69-71 | Calcareous ooze | 142.19 | 11.78 | 98.15 |
| 17H-2, 143-150 | Calcareous ooze | 142.93 | 11.59 | 96.57 |
| 17H-3, 69-71 | Calcareous ooze | 143.69 | 11.50 | 95.82 |
| 144-872B- | | | | |
| 4R-1, 19-21 | Limestone | 135.39 | 10.95 | 91.24 |
| 4R-1, 51-52 | Limestone | 135.71 | 11.29 | 94.07 |
| 4R-1, 68-71 | Limestone | 135.88 | 11.55 | 96.23 |

Notes: IC = inorganic carbon. CaCO₃ = carbonate carbon calculated as calcium carbonate.

matographic (Py-GC) analyses. During the time spent at Site 872, neither the Rock-Eval system nor the Geofina Py-GC were operating properly; therefore, no results are reported here. Visual inspection by light microscopy shows organic matter to be thermally immature, as judged from the light brown to yellow color of the particles.

Conclusions

The following conclusions can be made regarding the organic geochemistry at Site 872: (1) no volatile hydrocarbons were encountered at Site 872; (2) the pelagic cap sediments (Lithologic Unit I) have a calcium carbonate content of almost 100%; and (3) organic matter at this site is thermally immature with regard to hydrocarbon formation.

IGNEOUS PETROLOGY

Introduction

Three holes were drilled at Site 872 on Lo-En Guyot. Basalt was recovered in the bottom of each hole, although only small amounts were recovered from Holes 872A and 872C. Hole 872B penetrated 57.3 m into basalt, starting at 135.4 mbsf, with 41% recovery. Basalt was reached at 143.7 and 142.75 mbsf, with 0.29 and 2.06 m of recovery in Holes 872A and 872C, respectively. The interval and a description of each unit are in Table 8.

The uppermost basalt unit in each hole is an alkali olivine basalt. On the basis of petrographically determined texture, mineralogy, and alteration, Unit 1 in Hole 872A and Unit 5 in Hole 872B (the first basalt flow; Units 1–4 are conglomerates and fracture fill) appear to be from the same flow. Unit 1 in Hole 872C is quite different in texture and mineralogy from any unit in Hole 872B and is likely to have been from a different flow. Beginning in Section 144-872B-4R-1, 21 cm, Units 5–18 are a series of

differentiated basalt and hawaiite flows. Unit 11 may be a mugearite. Thick, brecciated flow tops occur in Unit 10 (Section 144-872B-5R-4, 24 cm) and several units downsection, suggesting that these flows were erupted subaerially. Below Unit 14 (Section 144-872B-7R-2, 0 cm), recovery is sufficiently complete to establish that the time interval between flows was short enough to preclude soil development on top of the flows.

This sequence of flows appears to represent the very latest shield stage or the alkalic-cap stage of hotspot volcanism.

Hole 872A

Twenty-nine centimeters of a severely altered, aphyric basalt were recovered in Hole 872A. The matrix is light brownish gray and has been altered to clay minerals. Abundant veins and vesicles filled with calcite, zeolites, and brown clays are also present. Much of the groundmass has been obscured by green and brown clays. The identifiable groundmass mineralogy is 8% iddingsite and green clay pseudomorphs after olivine; 56% plagioclase laths, most pseudomorphed by speckled brown clays; and 15% subhedral titanomagnetite grains and trace ilmenite needles, most pseudomorphed by hematite. This mineralogy is consistent with the unit being a differentiated alkali olivine basalt.

Hole 872B

Units 1–6

Units 1–6 include volcanic and biogenic materials recovered in Core 144-872B-4R-1. Only Unit 6 is large enough and fresh enough to be useful for igneous petrology and geochemistry, but the intercalated sediments are of particular interest in view of their Cretaceous faunas (see "Biostratigraphy" section, this chapter) and because they provide a minimum age for the underlying basalt.

Table 8. Summary of igneous units, Site 872.

| Unit | Core, section, interval (cm) | Description |
|------------|---|--|
| Hole 872A: | | |
| 1 | 144-872A-18X-1, 0–29 cm | Clinopyroxene basalt |
| Hole 872B: | | |
| 1 | 144-872B-4R-1, 0–13 cm | Volcanogenic sandstone |
| 2 | 144-872B-4R-1, 13–16 cm | Phosphatic pebble conglomerate with foraminifer limestone matrix |
| 3 | 144-872B-4R-1, 17–21 cm | Basalt pebble conglomerate with foraminifer limestone matrix |
| 4 | 144-872B-4R-1, at 28, 34, 50, 60, and 67 cm | Foraminifer limestone fracture filling in Units 5 and 6 |
| 5 | 144-872B-4R-1, 21–31 | Olivine basalt |
| 6 | 144-872B-4R-1, 33 cm, to -5R-2, 6 cm | Clinopyroxene basalt |
| 7 | 144-872B-5R-2, 6–11 cm | Aphyric basalt |
| 8 | 144-872B-5R-2, 11–43 cm | Aphyric basalt |
| 9 | 144-872B-5R-2, 43 cm, to -5R-4, 23 cm | Clinopyroxene basalt Subunit 9A flow-top breccia Subunit 9B massive flow |
| 10 | 144-872B-5R-4, 24 cm, to -6R-1, 67 cm | Aphyric basalt Subunit 10A flow-top breccia Subunit 10B massive flow |
| 11 | 144-872B-6R-1, 74–100 cm | Clinopyroxene basalt |
| 12 | 144-872B-6R-1, 101–126 cm | Aphyric basalt |
| 13 | 144-872B-7R-1, 0–65 cm | Clinopyroxene basalt |
| 14 | 144-872B-7R-2, 0 cm, to -7R-6, 43 cm | Clinopyroxene-olivine basalt Subunit 14A flow-top breccia Subunit 14B massive flow |
| 15 | 144-872B-7R-6, 43 cm, to -7R-7, 83 cm | Clinopyroxene basalt Subunit 15A flow-top breccia Subunit 15B massive flow |
| 16 | 144-872B-7R-7, 83 cm, to -9R-1, 5 cm | Clinopyroxene basalt Subunit 16A flow-top breccia Subunit 16B massive flow. |
| 17 | 144-872B-9R-1, 6 cm, to -9R-3, 90 cm | Aphyric basalt Subunit 17A flow-top breccia Subunit 17B massive flow |
| 18 | 144-872B-9R-3, 91 cm, to -9R-6, 60 cm | Olivine-clinopyroxene basalt Subunit 18A flow-top breccia Subunit 18B massive flow |
| 19 | 144-872B-9R-6, 60–72 cm | Very altered basalt |
| Hole 872C: | | |
| 1 | 144-872C-17X-CC, 48 cm, to -18X-2, 60 cm | Olivine basalt |

Unit 1 (Interval 144-872B-4R-1, 0–13 cm) is a pale yellow to light yellowish brown volcanogenic sandstone. Unit 2 (Interval 144-872B-4R-1, 13–16 cm) is a phosphatic pebble conglomerate. Dark brown phosphatic pebbles and occasional angular basalt clasts with 1–2 cm diameters are in a friable foraminifer limestone matrix. Unit 3 (Interval 144-872B-4R-1, 17–21 cm) is a conglomerate with subrounded to subangular, 0.5–5 cm basalt clasts in a white foraminifer limestone matrix. Unit 4 includes several fracture fillings of foraminifer limestone within the basalts of Units 5 and 6 (see “Biostratigraphy” section, this chapter).

Unit 5 (Interval 144-872B-4R-1, 21–31 cm) is a sparsely olivine-phyric basalt. Patches of brown clay obscure 30% of the groundmass. What remains is 10% iddingsite and green clay pseudomorphs after olivine, 15% hematite pseudomorphs after euhedral titanomagnetite, and 45% plagioclase laths, mostly pseudomorphed by brown speckled clays. This mineralogy is consistent with the unit being a differentiated alkali olivine basalt, indistinguishable from the basalt of Hole 872A, Unit 1.

Unit 6 (from Sections 144-872B-4R-1, 31 cm, to -5R-1, 150 cm) contains sparse, dark green phenocrysts. The matrix is yellowish brown and appears quite altered, but less so in the lower part of the unit where its color is grayer. It contains fewer than 1% olivine phenocrysts, which are unaltered and have anhedral, resorbed shapes subsequently rimmed with optically continuous skeletal overgrowths and 7% euhedral plagioclase phenocrysts. The groundmass consists of plagioclase microlites (An_{35–45}) arranged in a pilotaxitic texture, and 20% euhedral to subhedral titanomagnetite microphenocrysts. The texture and plagioclase composition of this lava suggest that it is an hawaiite.

Units 7–9 and 11–13

Units 7–13, excluding Unit 10, are six distinct lava flows with recovered thicknesses between 26 cm and 2.61 m. Flow boundaries were not recovered.

All these flows are aphyric or sparsely clinopyroxene-phyric basalts with microcrystalline groundmasses. Groundmass colors range from dusky reds and yellowish browns, indicative of oxidation and severe alteration to clay and zeolite minerals, respectively, to shades of medium and dark gray indicative of less alteration. Units 9 and 13 have mottled red and gray groundmasses.

Round to irregular vesicles occur in Units 8, 9, and 13. The abundances of vesicles are widely variable within each flow (5%–40%, with an average of about 20%), and they range in size from 0.25 mm to 1 cm. A small number of vesicles are lined with blue and green clay, but most are filled with calcite and white or pinkish orange zeolites. Larger vesicles typically have a 2-mm rim of the pinkish orange zeolite and a calcite-filled center. An X-ray diffraction (XRD) analysis of the pinkish orange zeolite indicated that it is the mineral chabazite.

Subhorizontal sparry calcite and zeolite veins are uniformly distributed throughout each flow. They are <1 to 7 mm in width and are spaced about 10–12 cm apart.

Unit 9 has been divided into Subunits 9A and 9B, separated by a gradational boundary between a more altered and oxidized upper zone (A), and a less altered and oxidized lower zone (B). In thin section, there are 5%–10%, subhedral, slightly pink (titaniferous?) augite phenocrysts, traces of titanomagnetite and <5% ilmenite microphenocrysts, and 80% plagioclase phenocrysts and microlites. This mineralogy suggests that this flow is a differentiated alkalic basalt or perhaps an hawaiite.

Unit 11 has 3% pseudomorphs after olivine, 55% euhedral plagioclase phenocrysts and microlites, subequal (about 5% each) abundances of euhedral titanomagnetite and ilmenite needles, both of which appear in reflected light to be fresh, trace, anhedral

potassic feldspar, biotite, and hornblende. The flow has been extensively altered to very bright green phyllosilicates (chlorite?) and brown speckled clays, which cover 25% of the groundmass in irregular 0.25–1 mm patches. The “chloritization” of the sample, which is a common characteristic of equivalent Samoan lavas, and the presence of biotite, hornblende, and potassic feldspar suggest that the flow is a mugearite.

Unit 13 is pervasively altered, with both phenocrysts and groundmass replaced by phyllosilicates. Pseudomorphs of plagioclase (47%), olivine (1%), titanomagnetite (7%), and accessory ilmenite can still be distinguished. Despite the alteration, 2% of unaltered olivine and clinopyroxene xenocrysts persist. The severity of alteration makes identification very difficult, but the mineralogy that can be discerned suggests that the flow was a differentiated alkali olivine basalt.

Units 10 and 14–18

Unit 10 and Units 14 through 18 are single flows, each with a relatively thick flow-top breccia above a massive base. Recovered thicknesses of brecciated flow tops vary from 19 cm to 3.28 m, whereas recovered thicknesses of massive flows vary from 91 cm to 3.39 m.

Clasts in the flow-top breccias are typically subangular and 1–10 cm across; occasional larger clasts, up to 30 cm, are present. They are aphyric (smaller clasts) to sparsely clinopyroxene-phyric (larger clasts). Colors vary within each flow top; usually clasts of both dark red and medium to dark gray are present. The Unit 16 flow top has very indistinct clast-matrix boundaries; all other flow tops have very distinct clast-matrix boundaries.

Except for Unit 18, in which all the clasts are nonvesicular, the clasts of the flow-top breccias have vesicle abundances varying from 0% to 50%. The vesicles are 0.5–10 mm in size, irregular to round in shape, and either filled with calcite and the pinkish orange zeolite (chabazite?) or lined with blue and green clays. A few are filled with dark green clay. Figure 25 is a photo of a typical portion of flow-top breccia.

The matrix around the clasts consists of sand- and granule-sized (2–4 mm), subrounded volcanoclastic grains. These are cemented by calcite and chabazite. Units 10 and 18 also have patches of dark green phyllosilicates in the flow-top matrix.

The massive portions of the flows are aphyric to sparsely clinopyroxene and olivine-phyric with microcrystalline groundmasses. Groundmass colors are medium gray where fresh, and yellowish, reddish, and greenish gray where more alteration has occurred. The massive portions of Units 14 and 16 have a more altered yellowish gray zone with dark iron staining along fractures in the lower halves, returning to fresher material about 30 cm above the top of the next unit.

All massive portions of the units are vesicular. Vesicles tend to be concentrated in subhorizontal bands on a scale of roughly 10–30 cm, with abundances ranging from 2% to 50%. As in the flow tops, vesicle centers are filled with calcite and a white zeolite, often inside a 2-mm rim of the pinkish orange zeolite; a few are empty and lined with blue and green clays.

Veins constitute 1%–4% of all these flows, increasing to 10% in the massive portion of Unit 18. They are 0.25–7 mm thick, filled with sparry calcite and zeolites, and are often subhorizontal. In Unit 18 the veins occur in subhorizontal anastomosing bands, 5–20 mm in width, spaced roughly every 5 cm (see Fig. 26). These veins give a strong impression of shearing, but no evidence for deformation of the intervening lavas exists.

Several of the contacts between the brecciated flow tops and massive bottoms were recovered within a single piece of core. The contact between the massive bottom of Unit 14 and the brecciated top of Unit 15 was also recovered. No evidence of soil develop-

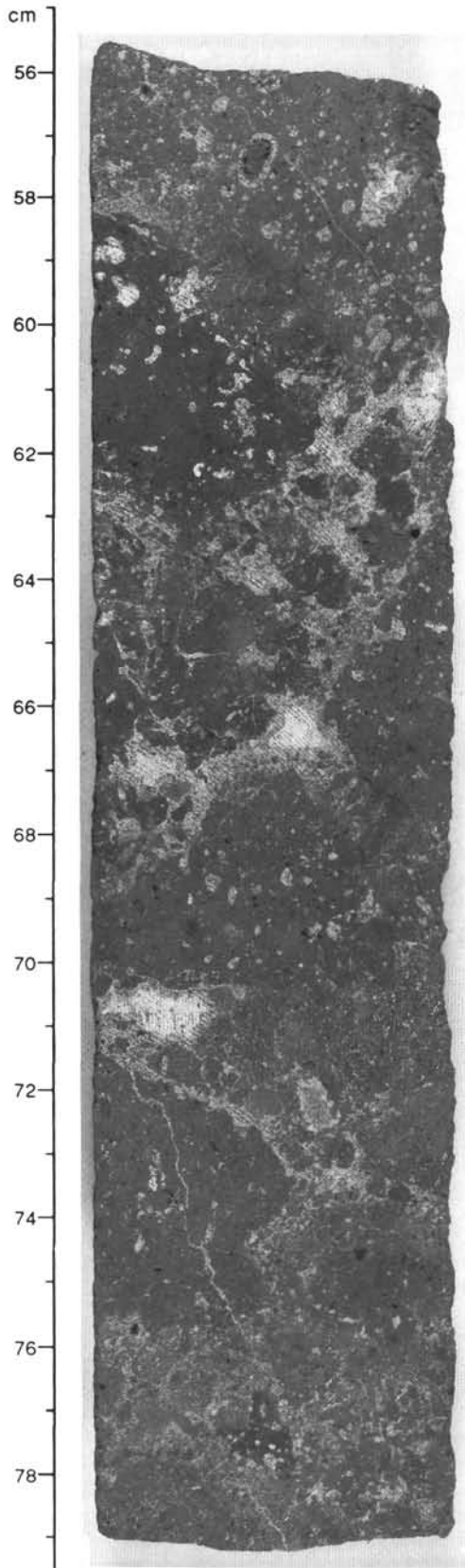


Figure 25. Interval 144-872B-7R-3, 55–80 cm, part of Igneous Subunit 14A. Flow-top breccia of 1–10 cm, subangular clasts in a volcanogenic sand matrix cemented by calcite (white) and the zeolite chabazite (light gray in photo, with very visible saw marks). Typical of the flow-top breccias in Hole 872B.

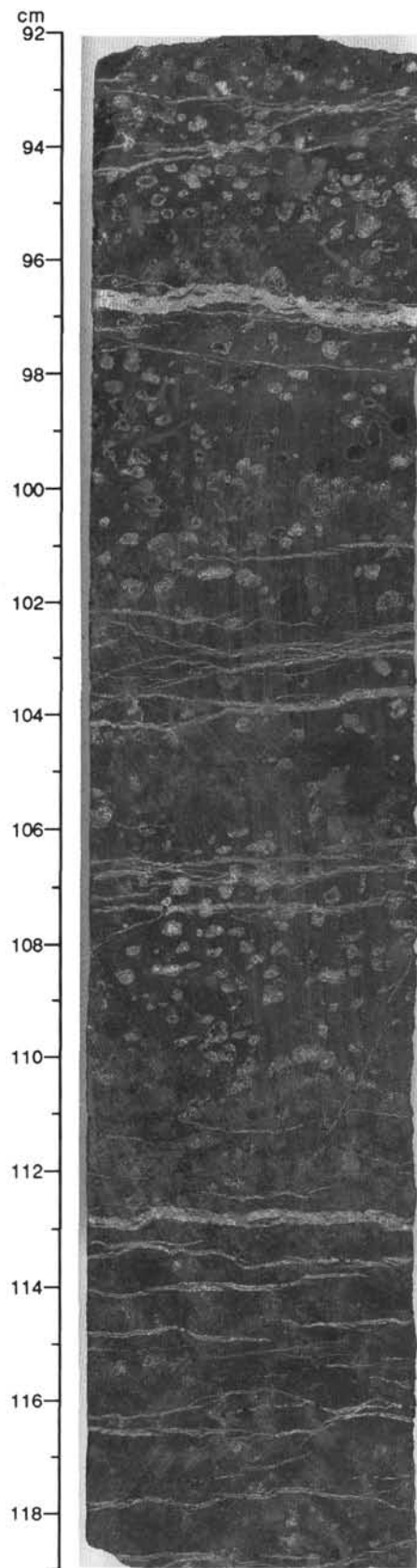


Figure 26. Interval 144-872B-9R-4, 92–119 cm, part of Igneous Subunit 18B. Vesicular, massive flow portion of Unit 18 with anastomosing veins of calcite. Vesicles are filled with calcite and chabazite.

ment at this contact or anywhere else in these flows is present; they appear to have been erupted subaerially in a short period of time.

In thin section, Units 10, 14, 15, 16, and 17 have 45%–70% plagioclase phenocrysts and microlites, often forming a slightly felted texture, and 8%–25% euhedral titanomagnetite microphe-nocrysts. Ilmenite is present in some of the flows. Mafic phe-nocrysts and microphenocrysts are present in small amounts in most of the flows. Many are now pseudomorphs after phyllosili-cates, and much of the groundmass of each flow has been ob-scured by green and brown clays. The low abundances of olivine and clinopyroxene, the lack of orthopyroxene, and the preponder-ance of plagioclase and titanomagnetite suggest that these lavas belong to a differentiated alkalic series. Units 14, 15, and 16 appear to be differentiated alkalic basalts. Unit 17, which lacks mafic phenocrysts, is probably an hawaiite.

Unit 18 has a groundmass very similar to the overlying flows; it is probably an hawaiite, based on the composition of the pla-gioclase (An_{30–35}) and on the low abundances (5% total) of oxide minerals. However, the lava contains 17% fibrous, subhedral pseudomorphs after olivine and 3% fresh, cracked, anhedral augites. These are unlikely to have been in equilibrium with the groundmass and are interpreted as xenocrysts.

Hole 872C

The basalt pieces recovered from Hole 872C appear to be from a single flow. They are aphyric, with a medium gray groundmass that consists of 15% iddingsite and green clay pseudomorphs after olivine; 4% ilmenite needles and 1% titanomagnetite grains, both replaced by hematite; 5% slightly pink (titaniferous), fresh augite; and 70% slightly altered (to clay) microlites of plagioclase. The mineralogy suggests that the sample is a differentiated alkali olivine basalt. However, the unit differs, by the presence of clinopyroxene microphenocrysts and a distinct subophitic texture, from the flow(s) sampled at the top of the basaltic units in Holes 872A and 872B, and thus is probably not the same flow.

PHYSICAL PROPERTIES

Introduction

The objectives of the physical properties measurement pro-gram at Site 872 were (1) to measure the standard shipboard physical properties and (2) to identify geotechnical units for downhole and cross-hole correlations. The standard shipboard physical properties program included (1) nondestructive mea-surements of bulk density, acoustic compressional velocity, and magnetic susceptibility, made using sensors mounted on the mul-tisensor track (MST); and (2) discrete measurements of index properties, vane shear strength, compressional wave velocity, and thermal conductivity (see “Explanatory Notes” chapter, this vol-ume). Shear strength was measured on the pelagic sediments using the Wykeham-Farrance vane shear device. Thermal conduc-tivity measurements were made using the needle-probe method in un lithified sediments (von Herzen and Maxwell, 1959); the slab method was used in basalts (Vacquier, 1985). Compressional wave velocities were measured using the digital sound velocime-ter (DSV) in the pelagic sediments and the Hamilton Frame (HF) on sample cubes of the basalts. All whole-round sections were passed through the MST-mounted sensors before being split; shipboard and shore-based whole-round samples were cut first from either end of the section.

Sediments recovered at Site 872 consist of un lithified nanno-fossil foraminifer ooze (Hole 872A, 0–30 mbsf; Hole 872C, 0–18 mbsf) and foraminifer ooze (Hole 872A, 30–144 mbsf; Hole 872C, 18–148 mbsf) forming the pelagic cap on the guyot. The pelagic sediments are very similar lithologically to those from

Site 871. Pelagic sediments from Holes 872A and 872C were sampled at intervals of 1.5 to 4.0 m. Basalt, altered and/or weath-ered to various degrees, underlies the pelagic sediments. The only limestone at this site was observed as infillings of lithified car-bonate in the basalt. Core recovery in the pelagic cap varied from 0% to 100%; however, the average recovery of pelagic cap sedi-ments was 85%. In contrast, core recovery in the basalts averaged only 25% (range of 0%–88% recovery). Basalts were sampled at each lithologic change where recovery permitted. As was the case with Site 871, samples were shared with other shipboard labora-tories where appropriate.

The pelagic oozes from Hole 872A suffered considerable disturbance from both drilling, handling, and splitting operations (see “Physical Properties” section, “Site 871” chapter, this vol-ume). To reduce disturbance to the pelagic sediments, special handling procedures were used for cores from Hole 872C. The liners were cut into sections and stored upright on the catwalk before making whole-round measurements and splitting the core. After allowing time for settlement, free water was drained off, the core liner was trimmed to the upper level of the sediments, and the core sections were capped. This process was generally suc-cessful in reducing the proportion of free water in each section and, hence, in improving the quality of whole-core measurements.

The results from physical properties measurements on the pelagic sediments and basalts are similar to those obtained at Site 871. Bulk density profiles for Hole 872C show a characteristic uniformity, with the exception of the uppermost 35 m of sediment, where some variation is observed (also seen at Site 871). There were two peaks in bulk density in the upper pelagic cap: one near 8 mbsf and the other near 28 mbsf. Physical properties data from Site 872 are presented in Tables 9 (index properties), 10 (thermal conductivity), 11 (DSV velocities), 12 (HF velocities), and 13 (vane shear strength).

Geotechnical and Properties Units

Pelagic Cap

Geotechnical Subunits 1A and 1B were defined through an examination of discrete measurements of physical properties (Figs. 27–29 and Table 9), and using the GRAPE density profiles (Fig. 30). At Holes 872A and 872C, Geotechnical Subunit 1A (Hole 872A, 0–30 mbsf, and Hole 872C, 0–32 mbsf) coincides with Lithologic Subunit IA. The lack of core recovery in Core 144-872A-3H at Hole 872A resulted in a gap in the density profile at an important point downhole, thus making the correlation between holes in the lower portion of Geotechnical Unit 1A uncertain.

The discrete density profile for Hole 872C shows two well-de-fined peaks at approximately 14 and 28 mbsf. Below 35 mbsf in Holes 872A and 872B, the measured bulk density of discrete samples of pelagic sediment is fairly uniform; dry-bulk densities are between 0.6 and 0.7 g/cm³ and wet-bulk densities are between 1.4 and 1.5 g/cm³.

The water content data reveal a trend toward a peak in water content at 50 mbsf in both Holes 872A and 872C (Figs. 27 and 29), despite moderate scatter. A second peak is also suggested at a depth of 85 mbsf in both holes. Below 50 mbsf, a gradual reduction in water content takes place. Errors in the determination of water content and wet-bulk density are introduced by the rapid draining of the foraminifer oozes on the workbench. Samples taken from the deepest part of the split core contain more water than those taken from the cut surface.

The GRAPE profiles, from 0 to 35 mbsf in Holes 872A and 872C, are in good agreement with each other when allowance is made for the shortened section lengths in Hole 872C. A series of large density peaks observed just above 30 mbsf in Hole 872A are found just below 30 mbsf in Hole 872C. A low-density interval

Table 9. Index properties data, Site 872.

| Core, section, interval (cm) | Depth (mbsf) | Wet-bulk density (g/cm ³) | Dry-bulk density (g/cm ³) | Grain density (g/cm ³) | Porosity (%) | Water content (% dry wt) |
|------------------------------|--------------|---------------------------------------|---------------------------------------|------------------------------------|--------------|--------------------------|
| 144-872A- | | | | | | |
| 1H-1, 40-42 | 0.40 | 1.50 | 0.76 | 2.81 | 75.00 | 104.30 |
| 1H-1, 130-132 | 1.30 | 1.45 | 0.69 | 2.61 | 76.50 | 118.40 |
| 1H-2, 100-102 | 2.50 | 1.46 | 0.69 | 2.69 | 77.60 | 119.50 |
| 1H-3, 100-102 | 4.00 | 1.52 | 0.76 | 2.78 | 76.70 | 107.00 |
| 1H-4, 100-102 | 5.50 | 1.52 | 0.76 | 2.70 | 76.70 | 107.00 |
| 1H-5, 100-102 | 7.00 | 1.49 | 0.74 | 2.80 | 75.40 | 107.80 |
| 2H-1, 100-102 | 8.50 | 1.48 | 0.73 | 2.73 | 75.80 | 110.10 |
| 2H-2, 100-102 | 10.00 | 1.49 | 0.74 | 2.70 | 75.60 | 107.90 |
| 2H-3, 100-102 | 11.50 | 1.51 | 0.76 | 2.75 | 75.20 | 104.70 |
| 2H-4, 60-62 | 12.60 | 1.50 | 0.75 | 2.74 | 75.00 | 105.70 |
| 2H-5, 120-122 | 14.70 | 1.53 | 0.81 | 2.82 | 73.60 | 96.70 |
| 2H-6, 20-22 | 15.20 | 1.48 | 0.70 | 2.79 | 78.30 | 119.00 |
| 4H-1, 30-32 | 26.80 | 1.51 | 0.78 | 2.66 | 73.80 | 100.90 |
| 4H-2, 30-32 | 28.30 | 1.63 | 0.96 | 2.74 | 68.40 | 75.30 |
| 4H-3, 30-32 | 29.80 | 1.56 | 0.86 | 2.78 | 70.50 | 86.30 |
| 4H-4, 30-32 | 31.30 | 1.43 | 0.65 | 2.83 | 78.70 | 128.60 |
| 4H-5, 30-32 | 32.80 | 1.45 | 0.67 | 2.78 | 78.10 | 123.90 |
| 5H-1, 80-82 | 36.80 | 1.45 | 0.67 | 2.80 | 79.00 | 127.10 |
| 5H-2, 80-82 | 38.30 | 1.44 | 0.65 | 2.75 | 79.50 | 130.80 |
| 5H-3, 80-82 | 39.80 | 1.42 | 0.63 | 2.75 | 79.70 | 134.80 |
| 5H-4, 80-82 | 41.30 | 1.44 | 0.62 | 2.75 | 82.40 | 142.00 |
| 5H-5, 80-82 | 42.80 | 1.42 | 0.63 | 2.82 | 80.00 | 137.20 |
| 6H-2, 130-132 | 48.30 | 1.38 | 0.58 | 2.66 | 81.40 | 152.20 |
| 6H-4, 125-127 | 51.25 | 1.41 | 0.61 | 2.70 | 80.60 | 141.00 |
| 6H-6, 80-82 | 53.80 | 1.43 | 0.62 | 2.71 | 81.40 | 140.50 |
| 7H-2, 35-37 | 56.85 | 1.39 | 0.59 | 2.72 | 81.20 | 147.80 |
| 7H-4, 100-102 | 60.50 | 1.42 | 0.63 | 2.78 | 79.40 | 134.50 |
| 7H-6, 50-52 | 63.00 | 1.40 | 0.61 | 2.71 | 79.60 | 139.10 |
| 8H-1, 100-102 | 65.50 | 1.44 | 0.67 | 2.59 | 77.60 | 123.50 |
| 8H-3, 100-102 | 68.50 | 1.42 | 0.63 | 2.75 | 79.60 | 135.30 |
| 8H-5, 80-82 | 71.30 | 1.40 | 0.62 | 2.67 | 79.50 | 137.90 |
| 8H-7, 7-9 | 73.57 | 1.44 | 0.65 | 2.68 | 79.50 | 131.00 |
| 9H-2, 80-82 | 76.30 | 1.39 | 0.60 | 2.73 | 80.50 | 144.50 |
| 9H-4, 63-65 | 79.13 | 1.43 | 0.66 | 2.75 | 78.50 | 127.90 |
| 9H-6, 47-49 | 81.97 | 1.39 | 0.60 | 2.74 | 79.70 | 142.00 |
| 10H-2, 50-52 | 85.50 | 1.40 | 0.59 | 2.72 | 81.20 | 147.30 |
| 10H-4, 50-52 | 88.50 | 1.49 | 0.73 | 2.73 | 76.00 | 110.30 |
| 10H-6, 50-52 | 91.50 | 1.40 | 0.62 | 2.71 | 79.60 | 138.80 |
| 11H-2, 66-68 | 95.16 | 1.44 | 0.66 | 2.75 | 78.70 | 127.30 |
| 11H-4, 50-52 | 98.00 | 1.49 | 0.75 | 2.67 | 75.80 | 108.20 |
| 13H-2, 116-118 | 104.66 | 1.48 | 0.73 | 2.69 | 76.20 | 111.40 |
| 13H-4, 70-72 | 107.20 | 1.43 | 0.65 | 2.65 | 78.20 | 128.50 |
| 13H-6, 39-41 | 109.89 | 1.43 | 0.65 | 2.81 | 78.50 | 129.00 |
| 14H-2, 60-62 | 113.60 | 1.48 | 0.73 | 2.69 | 75.80 | 109.80 |
| 14H-4, 50-52 | 116.50 | 1.52 | 0.80 | 2.86 | 73.60 | 98.00 |
| 14H-6, 25-27 | 119.25 | 1.53 | 0.79 | 2.77 | 74.50 | 100.00 |
| 15H-1, 110-112 | 122.10 | 1.45 | 0.67 | 2.71 | 79.00 | 125.50 |
| 15H-2, 110-112 | 123.60 | 1.44 | 0.66 | 2.78 | 79.20 | 128.30 |
| 15H-3, 110-112 | 125.10 | 1.43 | 0.64 | 2.73 | 79.80 | 132.80 |
| 15H-4, 110-112 | 126.60 | 1.44 | 0.66 | 2.81 | 79.20 | 128.90 |
| 15H-6, 110-112 | 129.40 | 1.44 | 0.65 | 2.72 | 79.80 | 130.60 |
| 16H-2, 100-102 | 133.00 | 1.52 | 0.77 | 2.73 | 76.10 | 105.70 |
| 16H-4, 100-102 | 136.00 | 1.51 | 0.77 | 2.78 | 75.40 | 104.50 |
| 16H-6, 100-102 | 139.00 | 1.47 | 0.71 | 2.72 | 77.10 | 115.70 |
| 17H-1, 80-82 | 140.80 | 1.52 | 0.77 | 2.80 | 75.40 | 103.80 |
| 17H-2, 80-82 | 142.30 | 1.54 | 0.80 | 2.75 | 75.20 | 99.70 |
| 17H-3, 135-137 | 144.30 | 1.55 | 0.83 | 2.75 | 72.70 | 92.30 |
| 144-872B- | | | | | | |
| 5R-1, 47-49 | 145.27 | 2.71 | 2.66 | 2.81 | 4.90 | 1.90 |
| 5R-3, 102-104 | 148.64 | 2.73 | 2.60 | 2.92 | 12.40 | 4.90 |
| 6R-1, 40-42 | 154.90 | 2.43 | 2.18 | 2.84 | 24.50 | 11.50 |
| 7R-1, 31-33 | 164.31 | 2.45 | 2.23 | 2.82 | 22.50 | 10.40 |
| 7R-4, 67-69 | 168.09 | 2.69 | 2.57 | 2.82 | 11.70 | 4.70 |
| 144-872B- (Cont.) | | | | | | |
| 7R-7, 74-76 | 172.37 | 2.42 | 2.18 | 2.91 | 24.60 | 11.60 |
| 8R-1, 70-72 | 173.80 | 2.51 | 2.31 | 2.72 | 20.60 | 9.20 |
| 8R-2, 89-91 | 175.35 | 2.82 | 2.73 | 2.85 | 9.40 | 3.50 |
| 8R-4, 6-8 | 177.48 | 2.87 | 2.79 | 2.88 | 7.70 | 2.80 |
| 9R-1, 46-48 | 183.06 | 2.35 | 2.01 | 2.74 | 34.40 | 17.70 |
| 9R-2, 92-94 | 184.90 | 2.85 | 2.75 | 2.95 | 10.20 | 3.80 |
| 9R-4, 14-16 | 186.72 | 2.43 | 2.13 | 2.78 | 30.80 | 14.90 |
| 9R-5, 131-133 | 189.29 | 2.44 | 2.14 | 2.91 | 30.70 | 14.80 |
| 144-872C- | | | | | | |
| 1H-6, 66-68 | 7.14 | 1.58 | 0.87 | 2.69 | 71.30 | 86.30 |
| 2H-2, 61-63 | 10.57 | 1.52 | 0.80 | 2.66 | 72.50 | 95.60 |
| 2H-3, 61-63 | 11.93 | 1.54 | 0.82 | 2.65 | 72.90 | 94.20 |
| 2H-4, 61-63 | 13.31 | 1.51 | 0.78 | 2.61 | 73.70 | 100.70 |
| 2H-5, 61-63 | 14.63 | 1.42 | 0.65 | 2.64 | 78.10 | 128.20 |
| 2H-6, 61-63 | 16.00 | 1.47 | 0.71 | 2.68 | 76.30 | 114.30 |
| 3H-2, 70-72 | 20.26 | 1.51 | 0.76 | 2.72 | 76.10 | 106.60 |
| 3H-3, 70-72 | 21.47 | 1.44 | 0.65 | 2.72 | 79.60 | 131.30 |
| 3H-4, 70-72 | 22.77 | 1.50 | 0.76 | 2.80 | 74.80 | 104.40 |
| 3H-5, 70-72 | 24.08 | 1.49 | 0.70 | 2.73 | 80.40 | 123.40 |
| 3H-6, 70-72 | 25.40 | 1.57 | 0.83 | 2.72 | 74.60 | 94.80 |
| 3H-7, 20-22 | 26.30 | 1.59 | 0.90 | 2.73 | 70.40 | 82.60 |
| 4H-1, 80-82 | 28.80 | 1.61 | 0.88 | 2.68 | 73.60 | 88.00 |
| 4H-2, 80-82 | 29.82 | 1.57 | 0.87 | 2.84 | 70.70 | 85.70 |
| 4H-3, 80-82 | 31.08 | 1.53 | 0.81 | 2.72 | 72.90 | 95.30 |
| 4H-4, 80-82 | 32.41 | 1.56 | 0.81 | 2.64 | 75.20 | 97.90 |
| 4H-5, 80-82 | 33.71 | 1.48 | 0.88 | 2.57 | 80.10 | 124.20 |
| 4H-6, 80-82 | 34.92 | 1.42 | 0.63 | 2.66 | 80.50 | 138.30 |
| 5H-2, 70-72 | 39.06 | 1.47 | 0.71 | 2.74 | 77.10 | 116.00 |
| 5H-3, 70-72 | 40.21 | 1.42 | 0.63 | 2.70 | 79.80 | 135.60 |
| 5H-4, 70-72 | 41.47 | 1.41 | 0.62 | 2.68 | 79.50 | 137.40 |
| 5H-5, 70-72 | 42.66 | 1.42 | 0.62 | 2.54 | 80.70 | 139.00 |
| 5H-6, 70-72 | 43.86 | 1.45 | 0.65 | 2.56 | 81.30 | 134.10 |
| 6H-2, 72-74 | 48.61 | 1.39 | 0.59 | 2.69 | 81.00 | 149.20 |
| 6H-4, 72-74 | 51.16 | 1.39 | 0.59 | 2.72 | 81.60 | 150.10 |
| 6H-6, 72-74 | 53.72 | 1.40 | 0.62 | 2.69 | 79.50 | 138.10 |
| 7H-1, 63-65 | 57.13 | 1.47 | 0.69 | 2.46 | 79.60 | 123.80 |
| 7H-3, 70-72 | 59.51 | 1.43 | 0.62 | 2.75 | 82.50 | 144.30 |
| 7H-5, 30-32 | 61.78 | 1.43 | 0.64 | 2.63 | 80.40 | 135.60 |
| 8H-2, 70-72 | 67.71 | 1.43 | 0.66 | 2.61 | 77.90 | 126.50 |
| 8H-4, 70-72 | 70.31 | 1.43 | 0.67 | 2.73 | 77.70 | 124.60 |
| 8H-6, 70-72 | 72.97 | 1.42 | 0.65 | 2.69 | 78.20 | 129.60 |
| 9H-2, 70-72 | 77.53 | 1.40 | 0.61 | 2.59 | 79.70 | 140.60 |
| 9H-4, 70-72 | 80.16 | 1.39 | 0.60 | 2.68 | 80.00 | 143.60 |
| 9H-6, 70-72 | 82.83 | 1.40 | 0.64 | 2.52 | 77.20 | 129.80 |
| 10H-2, 70-72 | 86.84 | 1.39 | 0.60 | 2.62 | 80.10 | 143.50 |
| 10H-5, 70-72 | 90.98 | 1.39 | 0.61 | 2.59 | 79.00 | 138.10 |
| 10H-6, 125-127 | 92.98 | 1.38 | 0.59 | 2.54 | 79.80 | 144.50 |
| 11H-2, 70-72 | 96.40 | 1.42 | 0.64 | 2.68 | 78.60 | 131.20 |
| 11H-4, 70-72 | 99.07 | 1.41 | 0.63 | 2.58 | 78.90 | 134.80 |
| 11H-6, 70-72 | 101.66 | 1.48 | 0.73 | 2.66 | 75.40 | 109.80 |
| 12H-2, 70-72 | 106.20 | 1.47 | 0.72 | 2.68 | 75.80 | 112.50 |
| 13H-2, 70-72 | 107.88 | 1.44 | 0.69 | 2.59 | 76.00 | 117.30 |
| 13H-5, 70-72 | 111.84 | 1.45 | 0.70 | 2.66 | 75.10 | 113.50 |
| 14H-3, 70-72 | 118.59 | 1.49 | 0.76 | 2.57 | 73.60 | 102.10 |
| 14H-5, 70-72 | 121.19 | 1.53 | 0.75 | 2.72 | 78.90 | 111.90 |
| 14H-7, 29-31 | 123.52 | 1.58 | 0.85 | 2.70 | 74.00 | 91.70 |
| 15H-1, 50-52 | 125.50 | 1.46 | 0.71 | 2.66 | 75.40 | 112.80 |
| 15H-3, 50-52 | 127.84 | 1.43 | 0.67 | 2.67 | 77.20 | 123.50 |
| 15H-5, 50-52 | 130.06 | 1.46 | 0.71 | 2.58 | 76.40 | 114.90 |
| 16H-2, 100-102 | 131.78 | 1.43 | 0.67 | 2.52 | 76.90 | 122.30 |
| 16H-4, 100-102 | 134.23 | 1.51 | 0.77 | 2.67 | 74.30 | 101.80 |
| 16H-6, 100-102 | 136.52 | 1.56 | 0.82 | 2.71 | 75.20 | 97.20 |
| 17X-2, 25-27 | 140.30 | 1.63 | 0.93 | 2.68 | 71.00 | 80.50 |

separating the two largest density peaks is noted at ~29 mbsf in Hole 872A and at ~31.5 mbsf in Hole 872C. This density low is associated with a peak in magnetic susceptibility values at these same depths in each hole (Fig. 31).

Magnetic susceptibility data plotted vs. depth (Fig. 31) show a "core" effect in which values are higher in the first section of each core. Values of magnetic susceptibility in pelagic carbonates within the core generally lie below zero, with the exception of the interval between 0 and 20 mbsf. No clear trend can be discerned with depth. Unusually high susceptibility values may be a function of drilling contamination, which was sometimes indicated in the white pelagic sediments by dark patches, probably derived from pipe dope.

Figure 32 shows the DSV velocity profile for Holes 872A and 872C (see Table 11). Both profiles show considerable scatter with no clear trend apparent. The velocity values, as was the case at Site 871, cluster around the value for seawater. The *P*-wave logger (PWL) data are generally poor as a result of the lack of signal strength and inadequate sediment-to-liner contact, despite the

improvements in core handling described earlier. Velocity values appeared to switch at random between 1400–1500 m/s and 2400–2500 m/s. It seems more likely that the lower values are "correct" as they agree with those (discrete) obtained by the DSV apparatus; these lower values were obtained at those points where signal strength was higher.

It was possible, using an empty liner, to demonstrate conclusively that the PWL has a bimodal characteristic when used with sediments that have poor contact with the liner. Compressional wave transmission through the sediment produced values of 1400–1500 m/s, whereas the higher values commonly obtained (2400–2500 m/s) were caused by compressional wave transmission around the inside of the liner. These higher values were associated with lower signal strengths and presumably poorer sediment-liner contact. In the case of the DSV apparatus, insertion of the transducers into the sediment usually caused cracking of the half-round core and hence poor contact between sediment and transducer. The experimental factors discussed above apply equally to the Site 871 results.

Table 10. Thermal conductivity data, Site 872.

| Core, section, interval (cm) | Depth (mbsf) | Thermal conductivity (W/[m · K]) | Error range (W/[m · K]) | Drift (K/min) |
|------------------------------|--------------|----------------------------------|-------------------------|---------------|
| 144-872A- | | | | |
| 1H-2, 50 | 2.00 | 1.49 | 0.007 | -0.010 |
| 1H-3, 50 | 3.50 | 1.42 | 0.005 | -0.001 |
| 1H-5, 50 | 6.50 | 1.22 | 0.004 | -0.013 |
| 2H-1, 41 | 7.91 | 1.42 | 0.016 | -0.025 |
| 2H-2, 100 | 10.00 | 1.23 | 0.006 | -0.037 |
| 2H-3, 100 | 11.50 | 1.12 | 0.006 | 0.000 |
| 2H-5, 100 | 14.50 | 1.09 | 0.003 | -0.002 |
| 4H-2, 100 | 29.00 | 1.41 | 0.004 | -0.014 |
| 4H-3, 100 | 30.50 | 1.48 | 0.004 | 0.002 |
| 4H-5, 100 | 33.50 | 1.36 | 0.005 | -0.024 |
| 5H-2, 100 | 38.50 | 1.33 | 0.005 | -0.009 |
| 5H-3, 100 | 40.00 | 0.67 | 0.004 | -0.007 |
| 5H-5, 100 | 43.00 | 1.03 | 0.004 | -0.014 |
| 5H-6, 30 | 43.80 | 1.02 | 0.003 | -0.003 |
| 6H-2, 50 | 47.50 | 1.53 | 0.002 | 0.018 |
| 6H-3, 50 | 49.00 | 1.53 | 0.005 | 0.011 |
| 6H-5, 50 | 52.00 | 0.96 | 0.005 | 0.027 |
| 6H-6, 50 | 53.50 | 1.03 | 0.002 | 0.006 |
| 7H-3, 50 | 58.50 | 0.81 | 0.010 | 0.006 |
| 7H-5, 50 | 61.50 | 0.96 | 0.003 | -0.028 |
| 8H-2, 50 | 66.50 | 1.38 | 0.006 | -0.010 |
| 8H-3, 50 | 68.00 | 1.31 | 0.003 | -0.001 |
| 8H-5, 50 | 71.00 | 1.06 | 0.004 | -0.012 |
| 8H-6, 50 | 72.50 | 1.03 | 0.003 | -0.001 |
| 9H-2, 50 | 76.00 | 1.21 | 0.006 | 0.000 |
| 9H-3, 50 | 77.50 | 1.38 | 0.004 | 0.027 |
| 9H-5, 50 | 80.50 | 1.21 | 0.004 | -0.015 |
| 9H-6, 50 | 82.00 | 1.04 | 0.003 | 0.008 |
| 10H-2, 50 | 85.50 | 1.20 | 0.003 | 0.031 |
| 10H-3, 50 | 87.00 | 1.58 | 0.003 | 0.032 |
| 10H-5, 50 | 90.00 | 1.01 | 0.003 | -0.074 |
| 10H-6, 50 | 91.50 | 1.03 | 0.005 | 0.004 |
| 11H-2, 50 | 95.00 | 1.26 | 0.004 | -0.006 |
| 11H-3, 50 | 96.50 | 0.99 | 0.006 | -0.020 |
| 11H-4, 50 | 98.00 | 1.06 | 0.004 | -0.075 |
| 11H-5, 50 | 99.50 | 0.96 | 0.004 | -0.033 |
| 13H-2, 50 | 104.00 | 2.21 | 0.004 | 0.020 |
| 13H-3, 50 | 105.50 | 1.71 | 0.002 | 0.003 |
| 13H-5, 50 | 108.50 | 1.43 | 0.005 | -0.004 |
| 13H-6, 50 | 110.00 | 1.03 | 0.003 | -0.002 |
| 14H-2, 50 | 113.50 | 1.58 | 0.004 | 0.015 |
| 14H-3, 50 | 115.00 | 1.43 | 0.005 | -0.048 |
| 14H-5, 50 | 118.00 | 1.39 | 0.067 | 0.031 |
| 14H-6, 25 | 119.30 | 1.03 | 0.003 | 0.005 |
| 15H-2, 50 | 123.00 | 1.37 | 0.005 | -0.024 |
| 15H-5, 50 | 127.50 | 1.12 | 0.003 | -0.016 |
| 15H-6, 50 | 129.00 | 1.07 | 0.002 | -0.003 |
| 16H-2, 50 | 132.50 | 1.40 | 0.002 | -0.041 |
| 16H-3, 50 | 134.00 | 1.37 | 0.006 | -0.008 |
| 16H-5, 50 | 137.00 | 1.30 | 0.003 | -0.001 |
| 16H-6, 50 | 138.50 | 1.22 | 0.003 | 0.020 |
| 17H-1, 50 | 140.50 | 1.66 | 0.005 | 0.031 |
| 17H-2, 50 | 142.00 | 1.93 | 0.003 | 0.046 |
| 17H-3, 50 | 143.50 | 1.34 | 0.006 | -0.009 |
| 17H-3, 10 | 144.10 | 1.27 | 0.002 | 0.025 |
| 144-872B- | | | | |
| 4R-1, 68 | 135.90 | 1.20 | 0.012 | -0.023 |
| 4R-1, 83 | 136.00 | 0.72 | 0.016 | -0.029 |
| 5R-1, 72 | 145.50 | 0.87 | 0.004 | -0.128 |
| 5R-2, 88 | 147.20 | 0.91 | 0.014 | -0.056 |
| 5R-3, 19 | 148.70 | 1.28 | 0.015 | -0.031 |
| 5R-4, 25 | 149.40 | 0.83 | 0.073 | -0.009 |
| 6R-1, 6 | 154.60 | 0.77 | 0.002 | -0.078 |
| 7R-1, 7 | 164.10 | 1.17 | 0.080 | 0.038 |
| 7R-4, 71 | 168.10 | 1.22 | 0.004 | -0.037 |
| 7R-5, 117 | 169.90 | 0.84 | 0.003 | -0.100 |
| 8R-1, 29 | 173.40 | 1.16 | 0.008 | 0.009 |
| 8R-1, 29 | 173.40 | 0.97 | 0.004 | -0.018 |
| 8R-3, 39 | 176.40 | 0.94 | 0.011 | -0.077 |
| 8R-3, 39 | 176.40 | 1.02 | 0.003 | -0.091 |
| 9R-1, 43 | 183.00 | 0.88 | 0.002 | -0.099 |
| 9R-2, 80 | 184.80 | 1.65 | 0.012 | 0.003 |
| 9R-3, 12 | 185.60 | 1.63 | 0.015 | 0.044 |
| 9R-4, 1 | 186.60 | 0.87 | 0.002 | -0.080 |
| 9R-5, 13 | 188.10 | 1.14 | 0.007 | -0.016 |
| 9R-6, 1 | 189.40 | 0.79 | 0.004 | -0.188 |
| 144-872C- | | | | |
| 4H-2, 50 | 29.50 | 1.74 | 0.002 | 0.011 |
| 4H-3, 50 | 30.80 | 1.61 | 0.003 | 0.000 |
| 4H-5, 50 | 33.40 | 1.21 | 0.004 | 0.002 |
| 4H-6, 50 | 34.60 | 1.04 | 0.002 | 0.000 |
| 12H-1, 50 | 105.00 | 1.41 | 0.005 | -0.028 |
| 12H-2, 50 | 106.00 | 1.33 | 0.004 | -0.010 |

Thermal conductivity profiles are given in Figure 33 and Table 10. These show moderate scatter, but an underlying uniformity within the pelagic sediments of Hole 872A. Values range from 0.9 to 1.6 W/(m · K). These values agree well with those from Site 871, although they lack the slightly higher trend above 40 mbsf seen in Hole 871A ("Physical Properties" section, "Site 871" chapter, this volume). Unfortunately, a software malfunction resulted in the loss of thermal conductivity data for Hole 872C.

Shear strength data from Holes 872A and 872C are given in Figure 34 and Table 13. These data suggest a strength "peak" at a depth of 70 mbsf in Hole 872A, but considerable scatter is present in the data, and the peak is not matched in Hole 872C. A general strength increase does occur, however, below 60 mbsf in Hole 872C. Values of shear strength generally range from 0 to 15 kPa. The test is described as undrained, but in these materials it is at least partially drained, even at the high deformation rate employed by the modified Wykeham-Farrance vane apparatus (see "Explanatory Notes" chapter, this volume). The majority of vane tests in the pelagic sediments did not feature a clear failure peak, and strength values may be considered as fully or partially "remolded" values. Because of the particle size (coarse silt to fine sand) of the pelagic ooze, the Torvane is considered an inappropriate technique.

Carbonate

Carbonate rock was recovered in very small amounts in Holes 872A and 872B, primarily infilling basalt fractures. The recovery did not permit any physical properties measurements to be conducted; thus, a separate physical property unit was not appropriate.

Basalt

Significant quantities of basalt were recovered only in Hole 872B between 135 and 193 mbsf. No major weathering profile was found. However, both basalt with vein fillings and brecciated basalt tended to crack and spall on drying, thus creating problems for the Hamilton Frame compressional wave velocity measurements. Basalts from Site 872 were less susceptible to cracking than basalts measured at Site 871 ("Physical Properties" section, "Site 871" chapter, this volume). Porosity was between 5% and 35% (Fig. 28). Hamilton Frame compressional wave velocities range from 3500 to 5600 m/s (Table 12). Velocity determinations were conducted out on orthogonal faces of the cube sample. Anisotropy coefficients are grouped around zero and the results generally show little anisotropy. What anisotropy was recorded was probably the result of micro-fissuring and veining in the sample. Samples were soaked for several hours before being tested. It was found, by experiment, that oven drying times needed to be extended beyond the usual 24 hr for the basalts if consistent results were to be obtained.

DOWNHOLE MEASUREMENTS AND SEISMIC STRATIGRAPHY

Logging Operations

Logging was attempted at Hole 872B by placing the bottom of the drill pipe at 151 mbsf, 14 m below the contact with basaltic basement, and lowering the geochemical tool string to calibration depth. Neither the primary geochemical tool string or its spare would calibrate properly, but the Shipboard Scientific Party finally decided to attempt the logging run anyway. Although the tool string could be lowered below the bottom of the drill pipe, it hung up only a few meters below that level, probably on a ledge within basement that we could not pass. Because the hole was shallow, the tool string was uncalibrated, and hole conditions

Table 11. DSV compressional wave velocity measurements, Holes 872A and 872C.

| Core, section, interval (cm) | Depth (mbsf) | Temperature (°C) | Velocity (m/s) |
|------------------------------|--------------|------------------|----------------|
| 144-872A- | | | |
| 4H-2, 69-76 | 28.70 | 21.40 | 1552.00 |
| 4H-2, 105-105 | 29.10 | 20.30 | 1512.90 |
| 4H-3, 80-87 | 30.30 | 19.90 | 1488.40 |
| 6H-2, 53-60 | 47.50 | 21.70 | 1477.20 |
| 8H-2, 77-84 | 66.80 | 20.30 | 1514.50 |
| 9H-4, 71-78 | 79.20 | 21.90 | 1504.60 |
| 9H-6, 63-70 | 82.10 | 20.90 | 1498.10 |
| 10H-2, 66-73 | 85.70 | 21.80 | 1562.60 |
| 10H-4, 60-67 | 88.60 | 20.80 | 1501.30 |
| 10H-6, 62-69 | 91.60 | 21.30 | 1499.70 |
| 11H-4, 32-39 | 97.80 | 21.30 | 1470.90 |
| 13H-2, 62-69 | 104.00 | 21.60 | 1511.20 |
| 13H-4, 59-66 | 107.00 | 21.10 | 1566.10 |
| 13H-6, 21-28 | 110.00 | 21.80 | 1514.50 |
| 14H-2, 34-41 | 113.00 | 22.10 | 1499.70 |
| 16H-6, 23-30 | 138.00 | 21.30 | 1457.80 |
| 11H-6, 32-39 | 101.30 | 21.00 | 1500.60 |
| 12H-2, 50-57 | 106.00 | 21.00 | 1507.20 |
| 13H-2, 35-42 | 107.50 | 21.00 | 1454.70 |
| 13H-5, 41-48 | 111.60 | 21.00 | 1451.60 |
| 14H-2, 70-77 | 117.30 | 21.00 | 1570.70 |
| 14H-3, 94-101 | 118.80 | 21.00 | 1581.50 |
| 14H-4, 74-81 | 120.00 | 21.00 | 1560.00 |
| 14H-5, 106-113 | 121.60 | 21.00 | 1423.20 |
| 14H-6, 73-80 | 122.60 | 21.00 | 1565.30 |
| 16H-2, 94-101 | 131.70 | 20.00 | 1577.90 |
| 144-872C- | | | |
| 1H-2, 41-48 | 1.41 | 22.00 | 1551.20 |
| 1H-3, 41-48 | 2.71 | 22.00 | 1500.60 |
| 1H-4, 42-49 | 4.13 | 21.00 | 1502.20 |
| 1H-5, 30-37 | 5.40 | 21.00 | 1505.50 |
| 1H-6, 36-43 | 6.84 | 21.00 | 1453.20 |
| 3H-5, 60-67 | 23.98 | 21.00 | 1540.80 |
| 4H-3, 45-52 | 30.73 | 21.00 | 1542.60 |
| 6H-2, 40-47 | 48.29 | 22.00 | 1503.90 |
| 7H-3, 34-41 | 59.15 | 22.00 | 1539.10 |
| 8H-2, 43-50 | 67.44 | 21.00 | 1513.80 |
| 9H-2, 40-47 | 77.23 | 21.00 | 1454.70 |
| 9H-4, 43-50 | 79.89 | 20.00 | 1572.50 |
| 10H-1, 43-50 | 85.43 | 22.00 | 1492.50 |
| 10H-5, 45-52 | 90.73 | 22.00 | 1495.70 |
| 10H-7, 22-29 | 93.37 | 21.00 | 1515.40 |
| 11H-2, 52-59 | 96.22 | 22.00 | 1512.10 |
| 11H-4, 38-45 | 98.75 | 21.00 | 1513.80 |
| 11H-6, 32-39 | 101.30 | 21.00 | 1500.60 |
| 12H-2, 50-57 | 106.00 | 21.00 | 1507.20 |
| 13H-2, 35-42 | 107.50 | 21.00 | 1454.70 |
| 13H-5, 41-48 | 111.60 | 21.00 | 1451.60 |
| 14H-2, 70-77 | 117.30 | 21.00 | 1570.70 |
| 14H-3, 94-101 | 118.80 | 21.00 | 1581.50 |
| 14H-4, 74-81 | 120.00 | 21.00 | 1560.00 |
| 14H-5, 106-113 | 121.60 | 21.00 | 1423.20 |
| 14H-6, 73-80 | 122.60 | 21.00 | 1565.30 |
| 16H-2, 94-101 | 131.70 | 20.00 | 1577.90 |

Note: DSV = digital sound velocimeter.

were bad, logging operations ended at that point and no log information was obtained.

Seismic Stratigraphy

An excellent single-channel seismic profile was obtained on two crossings of Hole 872B using a 200-in.³ water gun as a sound source. These data were recorded on a Masscomp computer, refiltered, and displayed (Fig. 35). The base of the foraminifer ooze (pelagic cap) is easily identified at 143 mbsf, where drill pipe penetration abruptly slowed, and at 1.62 s TWT on the seismic record. This reflector is easily substantiated by the 3.5-kHz record that also shows a pronounced "hardground" reflector at the same TWT. Below this horizon are other coherent reflections, the most prominent being at about 2.12 s TWT. These may be reflections from within basement, or possibly reflections from older sedimentary horizons covered by the lava flows sampled at Hole 872B.

Because no logging information was obtained at this site, the formation velocity of the foraminifer ooze was calculated from the interval traveltime to the basement reflection and the depth below seafloor was obtained from the drill-pipe penetration record. By this method, the 0.187 s, 143-m-thick section of foraminifer ooze has a formation velocity of 1.5 km/s, essentially the same as seawater.

SUMMARY AND CONCLUSIONS

Initial interpretation of the cores obtained at Site 872 indicate that a series of subaerial eruptions of differentiated alkali olivine basalt, possibly hawaiiites and mugearite, form the upper portion of the igneous basement at Lo-En Guyot. They appear to represent the very latest shield stage or the alkalic-cap stage of hotspot volcanism. Magnetic measurements demonstrate that the basalt is normally magnetized with the magnetization probably acquired at a paleolatitude of about 30°S.

Planktonic foraminifers and possibly calcareous nannofossils of late Turonian age are reworked into lower Santonian sediments filling the fractures in the basalt. On the basis of the biostratigraphic age of these organisms and other benthic organisms, it was determined that volcanism occurred before the late Turonian. Moreover, the association of middle neritic benthic foraminifers with planktonic organisms demonstrates that by early Santonian time, a relatively shallow pelagic environment was present on Lo-En Guyot, or, alternatively, transport of shallow-water material into a deeper site of deposition occurred at that time. The hypothesis that the Lo-En volcanic edifice existed and was submerged before late Turonian time is further supported by the occurrence of near-shore marine organisms of early Albian age recovered in dredges along the southern slope of this guyot. The backtracked location of Lo-En Guyot and other volcanic edifices that erupted during the mid Cretaceous (Lincoln et al., in press), agrees with the interpretation that Lo-En Guyot existed before the late Turonian and was located at a paleolatitude of 30°S.

The overall paucity of pelagic sediments, and the occurrence of highly phosphatized, manganese-oxide-encrusted lithoclasts of different origin and age (late Santonian, early Campanian, and late Paleocene) above the basalt in Holes 872A and 872B, suggest that for several millions of years the guyot experienced prevailing nondepositional conditions in an active current regime. A somewhat higher energy environment may have existed at the location of Hole 872C where only the youngest, slightly phosphatized chalk of middle Eocene age and one pebble with a Santonian matrix were recovered; alternatively, this may be a function of poor core recovery.

Continuous pelagic sedimentation was established on Lo-En Guyot only by late Oligocene time. The middle Eocene sediment thinly blanketing the conglomeratic chalk is overlain by a 140-m-thick sequence of upper Oligocene and Neogene pelagic carbonates. The hiatus associated with this middle Eocene to late Oligocene disconformity suggests that the seafloor may have been exposed for as long as 15 m.y. Calcareous microplankton stratigraphy indicates that sedimentation was relatively continuous from the late Oligocene through the Pleistocene, with only minor periods of nondeposition and/or erosion during the Miocene and possibly during the early Pliocene. The abnormally high ratio of planktonic foraminifers to nannofossils throughout most of the Oligocene and Miocene pelagic sequence suggests significant winnowing of the sediment. This current activity apparently waned during the Pliocene and Pleistocene, as indicated by the relative increase in the volume of nannofossils in the uppermost oozes.

An indirect relationship with Annewetak Atoll is confined to a few volcanic glass shards in a single pebble with a Campanian pelagic matrix from Hole 872B. These shards may be interpreted

Table 12. Hamilton Frame measurements of compressional wave velocity, Hole 872.

| Core, section, interval (cm) | Depth (mbsf) | Distance (mm) | Axes of measurement | Traveltime (μ s) | Corrected traveltime (μ s) | Measured velocity (m/s) | Velocity anisotropy index |
|------------------------------|--------------|---------------|---------------------|-----------------------|---------------------------------|-------------------------|---------------------------|
| 144-872B- | | | | | | | |
| 5R-1, 47-49 | 145.27 | 24.05 | a | 7.89 | 4.89 | 4918.20 | |
| 5R-1, 47-49 | 145.27 | 21.39 | b | 7.34 | 4.34 | 4928.57 | |
| 5R-1, 47-49 | 145.27 | 21.39 | c | 7.28 | 4.28 | 4997.66 | -0.01 |
| 5R-3, 102-104 | 148.64 | 23.61 | a | 8.02 | 5.02 | 4703.19 | |
| 5R-3, 102-104 | 148.64 | 21.50 | b | 7.41 | 4.41 | 4875.28 | |
| 5R-3, 102-104 | 148.64 | 21.35 | c | 7.45 | 4.45 | 4797.75 | 0.00 |
| 6R-1, 40-42 | 154.90 | 25.62 | a | 10.35 | 7.35 | 3485.71 | |
| 6R-1, 40-42 | 154.90 | 21.49 | b | 9.01 | 6.01 | 3575.71 | |
| 6R-1, 40-42 | 154.90 | 21.40 | c | 8.74 | 5.74 | 3728.22 | -0.05 |
| 7R-1, 31-33 | 164.31 | 25.98 | a | 10.23 | 7.23 | 3593.36 | |
| 7R-1, 31-33 | 164.31 | 21.46 | b | 8.97 | 5.97 | 3594.64 | |
| 7R-1, 31-33 | 164.31 | 21.44 | c | 8.75 | 5.75 | 3728.70 | -0.04 |
| 7R-4, 67-69 | 168.09 | 25.58 | a | 8.13 | 5.13 | 4986.36 | |
| 7R-4, 67-69 | 168.09 | 21.27 | b | 7.50 | 4.50 | 4726.67 | |
| 7R-4, 67-69 | 168.09 | 21.40 | c | 7.53 | 4.53 | 4724.06 | 0.03 |
| 7R-7, 74-76 | 172.37 | 22.25 | a | 9.16 | 6.16 | 3612.01 | |
| 7R-7, 74-76 | 172.37 | 21.50 | b | 8.84 | 5.84 | 3681.51 | |
| 7R-7, 74-76 | 172.37 | 21.39 | c | 9.11 | 6.11 | 3500.82 | 0.04 |
| 8R-1, 70-72 | 173.80 | 20.51 | a | 8.11 | 5.11 | 4013.70 | |
| 8R-1, 70-72 | 173.80 | 21.50 | b | 7.79 | 4.79 | 4488.52 | |
| 8R-1, 70-72 | 173.80 | 21.40 | c | 7.83 | 4.83 | 4430.64 | -0.04 |
| 8R-2, 5-7 | 175.39 | 25.02 | a | 7.83 | 4.83 | 5180.12 | |
| 8R-2, 5-7 | 175.39 | 21.48 | b | 6.72 | 3.72 | 5774.19 | |
| 8R-2, 5-7 | 175.39 | 21.35 | c | 6.72 | 3.72 | 5739.25 | -0.05 |
| 8R-4, 46-48 | 177.48 | 24.03 | a | 7.33 | 4.33 | 5549.65 | |
| 8R-4, 46-48 | 177.48 | 21.46 | b | 6.76 | 3.76 | 5707.45 | |
| 8R-4, 46-48 | 177.48 | 21.33 | c | 6.71 | 3.71 | 5749.33 | -0.02 |
| 9R-1, 59-61 | 183.07 | 21.98 | a | 10.29 | 7.29 | 3015.09 | |
| 9R-1, 59-61 | 183.07 | 21.65 | b | 9.94 | 6.94 | 3119.60 | |
| 9R-1, 59-61 | 183.07 | 21.51 | c | 9.94 | 6.94 | 3099.42 | -0.01 |
| 9R-2, 90-92 | 184.90 | 23.07 | a | 7.93 | 4.93 | 4679.51 | |
| 9R-2, 90-92 | 184.90 | 21.44 | b | 6.96 | 3.96 | 5414.14 | |
| 9R-2, 90-92 | 184.90 | 21.36 | c | 6.96 | 3.96 | 5393.94 | -0.07 |
| 9R-4, 130-132 | 186.72 | 20.89 | a | 8.51 | 5.51 | 3791.29 | |
| 9R-4, 130-132 | 186.72 | 21.83 | b | 8.48 | 5.48 | 3983.58 | |
| 9R-4, 130-132 | 186.72 | 21.49 | c | 8.86 | 5.86 | 3667.24 | 0.06 |
| 9R-5, 19-21 | 189.31 | 23.69 | a | 9.37 | 6.37 | 3719.00 | |
| 9R-5, 19-21 | 189.31 | 21.59 | a | 8.84 | 5.84 | 3696.92 | |
| 9R-5, 19-21 | 189.31 | 21.48 | b | 9.11 | 6.11 | 3515.55 | 0.05 |

Notes: a = direction perpendicular to split core plane, b = direction transverse to split core plane, and c = core axis; all axes orthogonal.

as evidence of the Campanian volcanic event that was responsible for the eruption of the basalts recovered by drilling in Anewetak Atoll.

REFERENCES*

- Berggren, W.A., Kent, D.V., and Flynn, J.J., 1985. Jurassic to Paleogene: Part 2. Paleogene geochronology and chronostratigraphy. In Snelling, N.J. (Ed.), *The Chronology of the Geological Record*. Geol. Soc. London Mem., 10:141-195.
- Berggren, W.A., Kent, D.V., and Van Couvering, J.A., 1985. The Neogene: Part 2. Neogene geochronology and chronostratigraphy. In Snelling, N.J. (Ed.), *The Chronology of the Geological Record*. Geol. Soc. London Mem., 10:211-260.
- Blow, W.H., 1969. Late middle Eocene to Recent planktonic foraminiferal biostratigraphy. In Brönniman, P., and Renz, H.H. (Eds.), *Proc. First Int. Conf. Planktonic Microfossils, Geneva, 1967*: Leiden (E.J. Brill), 1:199-422.

- Davis, A.S., Pringle, M.S., Pickthorn, L.B.G., Clague, D.A., and Schwab, W.C., 1989. Petrology and age of alkalic lava from the Ratak chain of the Marshall Islands. *J. Geophys. Res.*, 94:5757-5774.
- Edwards, L.E., 1985. Miocene dinocysts from Deep Sea Drilling Project Leg 81, Rockall Plateau, Eastern North Atlantic Ocean. In Roberts, D.G., Schnitker, D., et al., *Init. Repts. DSDP*, 81: Washington (U.S. Govt. Printing Office), 581-594.
- Head, M.J., Norris, G., and Mudie, P.J., 1989. Palynology and dinocyst stratigraphy of the Upper Miocene and Lowermost Pliocene, ODP Leg 105, Site 646, Labrador Sea. In Srivastava, S.P., Arthur, M., Clement, B., et al., *Proc. ODP, Sci. Results*, 105: College Station, TX (Ocean Drilling Program), 423-451.
- Hein, J.R., Kang, J.K., et al., 1990. Geological, geochemical, geophysical, and oceanographic data and interpretations of seamounts and C-rich ferromanganese crusts from the Marshall Islands, KORDI-USGS R.V. *Faranella* Cruise F10-89-CP. *Open-File Rep.—U.S. Geol. Surv.*, 90-407.
- Lancelot, Y., Larson, R., et al., 1990. *Proc. ODP, Init. Repts.*, 129: College Station, TX (Ocean Drilling Program).
- Lincoln, J.M., Pringle, M.S., and Premoli Silva, I., in press. Early and Late Cretaceous volcanism and reef-building in the Marshall Islands. In Pringle, M.S., Sager, W.W., Sliter, W.V., and Stein, S. (Eds.), *The Mesozoic Pacific*. Am. Geophys. Union, Geophys. Monogr. Ser.

* Abbreviations for names of organizations and publication titles in ODP reference lists follow the style given in *Chemical Abstracts Service Source Index* (published by American Chemical Society).

- Pringle, M.S., Jr., 1992. Geochronology and petrology of the Musicians Seamounts, and the search for hot spot volcanism in the Cretaceous Pacific [Ph.D. dissert.]. Univ. of Hawaii, Honolulu.
- Raitt, R.W., 1957. Seismic refraction studies of Eniwetok Atoll. *Geol. Surv. Prof. Pap. U.S.*, 260-S:685-698.
- Sager, W.W., Winterer, E.L., Firth, J.V., et al., in press. *Proc. ODP, Init. Repts.*, 143: College Station, TX (Ocean Drilling Program).
- Schlanger, S.O., 1963. Subsurface geology of Eniwetok Atoll. *Geol. Surv. Prof. Pap. U.S.*, 260-BB:991-1066.

- Vacquier, V., 1985. The measurement of thermal conductivity of solids with a transient linear heat source on the plane surface of a poorly conducting body. *Earth Planet. Sci. Lett.*, 74:275-279.
- Von Herzen, R.P., and Maxwell, A.E., 1959. The measurement of thermal conductivity of deep-sea sediments by a needle probe method. *J. Geophys. Res.*, 65:1557-1563.

Ms 144IR-105

NOTE: For all sites drilled, core-description forms ("barrel sheets") and core photographs can be found in Section 3, beginning on page 453. Forms containing smear-slide data can be found in Section 4, beginning on page 1017. Thin-section data are given in Section 5, beginning on page 1037.

Table 13. Wykeham-Farrance shear strength data, Holes 872A and 872C.

| Core, section, interval (cm) | Depth (mbsf) | Test type | Spring constant | Vane constant | Tension angle (degree) | Undrained shear strength (kPa) |
|------------------------------|--------------|-----------|-----------------|---------------|------------------------|--------------------------------|
| 144-872A- | | | | | | |
| 1H-2, 140-141 | 2.90 | WF | 31.27 | 0.23 | 1.00 | 0.70 |
| 1H-3, 100-101 | 4.00 | WF | 31.27 | 0.23 | 1.00 | 0.70 |
| 1H-5, 90-91 | 6.90 | WF | 31.27 | 0.23 | 0.50 | 0.35 |
| 2H-2, 92-93 | 9.92 | WF | 31.27 | 0.23 | 0.00 | 0.00 |
| 2H-5, 116-117 | 14.66 | WF | 31.27 | 0.23 | 0.00 | 0.00 |
| 4H-2, 115-116 | 29.15 | WF | 31.27 | 0.23 | 3.00 | 2.09 |
| 4H-3, 20-21 | 29.70 | WF | 31.27 | 0.23 | 1.00 | 0.70 |
| 5H-4, 112-113 | 41.62 | WF | 31.27 | 0.23 | 3.00 | 2.09 |
| 6H-2, 125-126 | 48.25 | WF | 31.27 | 0.23 | 0.00 | 0.00 |
| 8H-2, 102-103 | 67.02 | WF | 31.27 | 0.23 | 25.00 | 17.42 |
| 8H-3, 104-105 | 68.54 | WF | 31.27 | 0.23 | 14.00 | 9.76 |
| 9H-2, 124-125 | 76.74 | WF | 31.27 | 0.23 | 14.00 | 9.76 |
| 9H-4, 128-129 | 79.78 | WF | 31.27 | 0.23 | 6.00 | 4.18 |
| 9H-6, 119-120 | 82.69 | WF | 31.27 | 0.23 | 14.00 | 9.76 |
| 10H-2, 120-121 | 86.20 | WF | 31.27 | 0.23 | 12.00 | 8.36 |
| 10H-4, 110-111 | 89.10 | WF | 31.27 | 0.23 | 12.00 | 8.36 |
| 10H-6, 118-119 | 92.18 | WF | 31.27 | 0.23 | 12.00 | 8.36 |
| 11H-2, 129-130 | 95.79 | WF | 31.27 | 0.23 | 4.00 | 2.79 |
| 11H-4, 88-89 | 98.38 | WF | 31.27 | 0.23 | 0.00 | 0.00 |
| 13H-2, 110-111 | 104.60 | WF | 31.27 | 0.23 | 4.00 | 2.79 |
| 13H-4, 115-116 | 107.70 | WF | 31.27 | 0.23 | 1.00 | 0.70 |
| 13H-6, 118-119 | 110.73 | WF | 31.27 | 0.23 | 12.00 | 8.36 |
| 14H-2, 20-21 | 113.20 | WF | 31.27 | 0.23 | 1.00 | 0.70 |
| 15H-3, 80-81 | 124.80 | WF | 31.27 | 0.23 | 2.00 | 1.39 |
| 16H-4, 105-106 | 136.10 | WF | 31.27 | 0.23 | 1.00 | 0.70 |
| 144-872C- | | | | | | |
| 1H-2, 96-97 | 1.96 | WF | 31.27 | 0.23 | 0.00 | 0.00 |
| 1H-3, 97-98 | 3.27 | WF | 31.27 | 0.23 | 0.00 | 0.00 |
| 1H-4, 98-99 | 4.69 | WF | 31.27 | 0.23 | 4.00 | 2.79 |
| 1H-5, 87-88 | 5.97 | WF | 31.27 | 0.23 | 4.00 | 2.79 |
| 1H-6, 92-93 | 7.40 | WF | 31.27 | 0.23 | 5.50 | 3.83 |
| 3H-5, 117-118 | 24.55 | WF | 31.27 | 0.23 | 2.00 | 1.39 |
| 4H-3, 103-104 | 31.31 | WF | 31.27 | 0.23 | 4.00 | 2.79 |
| 5H-3, 95-96 | 40.46 | WF | 31.27 | 0.23 | 1.00 | 0.70 |
| 6H-2, 96-97 | 48.85 | WF | 31.27 | 0.23 | 0.00 | 0.00 |
| 7H-3, 92-93 | 59.73 | WF | 31.27 | 0.23 | 12.00 | 8.36 |
| 8H-2, 98-99 | 67.99 | WF | 31.27 | 0.23 | 5.00 | 3.48 |
| 8H-6, 100-101 | 73.27 | WF | 31.27 | 0.23 | 3.00 | 2.09 |
| 9H-2, 96-97 | 77.79 | WF | 31.27 | 0.23 | 11.00 | 7.67 |
| 9H-4, 99-100 | 80.45 | WF | 31.27 | 0.23 | 6.00 | 4.18 |
| 9H-6, 85-86 | 82.98 | WF | 31.27 | 0.23 | 3.00 | 2.09 |
| 10H-2, 99-100 | 87.13 | WF | 31.27 | 0.23 | 5.00 | 3.48 |
| 10H-5, 102-103 | 91.30 | WF | 31.27 | 0.23 | 7.00 | 4.88 |
| 10H-7, 32-33 | 93.47 | WF | 31.27 | 0.23 | 7.00 | 4.88 |
| 11H-2, 91-92 | 96.61 | WF | 31.27 | 0.23 | 2.00 | 1.39 |
| 11H-4, 92-93 | 99.29 | WF | 31.27 | 0.23 | 14.00 | 9.76 |
| 11H-6, 43-44 | 101.40 | WF | 31.27 | 0.23 | 2.00 | 1.39 |
| 12H-2, 104-105 | 106.50 | WF | 31.27 | 0.23 | 3.00 | 2.09 |
| 13H-2, 91-92 | 108.10 | WF | 31.27 | 0.23 | 5.00 | 3.48 |
| 13H-5, 98-99 | 112.10 | WF | 31.27 | 0.23 | 2.00 | 1.39 |
| 14H-1, 70-71 | 116.20 | WF | 31.27 | 0.23 | 6.00 | 4.18 |
| 14H-2, 70-71 | 117.30 | WF | 31.27 | 0.23 | 1.00 | 0.70 |
| 14H-3, 94-95 | 118.80 | WF | 31.27 | 0.23 | 2.00 | 1.39 |
| 14H-4, 74-75 | 120.00 | WF | 31.27 | 0.23 | 10.00 | 6.97 |
| 14H-5, 106-107 | 121.60 | WF | 31.27 | 0.23 | 2.00 | 1.39 |
| 14H-6, 73-74 | 122.60 | WF | 31.27 | 0.23 | 0.00 | 0.00 |
| 15H-1, 100-101 | 126.00 | WF | 31.27 | 0.23 | 43.00 | 29.96 |
| 16H-1, 12-13 | 130.10 | WF | 31.27 | 0.23 | 6.00 | 4.18 |
| 16H-2, 105-106 | 131.80 | WF | 31.27 | 0.23 | 14.00 | 9.76 |
| 17X-2, 47-48 | 140.50 | WF | 31.27 | 0.23 | 65.00 | 45.29 |
| 17X-2, 38-39 | 140.40 | WF | 31.27 | 0.23 | 60.00 | 41.81 |

Note: WF = Wykeham-Farrance vane.

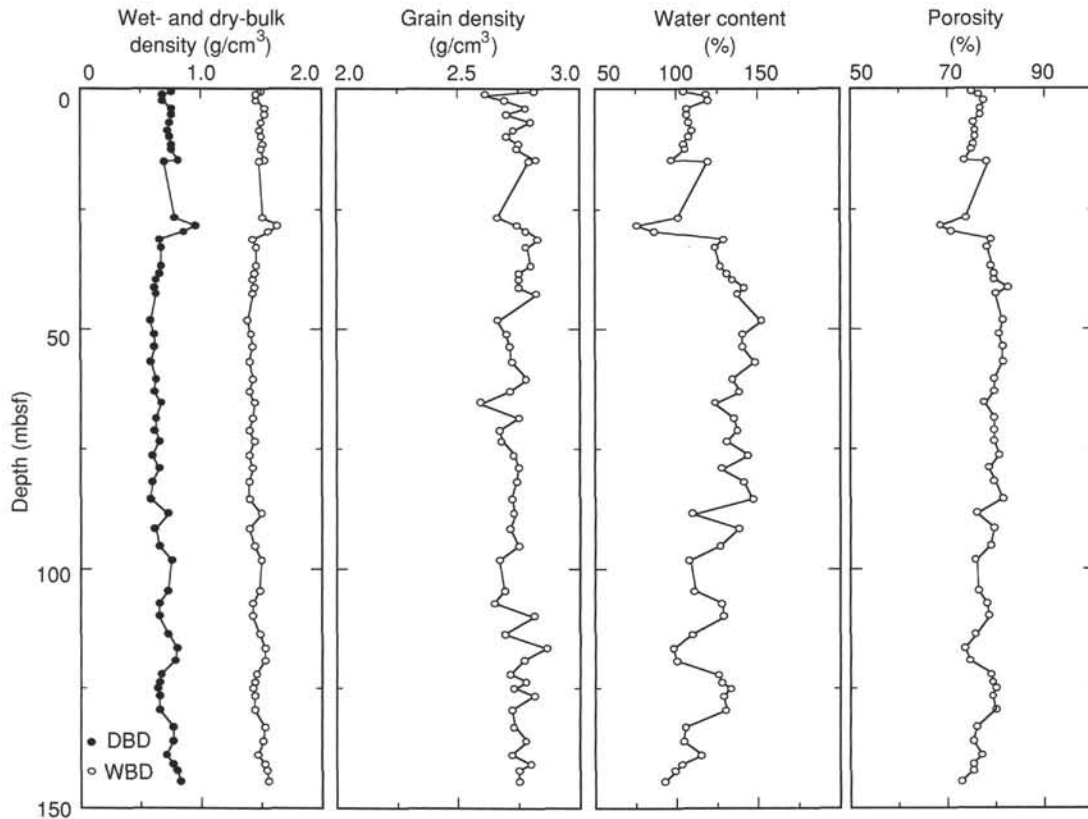


Figure 27. Measurements of index properties (wet- and dry-bulk density, grain density, water content, and porosity) vs. depth, Hole 872A.

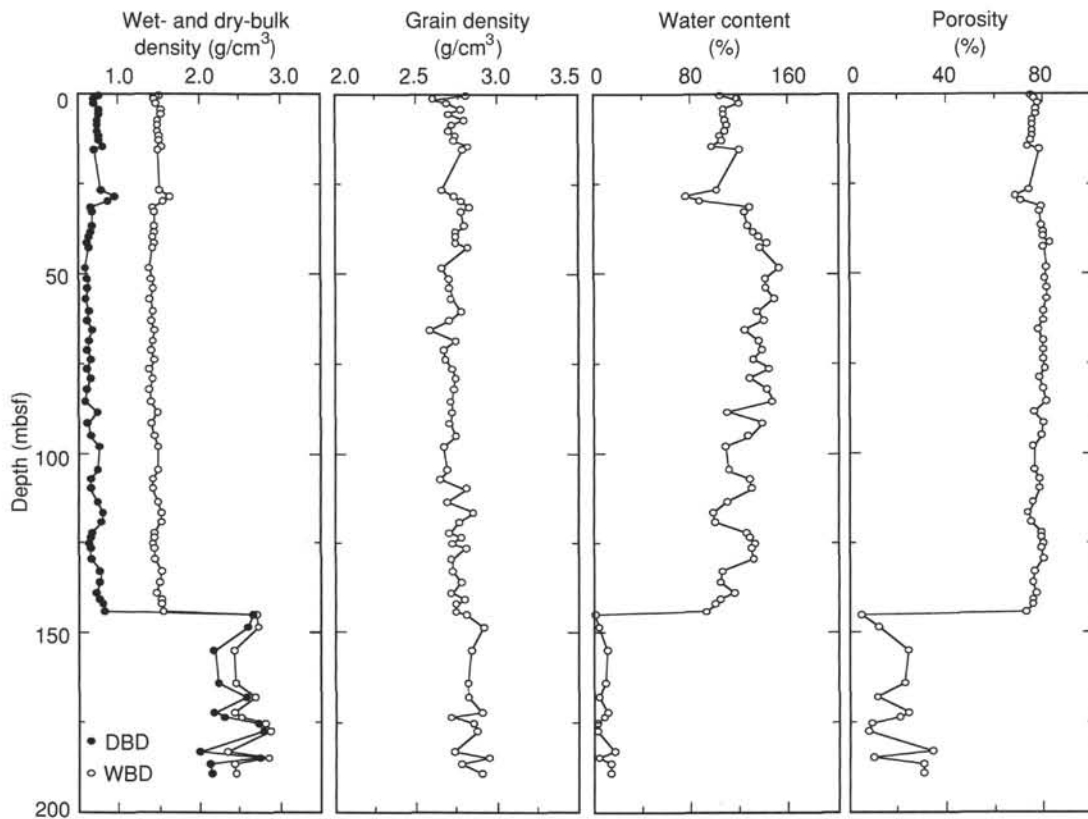


Figure 28. Measurements of index properties (wet- and dry-bulk density, grain density, water content, and porosity) vs. depth, Holes 872A and 872B.

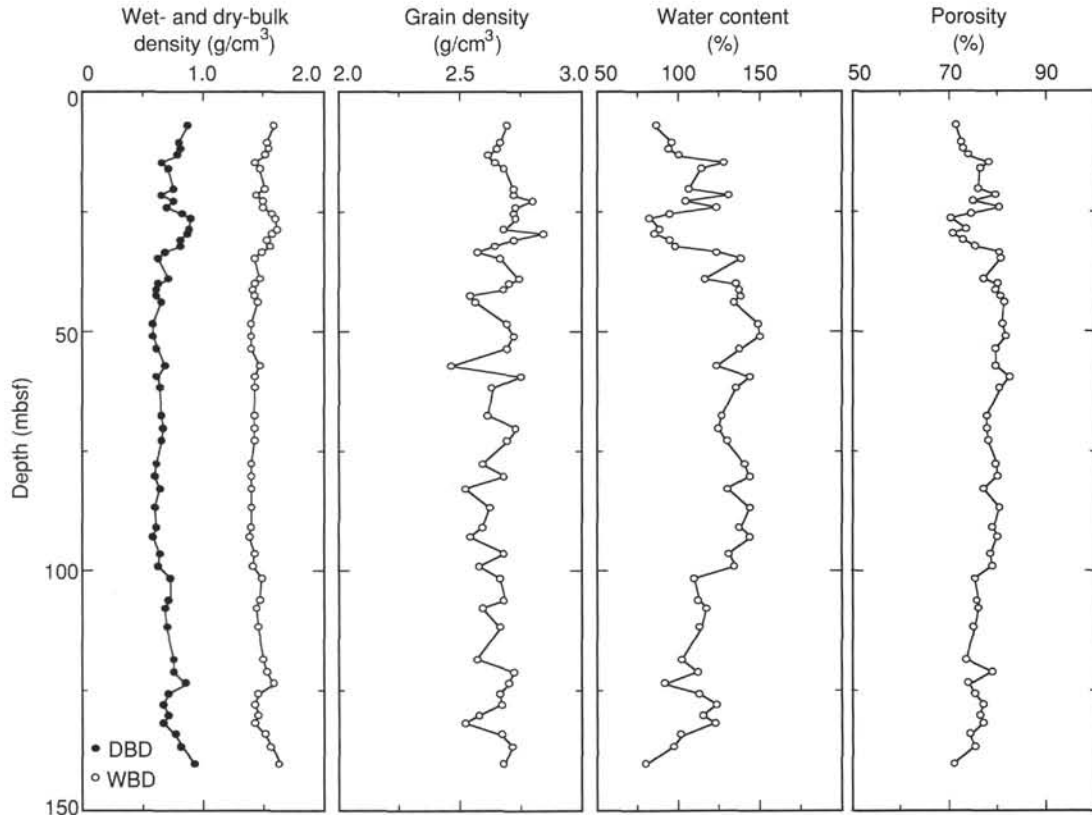


Figure 29. Measurements of index properties (wet- and dry-bulk density, grain density, water content, and porosity) vs. depth, Hole 872C.

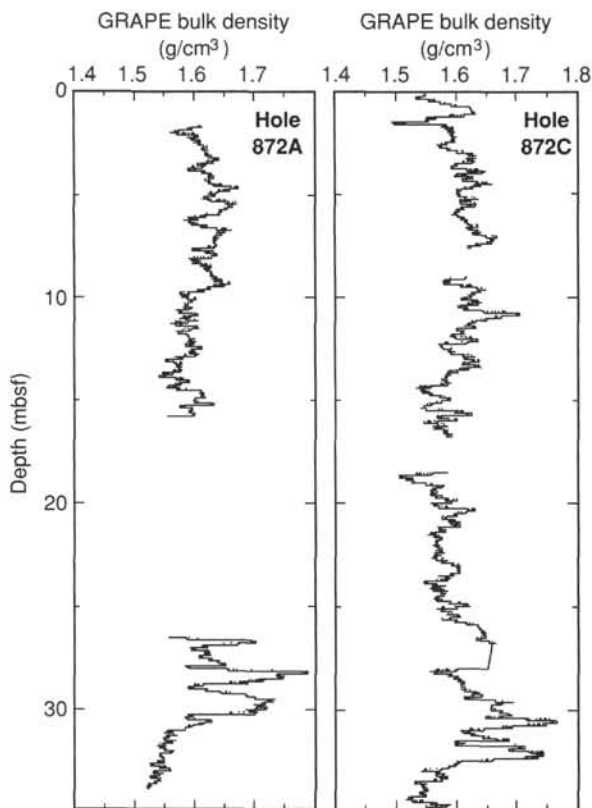


Figure 30. GRAPE bulk density vs. depth, Holes 872A and 872C.

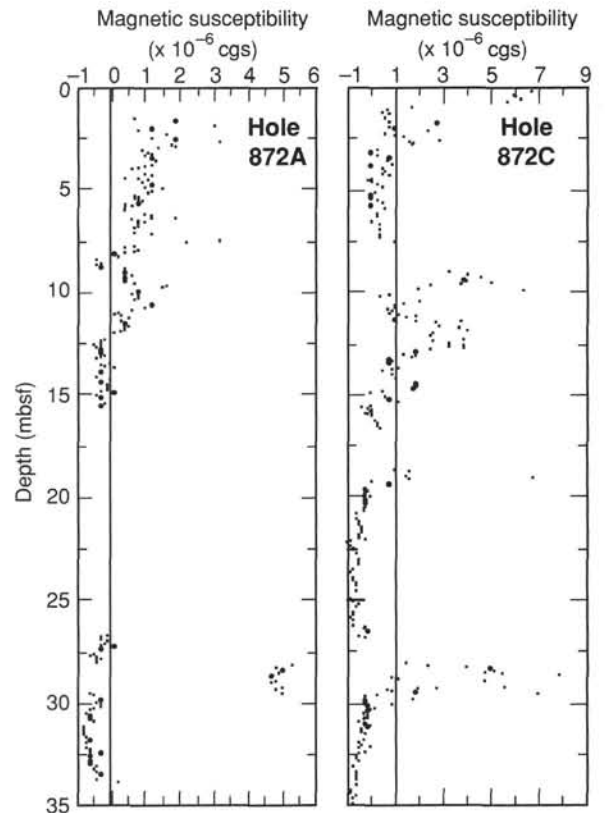


Figure 31. Magnetic susceptibility vs. depth, Holes 872A and 872C.

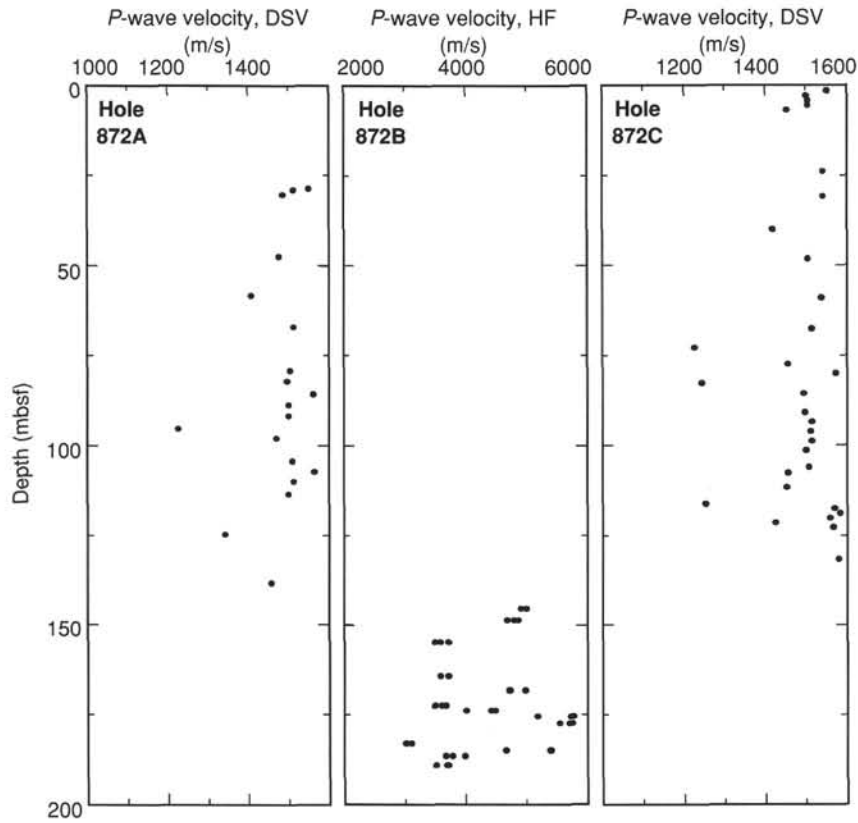


Figure 32. Digital sound velocimeter (DSV) and Hamilton Frame (HF) measurements of compressional wave velocity vs. depth, Holes 872A, 872B, and 872C.

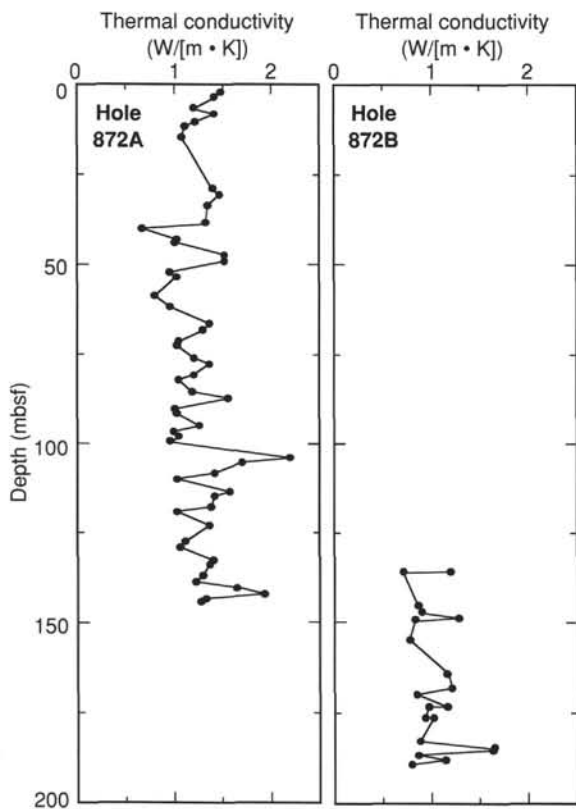


Figure 33. Thermal conductivity vs. depth for pelagic sediments in Hole 872A and basalts in Hole 872B.

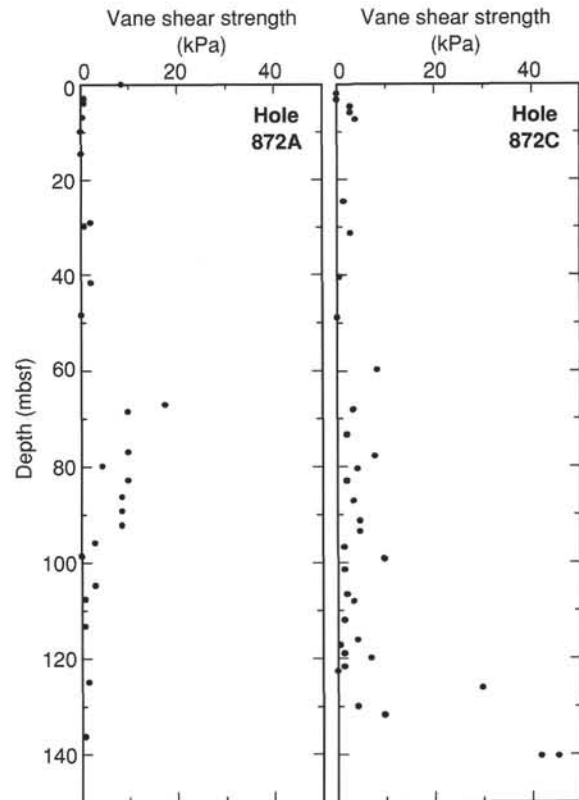


Figure 34. Vane shear strength vs. depth, Holes 872A and 872C.

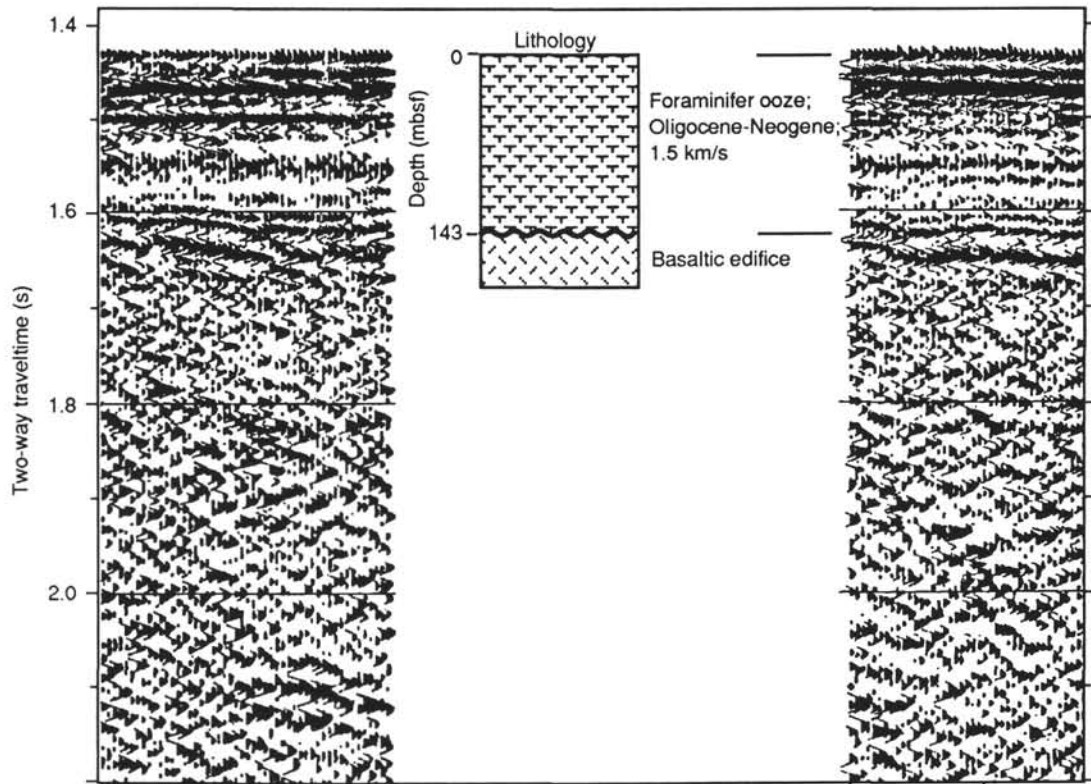


Figure 35. Lithostratigraphic correlations to the seismic stratigraphy section at Site 872. The major reflector corresponds to the basement/pelagic cap interface. Depth to basement is based on the drill-pipe penetration record. Formation velocity for the pelagic cap is based on that depth, and on the interval traveltime to the basement reflection from the seismic records.